ASSESSING NUTRIENT LOADS FROM IN-SITU FERTILIZER AMENDMENTS IN WILLARD SPUR

by

Joel Thomas Pierson

A thesis submitted to the faculty of
The University of Utah
in partial fulfillment of the requirements for the degree of

Master of Science

in

Geology

Department of Geology and Geophysics

The University of Utah

May 2014

Copyright © Joel Thomas Pierson 2014

All Rights Reserved

The University of Utah Graduate School

STATEMENT OF THESIS APPROVAL

The following faculty members served as the supervisory committee chair and members for the thesis of **Joel Thomas Pierson**.

Dates at right indicate the members' approval of the thesis.

William P. Johnson, Chair	1/9/14 Date Approved
Heidi M. Hoven, Member	1/29/14 Date Approved
Thure E. Cerling, Member	10/25/13 Date Approved

The thesis has also been approved by **John M. Bartley** Chair of the Department/School/College of **Geology and Geophysics** and by David B. Kieda, Dean of The Graduate School.

ABSTRACT

A research team studied relationships between nutrient loading and submerged aquatic vegetation (SAV) in the Willard Spur as related to increased nutrient loading by the Perry/Willard Regional Wastewater Treatment Plant (PWRWTP). *In-situ* plots containing slow-release nutrient amendments were constructed in the Willard Spur in 2012 and 2013. The water and sediment chemistry of the plots was monitored monthly in 2012 and bimonthly in 2013. Another team member assessed plant health metrics concurrently with surface water and sediment samples to determine short-term response of SAV to increased nutrient loading. In 2012 water and sediment analysis showed amendment affects from fertilizer amendments. In 2013 only the water column was amended. Nutrient concentrations in the water column did not show significant amendment effects, likely due to changes in fertilizer formulation. Laboratory and *in-situ* mesocosm tests provided surrogate settings in which nutrient release rates were measured under a variety of conditions. Release rate constants were obtained for a range of conditions through multivariate linear regression of data from these tests. Nitrogen isotopes provided evidence of perturbation of the system in the amended plots in 2012 and 2013. SAV health corresponded with the amount of fertilizer added to the plot, indicating that fertilizer amendments successfully bracketed a range of plant responses to nutrient loading.

In a separate study, depth profiles of dissolved and solid phase phosphorus and phosphorus mineral concentrations were examined in an impounded wetland before and after being drained and again following re-flooding to explore the potential benefit of periodic drying and oxidation of sediment. Surface water, pore water, and sediment nutrients were measured in order to monitor changes resulting from the drying and re-flooding process. The efficacy of Quantitative Evaluation of Minerals by SCANning (QEMSCAN) to determine mineral content in fine-grained sediment was also explored. Changes in phosphorus speciation in surface water, pore water, and sediment were observed in response to the drying and re-flooding process. Surface water dissolved phosphorus increased by 35% and pore water dissolved phosphorus increased by 50 to 125% following re-flooding between depths of 5 and 20 cm. Available phosphorus in the top 3 cm of sediment increased by approximately 10% after re-flooding.

TABLE OF CONTENTS

LIST OF FIGURES

LIST OF TABLES

ACKNOWLEDGEMENTS

Special thanks are due to my advisor, Dr. William P. Johnson, for his expertise, patience, and generosity. I am also very thankful for the insight and direction of Dr. Heidi M. Hoven and Dr. Thure E. Cerling. This thesis reflects the expertise and generosity of more people than can be listed here. You all know who you are. Finally, I would like to publicly thank my talented, generous, and lovely wife, Julia Pierson, for filling in when no one was available to help with fieldwork and happily helping me through any and every challenge that presented itself.

1. INTRODUCTION

1.1 Great Salt Lake Wetlands

Small wetlands and ponds are increasingly recognized in the scientific community as significant contributors to developing models of global cycles. Despite the small size of individual wetlands compared to larger inland lakes, recently updated inventories show that small lakes and ponds make up over half of the areal extent of the world's inland water bodies, covering an estimated 4.2 million km^2 (Downing, 2010). The collective rate of carbon burial in impounded wetland and pond sediment is up to three orders of magnitude greater than large lakes and oceans (Downing, 2010). Additionally, this author notes that small water bodies support a higher concentration of species per area than large water bodies

The wetlands surrounding the Great Salt Lake are no exception. Over the past century the wetlands of the Great Salt Lake (GSL) have been recognized as dynamic and essential ecosystem for migratory waterfowl. An estimated 3-5 million waterfowl (Vest and Conover, 2011) and approximately 500,000 shore birds (Gorrell et al., 2005) rely on the GSL and its wetlands for food during migration each year. For several decades, research has been directed towards maximizing the GSL wetlands for waterfowl habitat and population (Bellrose and Low, 1978).

The Great Salt Lake has approximately 250,000 ha of freshwater wetlands on its

north and east shorelines. Over 50,000 ha are managed, approximately 20,000 by private owners and 32,000 ha by federal and local government (Johnson, 2008). Managing freshwater inflows and water quality of these small water bodies is crucial for maintaining waterfowl habitat (Aldrich and Paul, 2002). Anthropogenic influences on the Great Salt Lake wetlands are extensive. The Jordan River is the primary input to Farmington Bay. Well over 1 million people live in the Jordan River watershed. Salt Lake County is home to 10 Superfund sites designated under Comprehensive Environmental Response, Compensation, and Liability Act (CERCLA). Most contamination is related to high trace metal content in soil and groundwater and is attributed to historic mining and smelting operations in the Salt Lake Valley (Waddell and Giddings, 2004). Agricultural runoff has also posed problems to the wetlands with high surface water nutrient concentrations measured in impounded wetlands throughout Farmington Bay (Hoven and Miller, 2009).

2. WILLARD SPUR NUTRIENT CYCLING

2.1 Background: Willard Spur Nutrient Cycling

The Willard Spur makes up the northeast arm of Bear River Bay (Figure 1). A series of dykes form the southern boundary of the Spur, separating it from the Willard Bay Reservoir, Harold Crane Waterfowl Management Area, and Great Salt Lake Minerals, Inc. The northern boundary of the Spur is formed by a system of dykes that separate the Willard Spur from impounded wetlands of the Bear River Migratory Bird Refuge (BRMBR) to the north.

The Spur lies partially within the boundaries of the BRMBR. The refuge was established in 1928 after a disproportionate diversion of freshwater inflow from the Bear River for agriculture led to outbreaks of avian botulism (Kadlec, 2002). The areas of the Willard Spur outside the BRMBR are hunted extensively for waterfowl.

In 2010 the Utah DWQ granted a Utah pollutant discharge elimination system (UPDES) permit to the newly constructed Perry/Willard Regional Wastewater Treatment Plant (PWRWTP). The decision met significant resistance from multiple groups, including the Utah Waterfowl Association and the Utah Airboat Association. In response to a petition to the Water Quality Board from Western Resources Advocates the DWQ undertook a study to evaluate possible deleterious effects of the PWRWTP effluent on the Willard Spur. The prevalence of vegetation in the open water of the Willard Spur

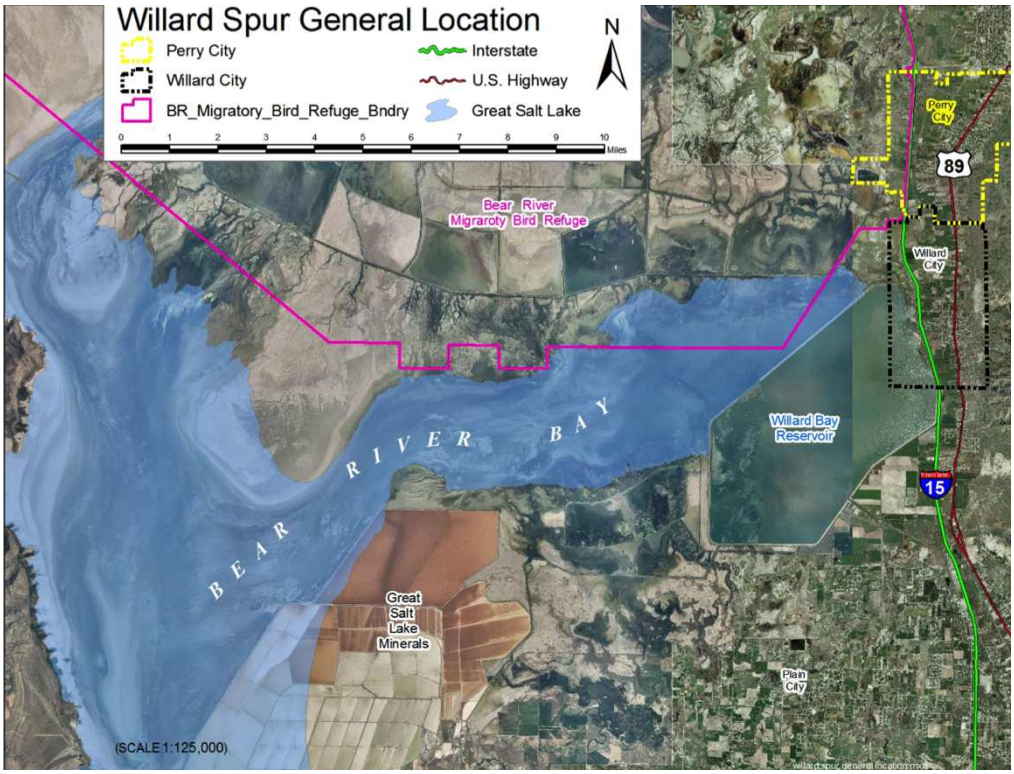

Figure 1. Map of Bear River Bay. Used with permission from utah.gov. URL: http://www.willardspur.utah.gov/images/maps/willardspurgenerallocation.jpg

highlights its capacity to support forageable plants for waterfowl and its importance to the Bear River Bay ecosystem. The false color image in Figure 2 represents vegetation in red.

The two main questions to be answered by the Willard Spur project were:

1) What are the potential impacts of the PWRWTP on the Willard Spur?
2) What will be required to provide long-term protection of Willard Spur?

The Utah DWQ put out requests for proposals to answer these and subsidiary questions associated with the Willard Spur study, including understanding the assimilative capacity of the Willard Spur and identifying sensitive biological indicators that respond to nutrient loading.

A proposal to study nutrient cycling from the research group from the University of Utah was funded by the Utah DWQ. This group includes Dr. William P. Johnson, Dr. Heidi Hoven, Dr. Ramesh Goel, Dr. Sam Rushforth, and Dr. David Richards. The primary goals of the nutrient cycling proposal were to:

1) Provide an understanding of the natural variability of biological processes and productivity related to nutrient cycling in the Willard Spur; and
2) Identify thresholds for nutrient response using biological indicators.

The research questions addressed by this proposal included:

1) How does the Willard Spur respond to nutrient loading in the water column and sediment?
2) What constitutes a negative or unacceptable response to nutrients by the SAV, macroinvertebrate community, phytoplankton, and macroalgae?
3) What threshold(s) to nutrient enrichment could be established relative to responses

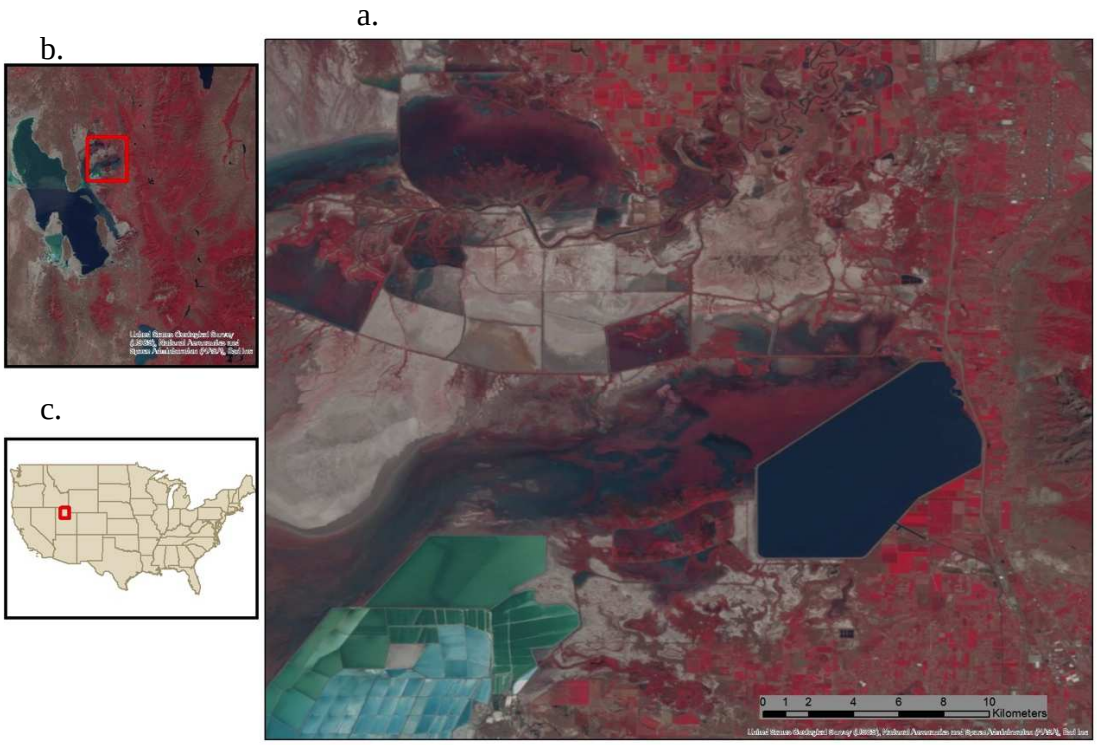

Figure 2. False color images show the proliferation of vegetation (represented in red) in the Willard Spur (a), contrasted by Willard Bay and Great Salt Lake Minerals, Inc. to the south and impounded wetlands in the BRMBR to the north. Also shown is the location of the Willard Spur relative to b) the Great Salt Lake and c) the contiguous United States.

of the biological indicator(s)?

During the spring of 2012 and 2013 the research group constructed *in-situ* plots in the Willard Spur in order to utilize wetland response metrics developed by Dr. Hoven in the presence of varying nutrient loads. The vegetation metrics are intended to assess the health of a wetland and "identify thresholds of significant change (impairment) that can be attributed to nutrients" (Hoven and Miller, 2009).

The response of the water column, sediment, and SAV to increased nutrient loading in the Willard Spur was observed from June through October in 2012 and April through July in 2013. Vegetation metrics were measured throughout the plots to characterize the response of the system under varying degrees of nutrient loading (Hoven et al., in preparation).

2.2 Methods

In April of 2012 and 2013 *in-situ* plots were constructed in a perennially submerged area of the Willard Spur. The plots were designed to mimic nutrient loading from the PWRWTP from April to October.

2.2.1 Experimental Design

Experimental design was established in March 2012 and appropriate changes were implemented in 2013.

2.2.1.1 2012 Willard Spur Nutrient Cycling Plots

The 2012 plots included sediment and water column fertilizer amendments, as described below.

2.2.1.1.1 Plot Location and Dimensions

Following acceptance of the proposal in March 2012, six *in-situ* plots were constructed in the Willard Spur perpendicular to surface water flow in April 2012. *Ex-situ* mesocosms were considered, however, it is impossible to replicate seasonal and daily temperature cycles in *ex-situ* experiments. Conditions in the Willard Spur, specifically temperature and water depth, can also vary significantly throughout the season. In dry years, the Willard Spur is cut off from the main body of the Great Salt Lake by a prominent sand bar. The location of the plots (Figure 3) was selected using satellite photos that indicated the areas of the Willard Spur more likely to remain water covered.

The plots were organized into two transects (Figure 3) with plots in each transect separated by 20 m. Three water column-amended plots (WS4, WS5, WS6) were installed 350 m upstream (northeast) of three sediment-amended plots (WS1, WS2, WS3). The amended areas of the plots were 6 m by 20 m for water column plots and 2.5 m by 20 m sediment plots was (see Appendix). The orientation, size, and spacing of the plots were intended to minimize influences from adjacent plots and ensure that all plots had similar plant communities. Galvanized steel posts were used to delineate the borders of the plots. The posts also provided a way to secure kayaks and canoes during sampling in order to avoid disturbing the plants and sediment during the study.

Figure 3. 2012 plots are shown in red and light blue and 2013 plots are shown in dark blue. Yellow circles indicate locations where PWRWTP effluent is discharged directly into the Willard Spur.

2.2.1.1.2 Amendment Ranges

The water and sediment amendments were intended to simulate ambient, mid-range, and high range nutrient loading to the Willard Spur water column and sediment. In 2012, high and low target concentrations for dissolved phosphorus (PO_4-P) in the water column were 0.4 mg/L and 0.1 mg/L, respectively. The high and low target concentrations for available phosphorus in the sediment were 200 mg/kg and 100 mg/kg, respectively. Water column and sediment target concentrations for phosphorus were established relative to phosphorus concentrations in Willard Spur surface water and sediment measured in 2011 by the Utah DWQ (Ostermiller, 2012).

2.2.1.1.3 Fertilizer Amendments

Osmocote Smart Release™ fertilizer was deployed in April 2012. Woven nylon bags were filled with 0.4 kg of fertilizer and suspended in the water column or buried in the sediment. Table 1 shows the approximate mass of fertilizer in each plot in 2012.

To amend water column nutrient concentrations, bags of Osmocote™ were suspended about 10 cm below the water surface from five ropes extending between posts 20 m across the plots. The ropes were lowered as the water level dropped throughout the summer.

To amend the sediment nutrient concentrations, bags of Osmocote™ fertilizer were pushed 10-20 cm into the sediment, which was sufficiently soft (mud) to deform and cover each bag. The mass of fertilizer placed in the sediment was calculated by estimating the volume of sediment affected by each bag of fertilizer and a bulk density for the sediment.

Table 1. Mass of nutrients in 2012 sediment and water column amendments.

	kg/plot			
	P	**NO_3 -N**	**NH_4-N**	**Urea-N**
2012 High Sediment	9.6	16.0	14.4	0.0
2012 Low Sediment	4.8	8.0	7.2	0.0
2012 High	8.0	13.4	12.1	0.0
2012 Low	2.0	3.4	3.1	0.0

2.2.1.1.4 Sample Schedule

Following site set up and monitoring, regular sample events were conducted monthly between June and October. The Appendix contains tables describing the samples collected for water and sediment chemistry, nutrient flux, and biota in more detail. Biweekly monitoring of dissolved nutrients occurred between monthly sample events in 2012.

2.2.1.2 2013 Willard Spur Nutrient Cycling Plots

The 2013 experimental design only included fertilizer amendments in the water column. In addition, improvements from the 2012 design were worked into the experimental design in order to avoid complications encountered during the 2012 field season.

2.2.1.2.1 Plot Location and Dimensions

Several changes to the experimental design were implemented for the 2013 experiment. Nutrient amendments in 2013 only targeted the water column in order to reflect the waterborne loads from the PWRWTP. Amendment plots included three water column amendments and one control. Four 6 m x 20 m water amendment plots were constructed in April 2013, about 70 m northeast of the 2012 water amendment plots.

Just as in 2012, satellite photos were used to orient the 2013 plots with their widest dimension perpendicular to the direction of surface water flow and in a location perennially submerged. One transect was formed by the high, medium, and low water column plots (Figure 3: WS7, WS8, WS9). These three plots were separated by 20 m,

just as in 2012. The control plot was located about 90 m upstream (northeast) of the amended plots. In addition to the control plot, ambient sediment and water column samples were collected outside of the constructed plots. For the ambient site, a single post (identical to the posts used to delineate the borders of the four plots) was placed 30 m northwest of the control plot, forming a second transect (Figure 3: WS10, WS11). This post provided an attachment for kayaks and canoes during sampling.

2.2.1.2.2 Amendment Ranges

A larger range of water column amendments was possible in 2013 with the elimination of sediment plots from the experimental design. Three levels of nutrient loading in the water column were planned for the 2013 plots. In 2012, plant response to nutrient loading was observed for high and low water column plots, though differences in nutrient concentrations between plots was minimal and well below the target concentrations (See results in Section 2.3**)**. Therefore three water column amendments were constructed in 2013 to assess plant response in a larger range of nutrient loads.

The high water column plot had approximately the same amount fertilizer in 2012 and 2013. Likewise, the amount of fertilizer in the 2013 medium water column plot was similar to the low water column amendment in 2012. The low water column plot in 2013 contained half the fertilizer of the 2012 low and 2013 medium water column amendments in order to further bracket the range of nutrient loads potentially driving impairment of plant health.

2.2.1.2.3 Fertilizer Amendments

The type of fertilizer used in 2013 was different from 2012 in order to promote dissolution during the relatively cold water period of April and May, which ranged between 40 °F and 55 °F in 2012. Based on PO_4-P and NO_3-N data from 2012 amendment plots, the Osmocote Smart Release™ fertilizer did not release significant amounts of nutrients until June, which may be expected since the polymer coating is designed to release nutrients above 60 °F.

In order to promote dissolution of nutrients into the water column during both colder and warmer temperatures, a different mixture of fertilizers was used in the 2013 amendment. Table 2 shows the mass of nutrients added to the water column amendments in 2013. The mixture was made up of approximately 60% Osmocote™ (the same fertilizer used in 2012), approximately 37% coated urea, and about 3% soluble urea. The urea fertilizers were designed to provide nutrient release during the cool water temperatures expected during the first 90 days of the experiment.

A different method for deploying bags of fertilizer was used in 2013 in order to remove artifacts from the fertilizer deployment in the water column in 2012. The 2012 experiment was complicated by the ropes and posts used to construct the plots. The floating ropes used to suspend the bags of fertilizer in the water column trapped drifting SAV debris. This debris consisted of plants uprooted during wind events and grazing as well as branches and leaves that are released naturally throughout the growing season. The debris formed mats above the plots with a thickness of up to 35 cm, at which point the mat became dense enough to sink and collapse onto the SAV below (Figures 4a). This debris was removed from the plot weekly until a fence was constructed around the plots

Table 2. Mass of nutrients in 2013 water column amendments.

	kg/plot			
	P	**NO_3-N**	**NH_4-N**	**Urea-N**
2013 High	5.6	9.3	10.2	23.4
2013 Medium	1.3	2.2	2.4	5.5
2013 Low	0.7	1.1	1.2	2.8

to exclude additional debris from entering the plot areas.

In 2013, rather than suspending fertilizer bags in the water column from ropes strung across the plots, wooden stakes were embedded in the sediment (Figure 4b). Between 1 and 4 bags of fertilizer were attached to the top of each stake about 10 cm to 25 cm above the surface of the sediment. The lines of stakes followed the same pattern as the ropes, five lines extending 20 m across the plots. The number of stakes on each line varied between 9 and 19, depending on the mass of fertilizer placed in the plot. The Appendix shows the 2013 experimental design. Half of the control plot reflected the pattern of the stakes in the low and medium treatment plots while the other half reflected the pattern of stakes in the high treatment plot.

2.2.1.2.4 Sample Schedule

The timing of intensive sampling events in 2013 was scheduled for the early months of high growth observed between April and July of 2012. Capturing the conditions leading up to plant senescence observed during late May and June of 2012 was a primary objective for the 2013 sampling season. Plots were installed in early April 2013 and sampling began in mid-April. Between mid-April and the end of July water samples were collected every two weeks and sediment samples were collected every month. Sampling ended in late July after plant senescence was observed in May and June and water levels had dropped, making canoe access to the sites impossible. Additional squeezer core sediment samples described in Section 2.1.3 were collected in 2013 to supplement the information from homogenized sediment samples collected in 2012.

a. b.

Figure 4. Amendment techniques for a) 2012: Plant debris collecting on ropes within the plots. The darker areas show where the mat was sufficiently dense enough to collapse onto the plants below. b) 2013: Underwater photo of submerged fertilizer bags attached to a stake and embedded in the sediment.

2.2.2 Field Methods

Surface water and sediment samples were collected by canoe, transported on ice, and stored in the refrigerator or freezer until analysis. Unfiltered samples for carbonaceous BOD, general chemistry, and nutrients were collected in plastic bottles supplied by the Utah State Health Laboratory. Filtered and unfiltered samples for nutrient analysis were preserved with 0.5% H_2SO_4. Filtered trace metal samples were collected in acid-leached LDPE bottles and acidified using 2.4% trace metal grade HNO_3.

For most sample events in 2012 and 2013, three samples were collected per plot. More detail describing the number of samples during each sample event collected and the specific analyses run is found in the Appendix. Filtered samples were collected using a GeoTech ™ peristaltic pump. Teflon™ tubing was submerged into the middle of the water column. Water was forced through the high-capacity capsule filters (0.45 µm GeoTech Dispose-a-filter ™). Both the tubing and capsule filters were rinsed with 10% HCl prior to use in the field. At least two volumes of water were flushed through Teflon™ tubing and filter system between sample sites within a plot. The Teflon™ tubing was rinsed between plots with 10% HCl and flushed with sample water and a new filter was used for each plot.

Field parameters were measured using YSI Professional Plus multimeter probe. Temperature, dissolved oxygen (DO), pH, and conductivity were collected for each plot. Prior to each sample event the probe was calibrated for conductivity and pH using commercial standards (GeoTech). DO was calibrated using a one-point calibration method in water-saturated air.

Sediment samples were collected using a 1-inch copper pipe in three to four

random areas throughout the plots. The top 10 cm of the sediment was retained and 8-10 samples per plot were homogenized in a plastic bag. In 2013 squeezer core samples were collected in 2-inch plastic core and kept on ice until squeezed on shore. The squeezer core is outfitted with threaded holes to allow for extraction of pore water from the sediment. Porex™ rods were inserted into the sediment core and attached to syringe filters (Whatman 0.45 μm PES) and syringes (Figure 5). Pistons compressed the core from both sides, forcing pore water into the syringes (method modified from Carling et al., 2013).

2.2.3 Laboratory Methods

Samples were processed according to standard operating procedures developed by laboratories at the University of Utah, Utah State University, and the Utah State Health Laboratory, as described below.

2.2.3.1 Surface Water Methods

The laboratories and associated methods for each parameter are provided in the Appendix. Quantification limits were established for each sample batch run following regular sample events. The highest value of trip blank, field blank, method blanks, or established limits of detection for the instrument were used to set the quantification limit for sample runs. For all samples analyzed in the Johnson Lab at the University of Utah method blanks were run every ten samples and matrix spikes for every batch. Nutrient concentrations below the quantification limit were set at one-half the quantification limit for statistical analyses.

Figure 5. Sediment squeezer apparatus with attached syringe filters and syringes.

Trace element extractions were performed by digesting sediment subsample in 20 ml of 5% (v/v) trace metal grade HCl for three days at room temperature, followed by centrifugation and analysis of supernatant as a water sample. A quadrupole inductively coupled plasma mass spectrometer (ICP-MS) with a collision cell was used to measure trace elements in surface water samples and sediment sample supernatant. A list of elements analyzed is provided in the Appendix.

Most samples submitted to the Utah State Health Laboratory were analyzed within 30 days of collection, except for carbonaceous BOD samples that were analyzed within two days. Major anion concentrations were measured within 72 hours of sampling using ion chromatography. Mercury samples were analyzed within three months of sampling.

2.2.3.2 Sediment Methods

Sediment samples were sub-sectioned for analysis at the Johnson Lab, Utah State University Analytical Laboratory (USUAL), and the Stable Isotope Ratio Facility for Environmental Research (SIRFER). Samples for the USUAL lab were refrigerated and submitted within 3 days of collection. USUAL provided analysis for ammonia-N and nitrate-N (from 2N KCl extract) and available phosphorus using the Olsen $NaHCO_3$ method (Poulton et al., 2012). All sediment nutrient concentrations were above the analytical detection limit provided by the Utah State University Analytical Laboratory.

Sediment samples prepared for C/N analysis at SIRFER were dried overnight in an oven at 100 °C within 5 days of collection. Dried samples were crushed using a Retsch ball mill. Samples for organic carbon and nitrogen analysis were prepared by treating

crushed and dried sediment with 0.5 N HCl until the pH of the mixture dropped below 5. The leftover sediment was rinsed with DI water and dried using a vacuum Buchner funnel and dried in an oven at 70°C. The SIRFER lab analyzed carbon and nitrogen isotopes using a Delta Plus isotope ratio mass spectrometer (Finnigan-MAT, Bremen Germany) interfaced with an Elemental Analyzer (model 1110, Carla Erba, Milan, Italy). Instrument precision for $\delta^{13}C$ and $\delta^{15}N$ is ± 0.15 ‰ and ± 0.2 ‰, respectively. Carbon and nitrogen isotope data met all quality assurance-quality control standards established by the SIRFER lab.

2.2.4 Release Rate Experiments

Osmocote™ has been used with favorable results in other large-scale nutrient enrichment studies (Baggett et al., 2010; Furman and Heck, 2008; Heck et al., 2000) where nutrient release rates were measured in the laboratory and field. For this study, tests were conducted in laboratory and *in-situ* settings to better understand dissolution characteristics of the fertilizers used in 2012 and 2013. Multiple conditions were tested in order to expand on previous experiments described in the literature and increase the range of known release rates for different conditions.

2.2.4.1 Bucket Release Rate Tests

The bucket scale release rate test analyzed Osmocote™ dissolution in a relatively closed system in a laboratory setting. New and used bags containing approximately 0.4 kg of Osmocote™ were placed in three gallons of water in five-gallon plastic buckets open to the atmosphere. Samples were collected over the course of four weeks and

filtered using 0.45 µm syringe filters. Because the release of nutrients from Osmocote™ is temperature dependent, tests were conducted at two temperatures that bracketed the expected temperatures in the field. During the first two weeks of the experiment, the buckets were kept indoors at temperatures near 60 °F. During the second two weeks, buckets were kept outdoors with daily high temperatures ranging between 70 and 85 °F.

2.2.4.2 Mesocosm Release Rate Tests

The mesocosm scale release rate experiments analyzed dissolution rates in the field from bags of Osmocote™ used in 2012 and from bags of the mixture of fertilizers used in 2013. Two mesocosms designed by the Utah Division of Water Quality were installed in the Turpin (GSLI-013) impounded wetland in Farmington Bay. Turpin was chosen for the location of the experiment as Willard Spur water levels dropped below 2 inches in August 2013. Rapid changes in the water levels were unlikely as the Utah Division of Wildlife Resources controls water levels in impounded wetlands in the Farmington Bay Waterfowl Management Area.

The source of water to Turpin Unit is the Jordan River. The Jordan River flows through industrial areas in the Salt Lake Valley and is heavily influenced by anthropogenic contaminants (Naftz et al., 2008). Background concentrations of dissolved phosphorus (0.75 mg/L) are more than one order of magnitude greater than those of the Willard Spur (0.035 mg/L).

The walls of the mesocosms were made of Lexan™ plastic and were pressed down into the sediment in order to avoid large amounts of flow in or out of the mesocosm. The mesocosms were not completely watertight, however, since a small gap

in the mesocosm wall allowed the water levels inside to slowly equilibrate with water levels outside the mesocosm. This flux was not expected to lead to significant loss of nutrients during the experiment since flow was into the mesocosm. This is based on the observation that levels inside the enclosure gradually increased from 0.50 m to 0.54 m over the course of the experiment in response to the same increase outside the mesocosm.

Four bags containing 0.4 kg of fertilizer were attached to a wooden stake and placed in the center of each mesocosm. This deployment system was identical to the fertilizer deployment method in the 2013 high water column test plot. Bags of Osmocote™ fertilizer, identical to those used in 2012, were placed in the center of one mesocosm and the 2013 mixture of fertilizers was placed in the other.

Filtered and unfiltered samples for nutrient analysis were collected periodically over 12 days. A GeoTech ™ peristaltic pump was used to collect composite samples. Teflon™ tubing was submerged into the middle of the water column and moved in a uniform pattern throughout each mesocosm in order to collect a representative sample. The same method was used for filtered samples with the addition of forcing the water through high-capacity capsule filters (0.45 μm GeoTech Dispose-a-filter ™). At least two volumes of water were flushed through the system between sample sites. Dissolved nutrients were measured in the Johnson Lab using ion chromatography. Total and dissolved nutrient samples were sent to the Utah State Health Laboratory for analysis.

2.3 Results

There are three sections of results: 2012 field results, 2013 field results, and subsidiary laboratory and field results designed to quantify nutrient release rates from the

fertilizer amendments in the field.

2.3.1 2012 Field Results

2012 field results include concentration measurements from two phases, surface water and sediment, as described below.

2.3.1.1 2012 Surface Water

Trace elements were measured to confirm concentrations in the six test plots were equivalent, and therefore not driving any observed differences between the plots, as described below. In addition, nutrient concentrations were monitored to determine whether target concentrations were reached.

2.3.2.1.1 Trace Elements

Water column trace element concentrations were similar between treatments and most likely were not responsible for any differences in observed biological responses among the test plots. This is shown by the equivalence of filtered trace element surface water concentrations in both water-amendment and sediment-amendment test plots (Appendix). The samples were collected six weeks following deployment of Osmocote™ in 2012; hence, deployment of Osmocote™ did not significantly alter trace element concentrations among the plots.

2.3.2.1.2 Nutrients

The highest surface water phosphate concentrations corresponded with the warmest months in terms of surface water temperatures; i.e., September and October were 7-12 °C cooler than August. Notably, the highest dissolved phosphorus concentrations were measured in the high water column plot for each sample event (Figure 6b and 7b). The surface water concentrations for dissolved phosphate were far below the target concentrations of the high and low water column amendments, 0.4 mg/L and 0.1 mg/L, respectively.

As was observed for phosphate, increased NO_2-N + NO_3-N concentrations corresponded with the warmest months. Again, the highest NO_2-N + NO_3-N concentrations occurred in the high water column plot for each sample event (Figures 6a and 7a), as was observed for dissolved phosphorus. In contrast to phosphate, a surface water target concentration for nitrate was not established. Additional surface water nutrient concentrations were measured and are available in the Appendix.

2.3.1.2 2012 Sediment

In 2012, several constituents were analyzed. Trace elements were measured to confirm concentrations in the six test plots were equivalent, and therefore not driving any observed differences between the plots, as described below. In addition, nutrient concentrations were monitored to determine whether target concentrations were reached. Carbon and nitrogen content and stable isotopes were measured in order to further examine potential propagation of nutrients into the sediment.

a.

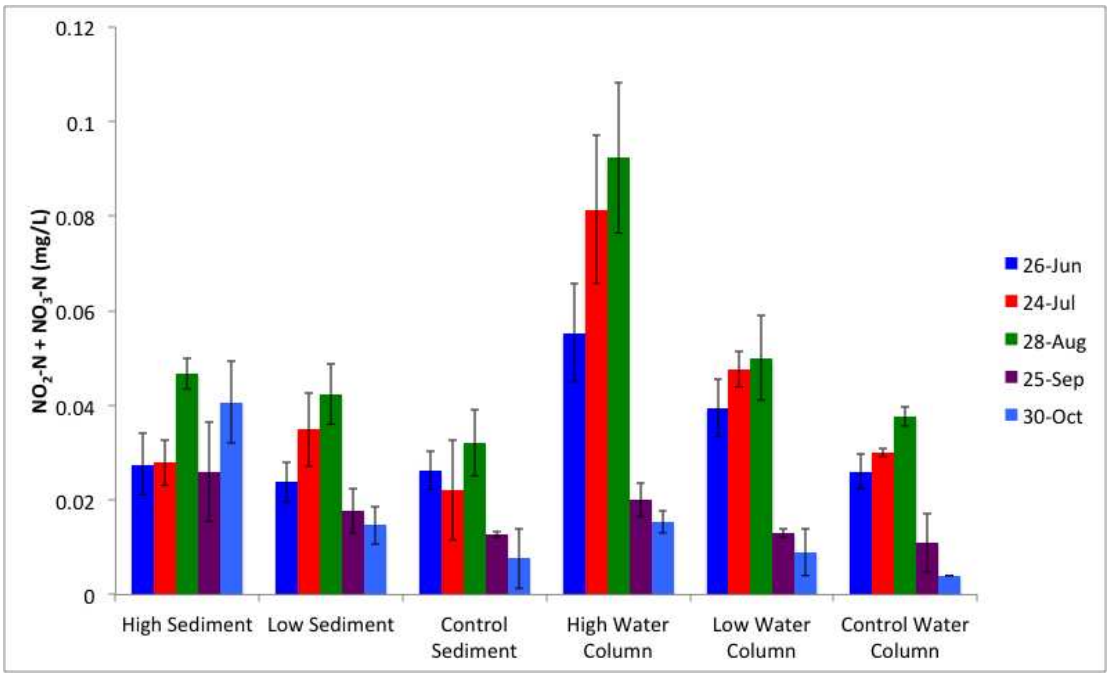

b.

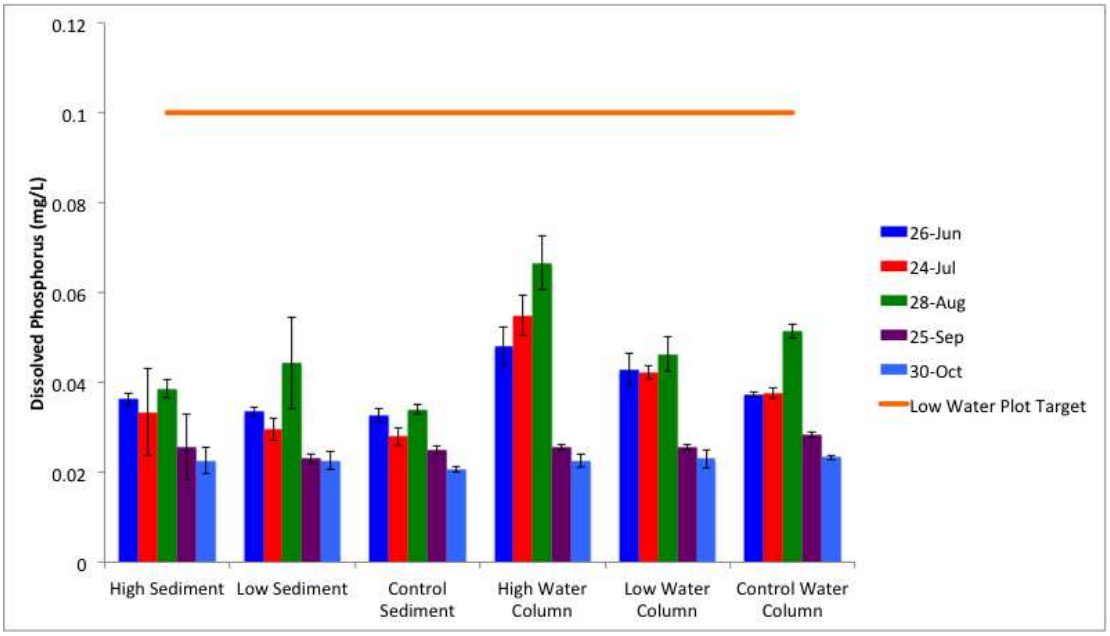

Figure 6. Dissolved surface water concentrations for a) NO_2-N + NO_3-N correspond with b) dissolved phosphate concentrations showing elevated levels in the high water column plot. Error bars represent one standard deviation (n=3 except for June samples where n=4, excluding June Control Water Column where n=3). All bars in bar plots that show concentrations in plots through time are arranged chronologically from left to right (e.g., bars in Figure 12 in the High Sediment plot represent 26-Jun, 24-Jul, 28-Aug, 25-Sep, and 30-Oct from left to right).

a.

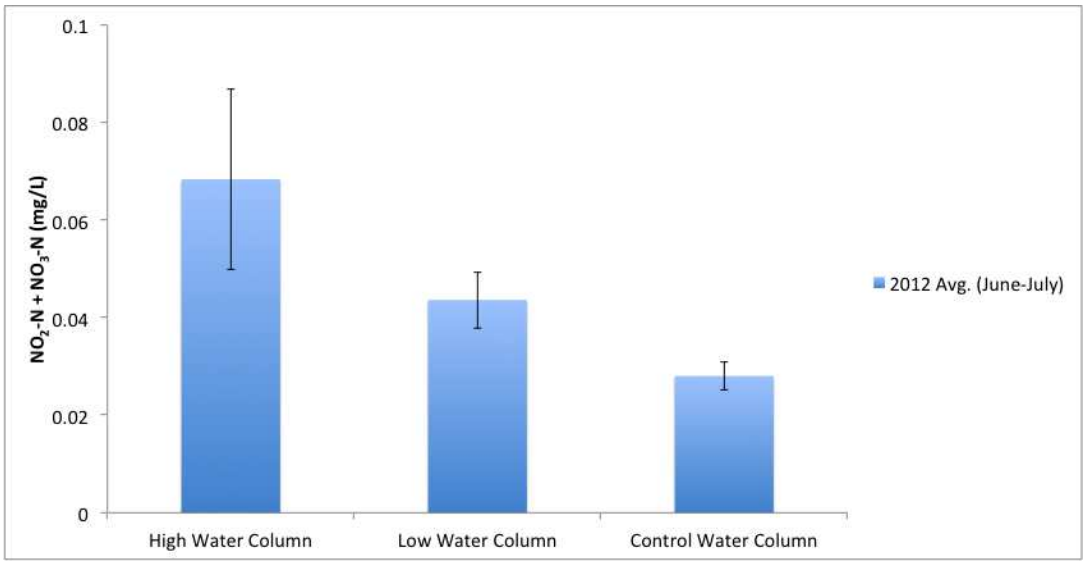

b.

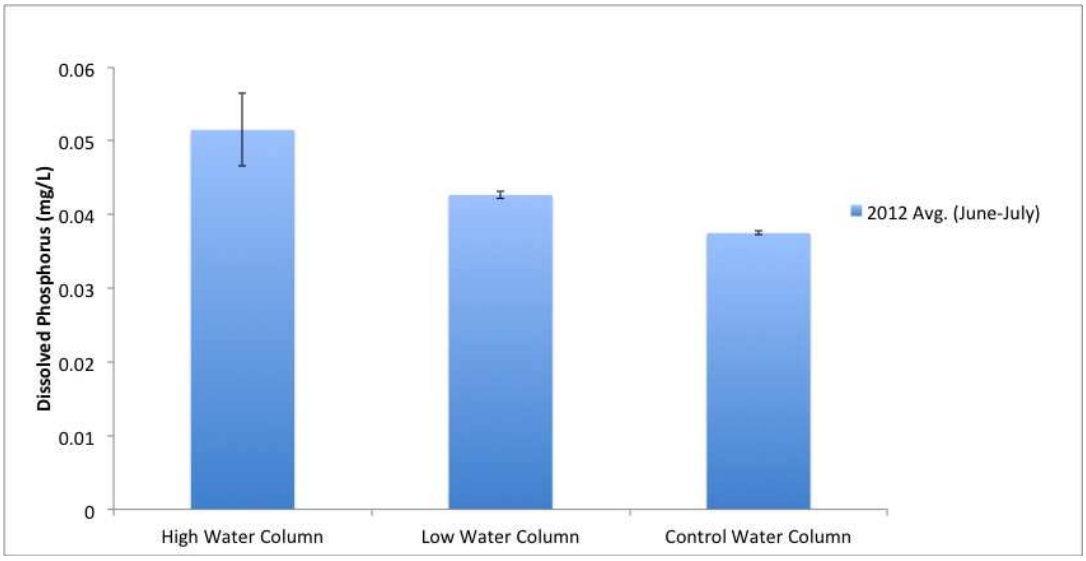

Figure 7. Significant variation between amendments and controls was observed in 2012 for a) dissolved NO_2-N+NO_3-N and b) dissolved P averages from June and July. Error bars represent one standard deviation (n=12 for all locations except for Ambient where n=4).

2.3.1.2.1 Trace Elements

Sediment trace elements (see Appendix) did not likely drive differences in biological responses between plots. Sediment samples for trace element were collected six weeks after the Osmocote was deployed therefore the Osmocote did not significantly alter sediment trace element concentrations.

2.3.1.2.2 Nutrients

Sediment phosphorus concentrations in the high sediment plot were significantly higher than low sediment plots. Yearly averages for phosphorus concentrations in sediment-amended plots (Figure 8b) were approximately half of the target concentrations for the high and low amendments, 200 mg/kg and 100 mg/kg, respectively.

Sediment nitrate concentrations were elevated in high and low sediment-amended plots (Figure 8a). Temporal variability observed in sediment nitrate and phosphorus concentrations (Figure 8) may be attributed to the size of the sediment cores collected and collecting cores in discreet locations. Nutrient concentrations in the sediment collected in the core were dependent on proximity of sediment cores to bags of Osmocote and the rate of propagation of nutrients into the sediment. C:N ratios and % N also indicated increased nitrogen in the sediment in sediment amended plots. This information is available in the Appendix.

2.3.1.2.3 C/N Isotopes

Nitrogen isotope data for sediment and plant leaves show isotope effects in sediment amendments. Sediment $\delta^{15}N$ values were enriched in the high and low sediment

a.

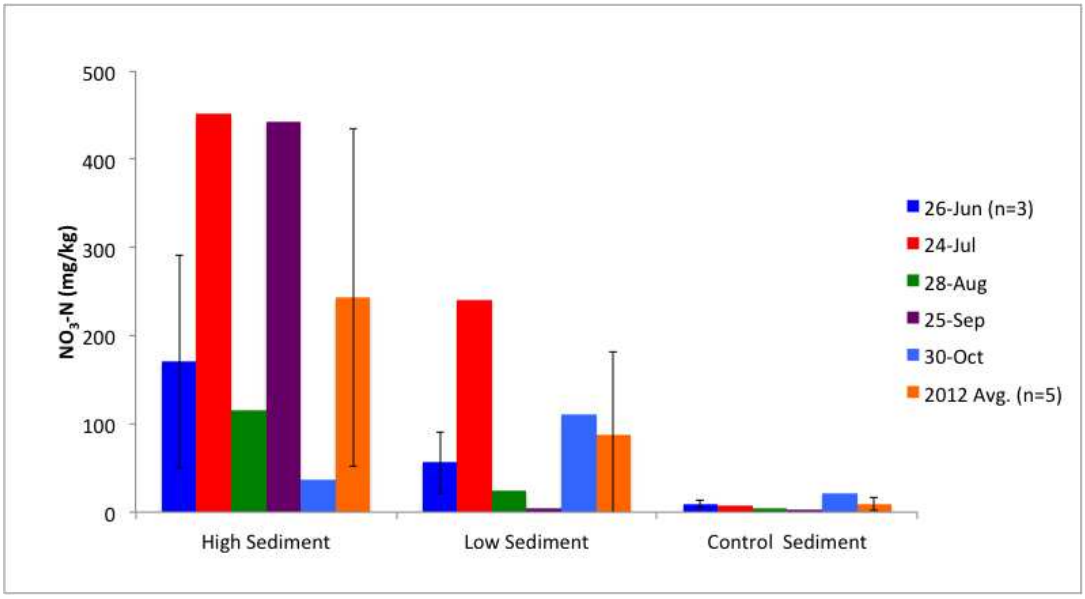

b.

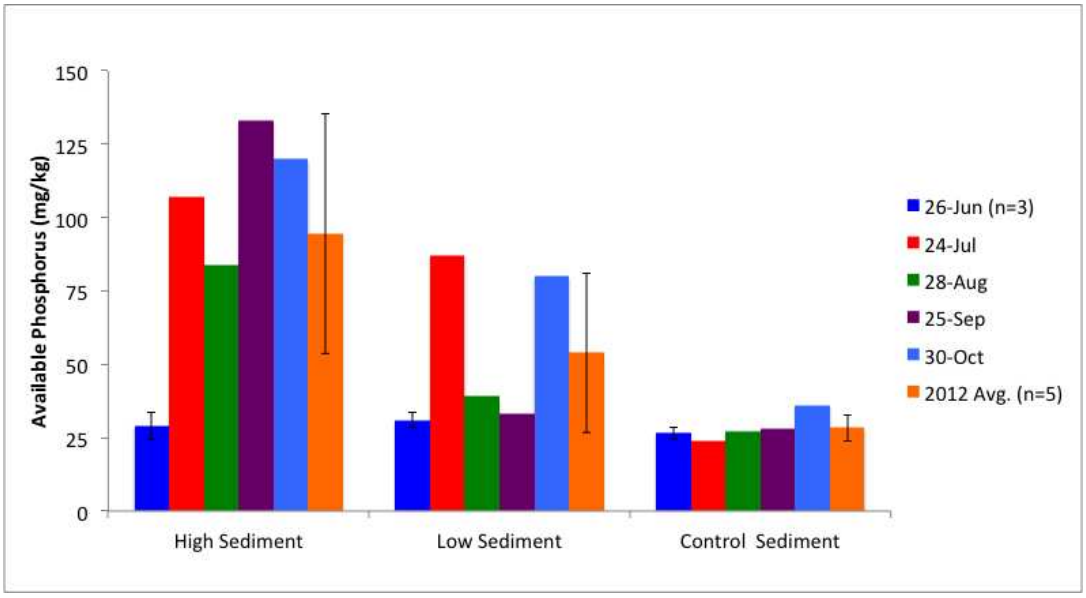

Figure 8. Elevated concentrations are observed in sediment-amended plots of a) nitrate and b) available phosphorus and nitrate. Error bars for June results represent one standard deviation (n=3).

plots relative to the water column amendments and the sediment control plot (Figure 9).

Isotope differences (Δ) shown in Figure 10 represent the deviation of nitrogen isotope values for sediment and SAV leaves in amended sediment plots relative to the control sediment plot. The high sediment plot had $\Delta^{15}N_{amendment-control}$ averaging approximately 1.5‰ in the sediment and -1.5‰ in SAV leaves.

2.3.3 2013 Results

2013 field results also include concentration measurements from two phases, surface water and sediment, though only the water column was amended with fertilizer.

2.3.3.1 2013 Surface Water

In 2013 average concentrations of dissolved NO_2-N + NO_3-N for all sample dates were approximately equal among all plots, regardless of amendment (Figure 11.a). The same was true for dissolved phosphorus (Figure 11.b). NO_2-N + NO_3-N concentrations are greatest in the high water column amendment for only two of eight sample events in 2013. There are no sample events where the highest dissolved phosphorus concentration was measured in the high water column amendment. Dissolved NO_2-N + NO_3-N and dissolved P averages during the warmer months, June and July 2013 (Figures 12.a and 12.b), do not show significant amendment effects that were observed during the same months in 2012 (Figure 7.a and 7.b). Additional nutrient concentrations were measured and results are available in the Appendix.

Equivalent concentrations were observed among all amendments and control and ambient plots. This indicates that dissolution of nutrients into the water column was

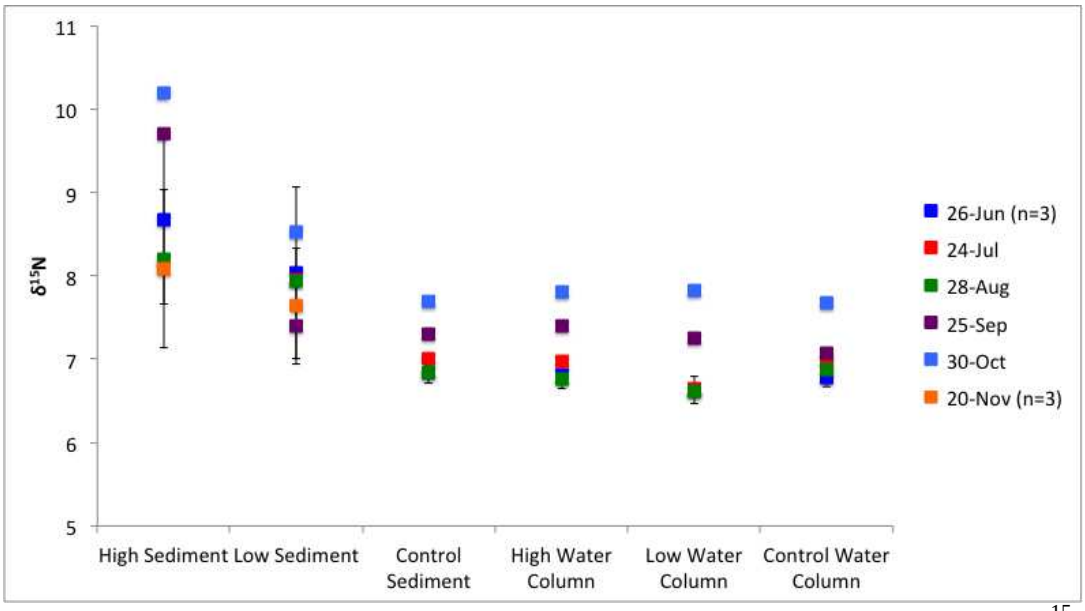

Figure 9. Isotope ratio mass spectrometry (IRMS) sediment results show enriched $\delta^{15}N$ values in the amended sediment plots. Error bars for June and November results represent one standard deviation (n=3).

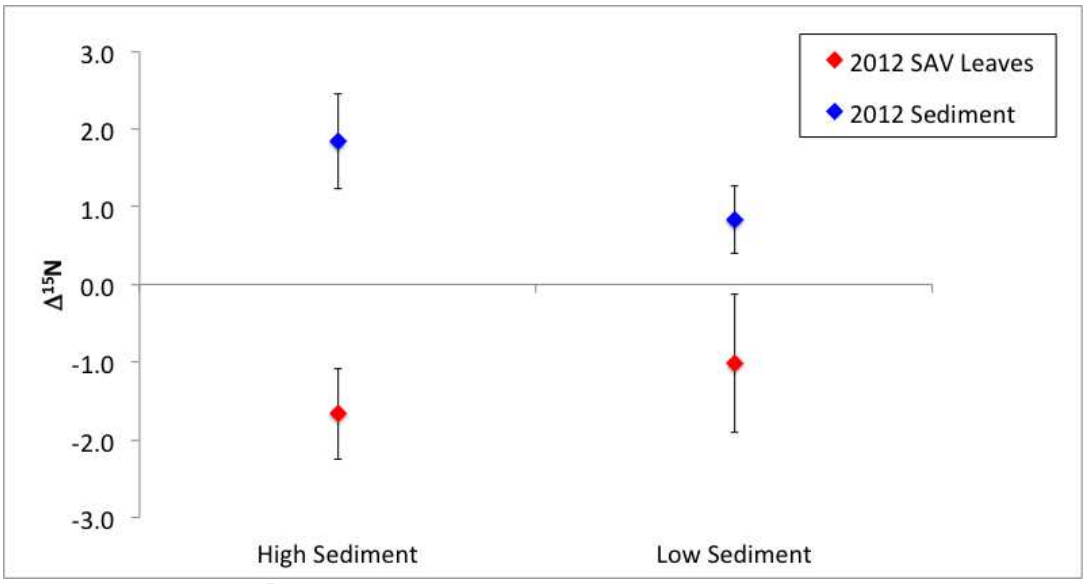

Figure 10. Average $\Delta^{15}N$ values indicate fractionation in the sediment amendment plots. For each month, $\delta^{15}N$ values from control plots were subtracted from $\delta^{15}N$ values from amendments (n=3 for SAV leaves and n=7 for sediment). SAV leaves data source Hoven et al., 2013.

a.

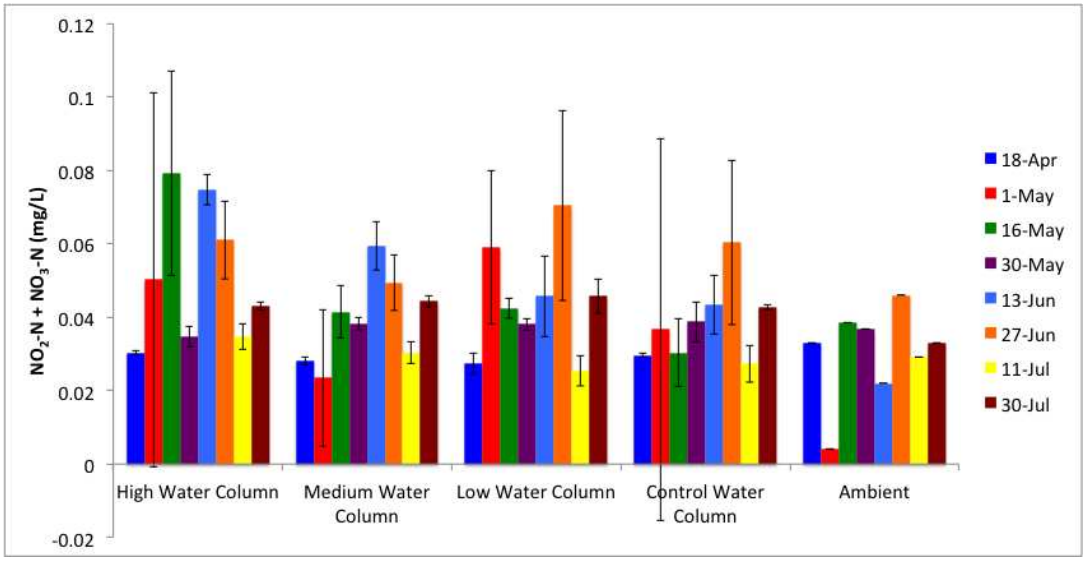

b.

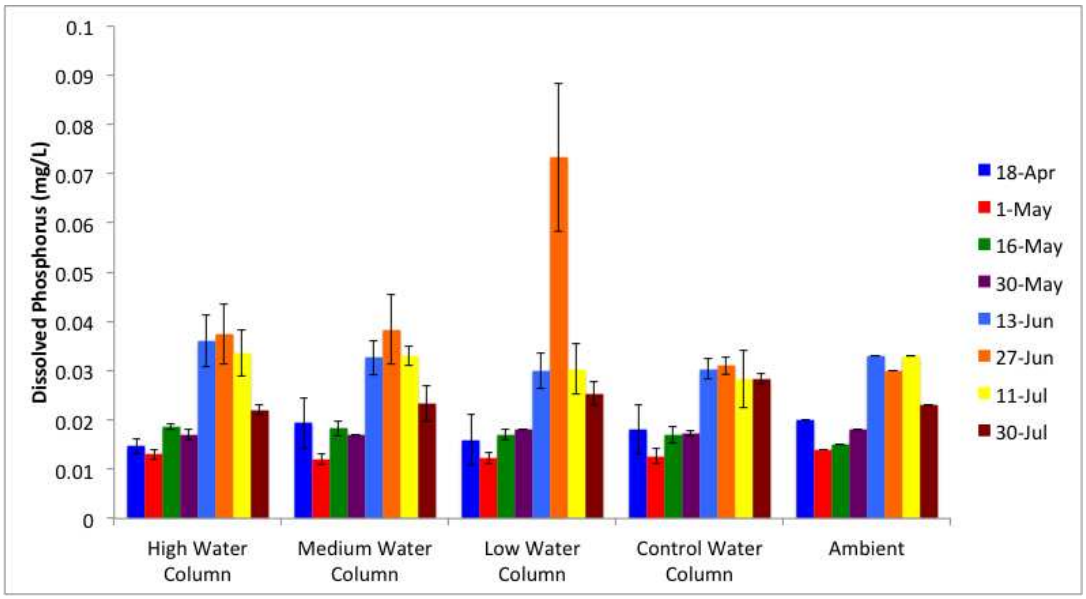

Figure 11. 2013 surface water concentrations for dissolved a) NO_2-N + NO_3-N and b) dissolved P do not show a clear trend between amendment and control plots.

a.

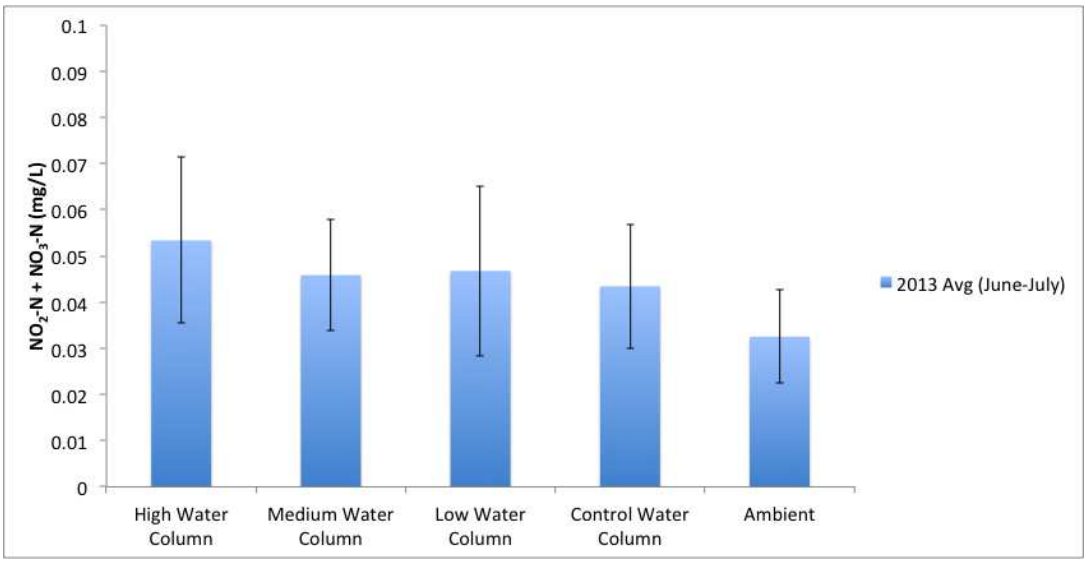

b.

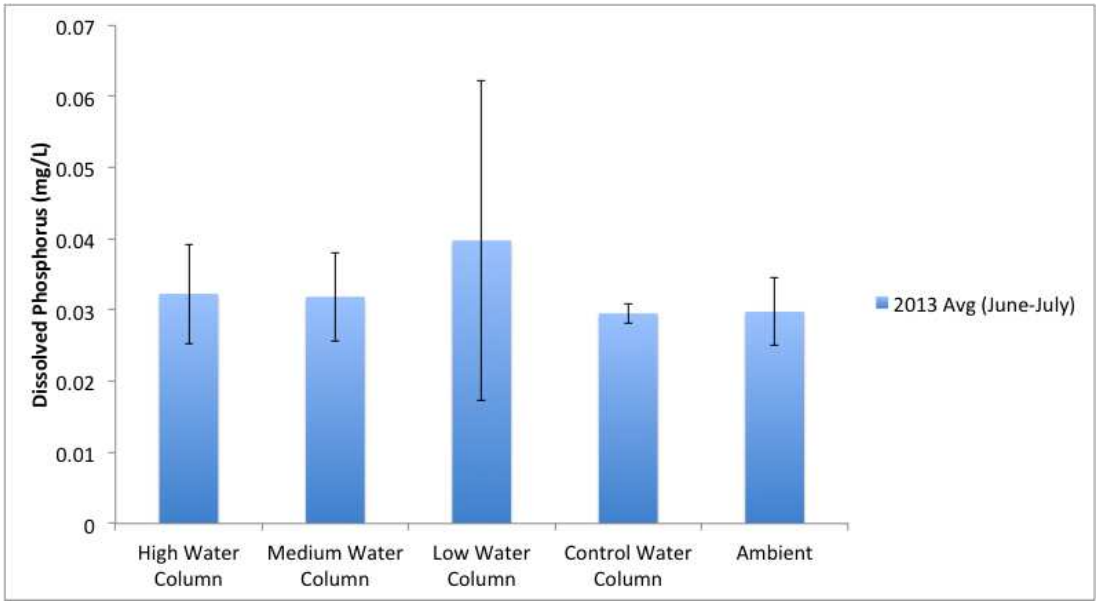

Figure 12. Significant variation between amendments and controls was not observed in 2013 for a) dissolved NO_2-N+NO_3-N and b) dissolved P averages from June and July. Error bars represent one standard deviation (n=12 for all locations except for Ambient where n=4).

approximately balanced by dilution and loss of nutrients from the water column (e.g., nutrient removal by biota, precipitant settling, etc.).

2.3.3.2 2013 Sediment

Because the sediment was not amended in 2013, sediment phosphorus and nitrate were equivalent between plots. Sediment nutrient measurements from 2013 are available in the Appendix. Likewise, $\delta^{15}N$ values did not vary between plots (Figure 13).

Additional sediment cores were collected in 2013 in order to characterize variation of nitrogen isotopes with depth (Figure 14). Squeezer cores were used to remove sediment pore water and then extrude sediment in 2 cm sections. These sections represented horizons within the sediment from 0-12 cm.

The average of $\delta^{15}N$ values observed from the squeezer cores was similar to $\delta^{15}N$ values of homogenized samples, approximately 7‰. However the top horizon from the high water column amendment collected in June has a $\delta^{15}N$ value near 5.5‰, the lowest value measured in Willard Spur sediment in 2012 and 2013.

2.3.3 Quantifying Nutrient Release Rates to Water Column

In order to estimate the nutrient release rates from the fertilizer amendments into the water column in amended plots, two types of release rate experiments were performed: small volume bucket tests which were portable to allow temperature control, and mesocosm tests involving much larger volumes in the field as well as biological response to nutrient addition.

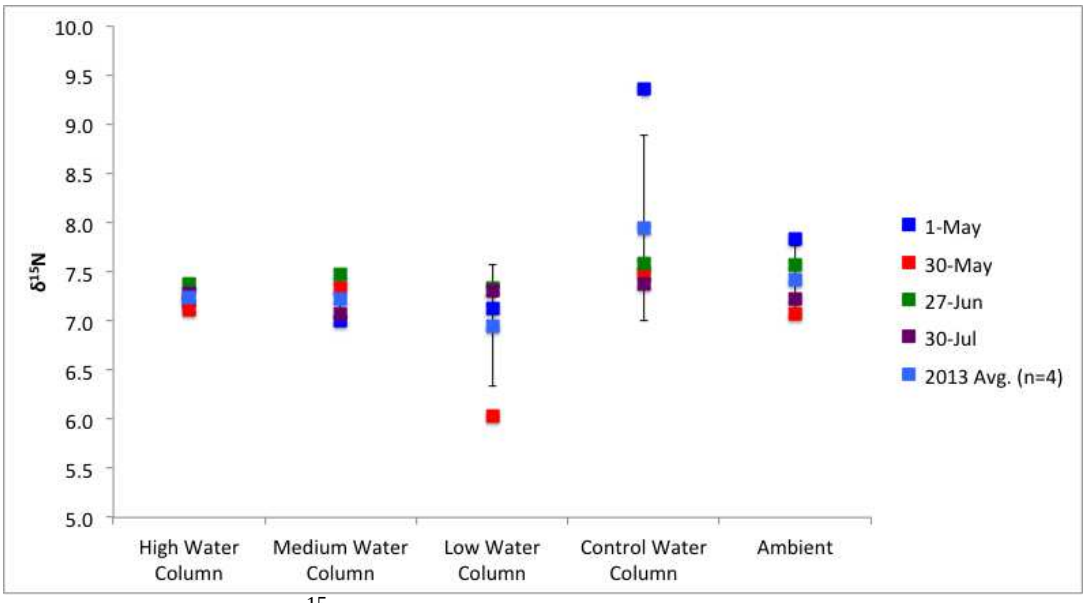

Figure 13. In 2013 total $\delta^{15}N$ values were similar between amended and control plots.

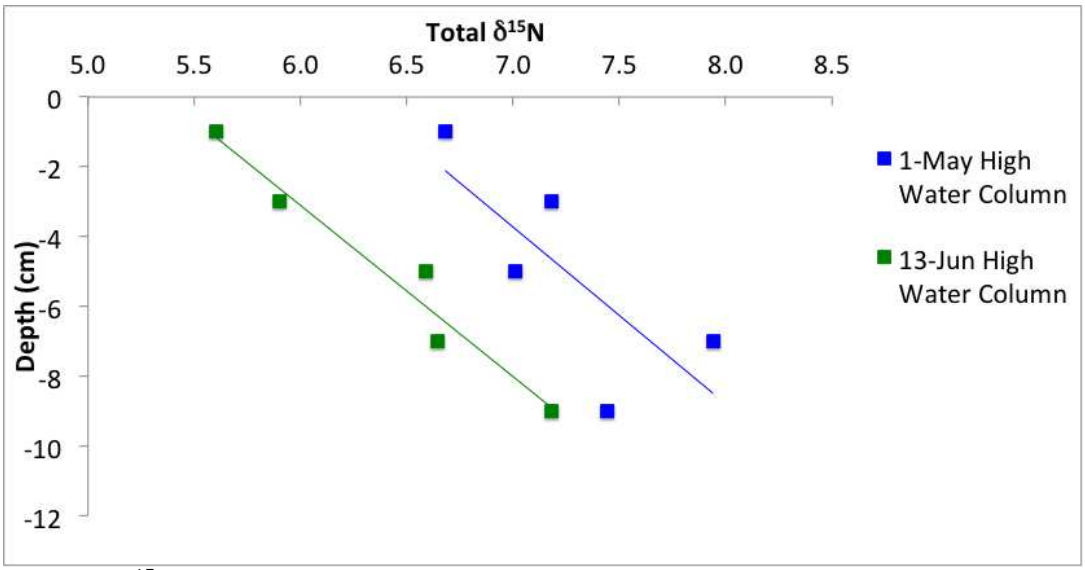

Figure 14. $\delta^{15}N$ values from 2013 high water column plots in sediment horizons between 0 and 10 cm.

2.3.3.1 Bucket Test Results

The release rates for NO_3-N and PO_4-P were calculated using measured concentrations from the indoor and outdoor tests (Figure 15). Throughout the bucket test it was clear that the results were not significantly affected by potential depletion of the nutrient source or saturation limits of the solution, based on the fact that the release of nutrients was linear (Figure 15). This was true even for the fertilizer that had been in the field for approximately 3.5 months prior to the experiment. However, the "initial burst" at warmer temperatures that was observed in other studies (Heck et al., 2000) was not observed for bags that had previously been used in the field.

The bucket tests indicate a significant difference in release rates of nutrients between temperatures near 60 °F and temperatures near 80 °F. Figure 15 shows nutrient release rates for NO_3-N and PO_4-P from bucket tests. New bags released NO_3-N into the water at a rate of about 0.101 g/day in cool temperatures and 0.980 g/day in warm temperatures. Likewise for PO_4-P, changes in concentration increased from 0.00530 g/day in cool temperatures to 0.0855 g/day in warm temperatures. Bags of Osmocote™ that were deployed in the field for 3.5 months and then used in buckets released NO_3-N and PO_4-P at 10% and 15%, respectively, of the rate of new bags at warmer temperatures.

2.3.3.2 Mesocosm Test Results

Dissolved oxygen measurements in both mesocosms (Figure 16) indicated an increase in biological activity due to the nutrient amendments. The Osmocote™ mesocosm experiment (Figure 16a) shows a significant shift in DO in the system earlier than the 2013 fertilizer mixture. This DO shift is likely caused by eutrophication where

a.

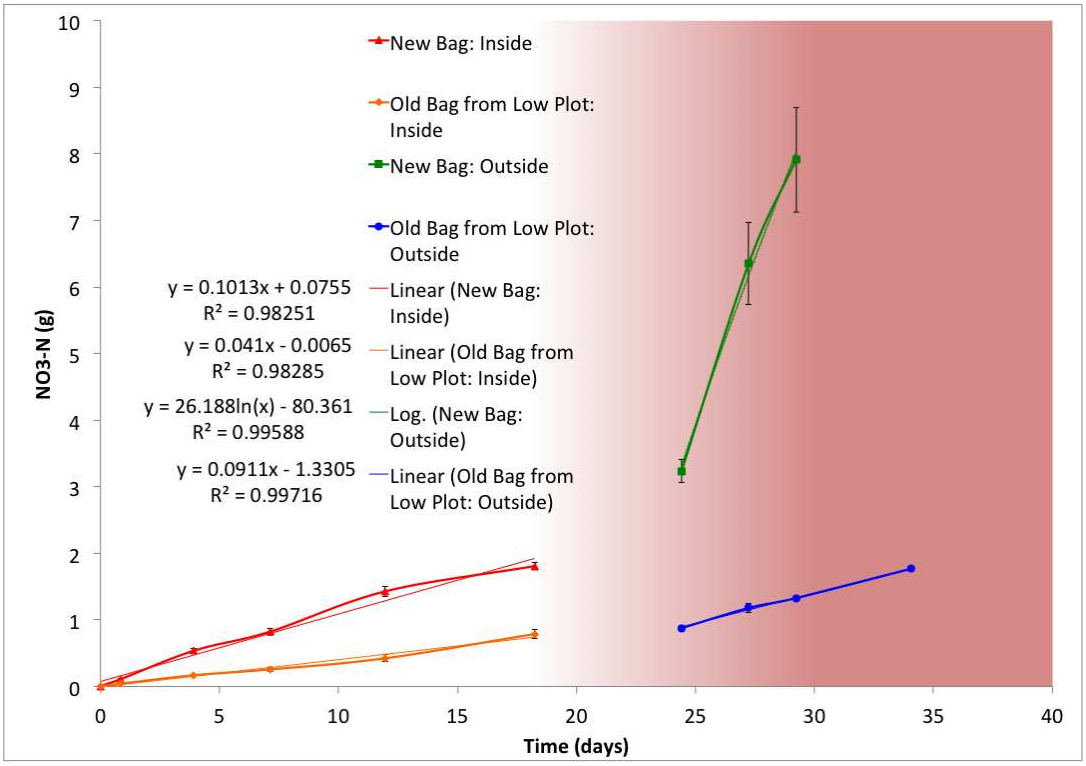

b.

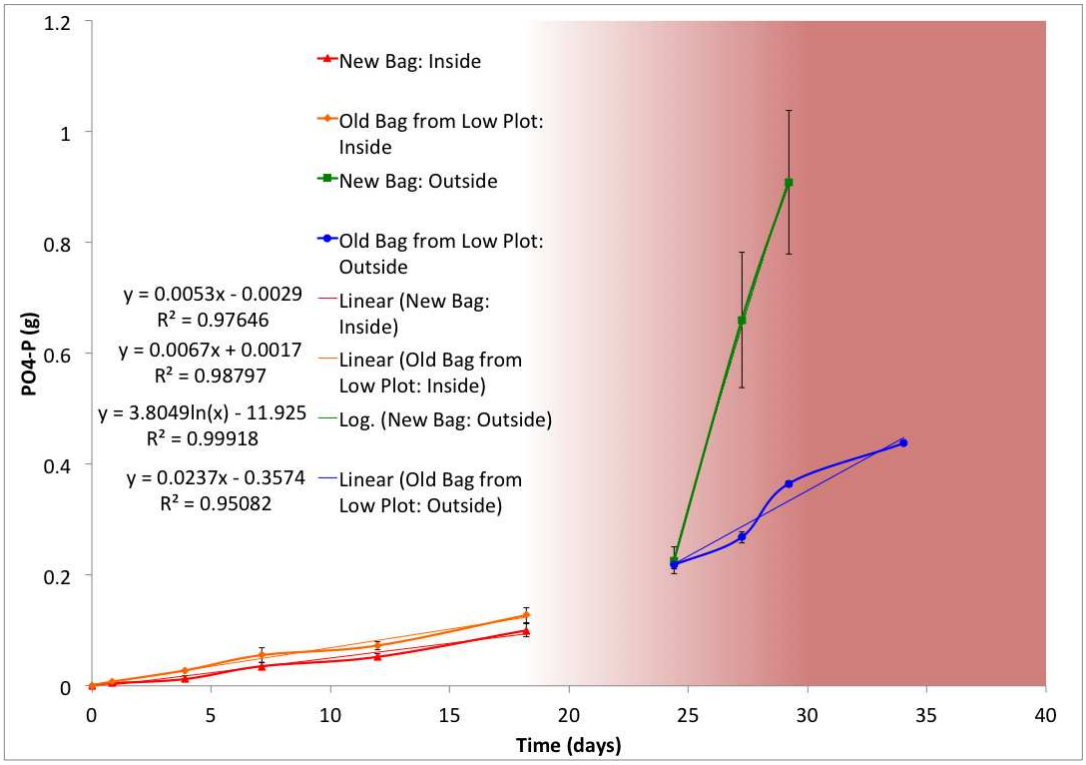

Figure 15. Results from bucket dissolution tests for a) NO_3-N and b) PO_4-P. White areas indicate temperatures averaging 13°C (volume of water for test = 11.3 L). Red shading indicates outdoor tests and temperatures averaging 29°C (volume = 9.5 L).

a.

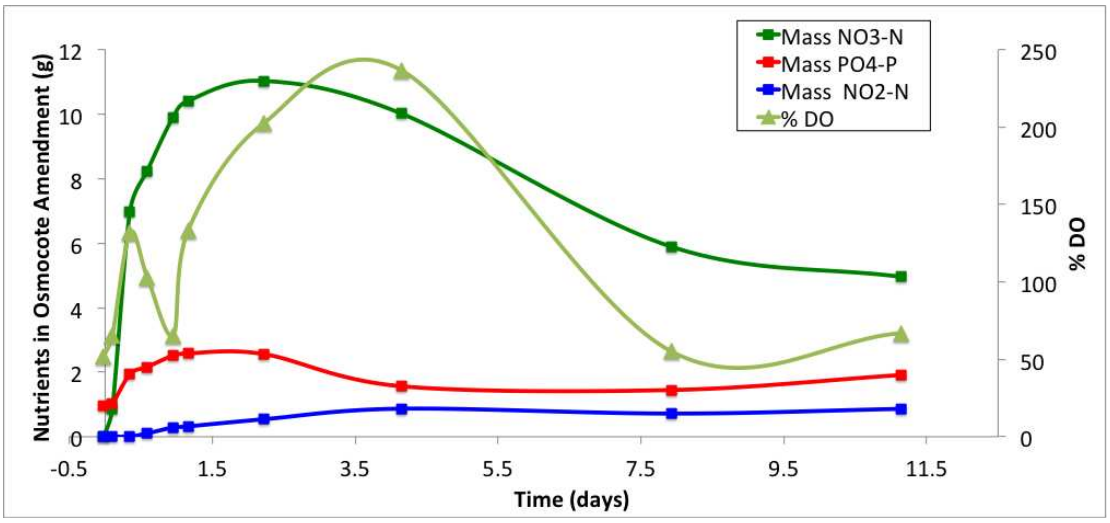

b.

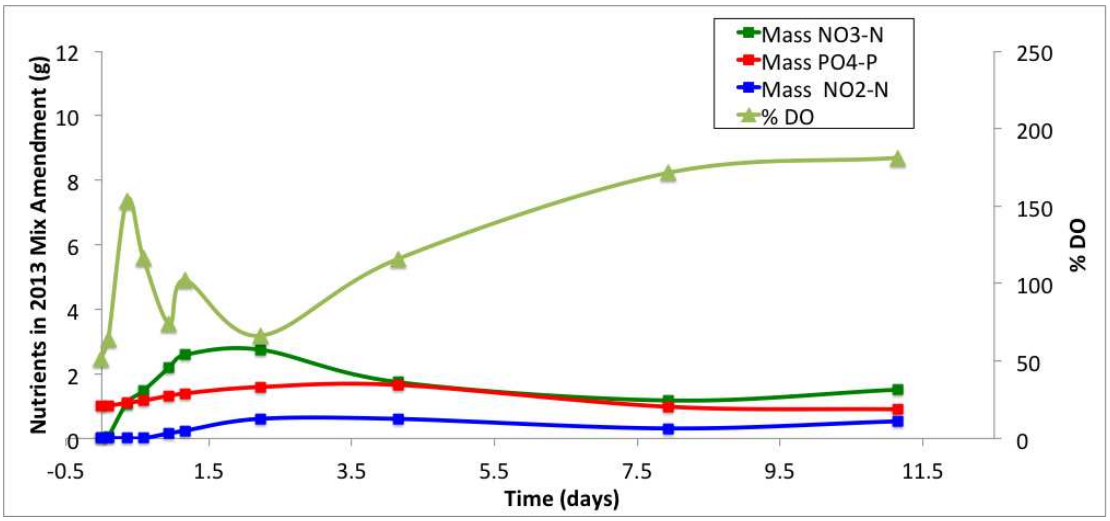

Figure 16. Mass of nutrients in the water column for a) the Osmocote™ amendment and b) the 2013 mix amendment.

excessive biomass production consumes the DO. A subsequent further decrease in DO coincides with the decomposition of biomass (McCormick and Laing, 2003).

Mesocosm tests revealed differences between release rates for fertilizers used in 2012 and 2013 (Figure 16). A rapid increase in nutrient mass in the water column was observed for NO_3-N and PO_4-P in both amendments. However, the sharp spike in nutrient concentrations was most prevalent in the Osmocote™ only amendment. The maximum change in NO_3-N mass inside the mesocosm from the 2013 fertilizer amendments was 21% of the Osmocote™ amendment. Similarly, the change in PO_4-P mass from the 2013 fertilizer amendments was only 16% of the Osmocote™ amendment.

After approximately two days, nutrient concentrations in both mesocosms decreased and NO_2-N concentrations gradually increased. An increase in DO was observed in both mesocosms that correlated with the decrease in nutrients. The DO increase was more rapid in the Osmocote™ amendment but was not sustained throughout the experiment. DO was measured every six hours in the first one and one-half days of the experiment and shows diel cycles. All DO measurements after the first two days were sampled between 12 and 4 PM, with the exception of the value near day 8, which was measured at 9 AM.

2.3.3.3 Determining Nutrient Release Rate Constants from Buckets and Mesocosms

Release rate constants relate the release rate of a given nutrient (to the water column) (R_{nutr}) to the mass of solid phase nutrient present in the system (Equation 1):

$$R_{nutr} = k_{release}\left(f_{fert}^{nutr}\left(M_{fert}\right)\right) \quad (1)$$

where $k_{release}$ represents the release rate constant, f^{nutr}_{fert} is the mass fraction of nutrient in the fertilizer, M_{fert} is the mass of solid fertilizer in the system.

Data from the bucket tests (Figure 15) and mesocosm tests (Figure 16) was used to obtain release rate constants as a function of temperature, time, and the composition of the fertilizer. The slope of the line of best fit for each bucket test condition (new bags inside, new bags outside, old bags inside, old bags outside) represented the release rate (g_{nutr}-day^{-1}). The release rate was converted to a rate constant (day^{-1}) by normalizing the release rate (or flux) to the mass of the nutrient in the solid phase fertilizer. This provided a rate constant for the fertilizer associated with the temperature and time submerged in water under each of the four conditions in Figure 15.

Bucket tests were not conducted for the 2013 mixture of nutrients; therefore the mesocosm tests were used to compare the release rate of nutrients into the water column from the 2012 and 2013 fertilizer mixtures. Assuming that uptake was negligible at the beginning of the mesocosm experiments (i.e., DO follows a normal diel cycle; e.g., first 1.5 days) the subsequent larger increase in DO (Figure 16) likely reflects growth of photosynthetic organisms in response to the amendment. Under these initial conditions (e.g., first 1.5 days) nutrient release is assumed to dominate over uptake, and the release rate is obtainable from the slope of the nutrient concentration versus time (Figure 16).

The NO_3-N and PO_4-P release rate for the 2013 mixture was 21% and 16%, respectively, of the release rate from the 2012 Osmocote™ during the early stages of the mesocosm experiment (Figure 16). These ratios (0.21 and 0.16) were multiplied against

the release rate constants for the 2012 Osmocote mixture (bucket tests) (Figure 15) to estimate temperature and deployment time dependencies of release rate constants for NO_3-N and PO_4-P release from the 2013 mixture. Table 3 shows the release rate constants from bucket and mesocosm tests.

It should be noted that the release rate constants lump multiple processes. For example, rate constants for NO_3-N release subsume processes beyond release from fertilizer, specifically transformations of ammonia and urea to nitrate. This is indicated by the formation of nitrite during the mesocosm experiment (Figure 16), which is an intermediate substrate in the transformation of ammonia to nitrate. The release rates and removal rates of nitrogen from the fertilizer determined in this study are complicated by two forms of nitrogen in Osmocote™ (nitrate and ammonia) and urea found in the 2013 mixture of fertilizers. The chemical transformation of ammonia and urea to nitrate require two and three steps, respectively, and the corresponding rates of hydrolysis and nitrification contribute to the lumped release rate constant that we report.

Whereas the bucket and mesocosm tests define release rate constants dependences on temperature and deployment time, they do so for a limited range of values. To expand the range of temperature and deployment time values to match conditions in the amended plots, multivariate linear regression was used. In order to avoid negative estimated release rates, which might result from field temperatures and deployment times outside the range provided by the bucket tests, two rate constants were added to the regressed data (at 300 days at 12°C and 28°C). These rate constants better constrained the regressions at the upper end of the deployment time and the lower and upper ends of the temperature range experienced in the Willard Spur. These estimated minimum and maximum rate constants

Table 3. Release rate constants from bucket and mesocosm tests.

		NO3-N		PO4-P	
Deployment Time (days)	Temp (C)	2012 rate constant (1/days)	2013 rate constant (1/days)	2012 rate constant (1/days)	2013 rate constant (1/days)
78.00	12.8	1.1E-03	2.4E-04	2.8E-04	4.5E-05
78.86	12.8	1.1E-03	2.4E-04	2.8E-04	4.5E-05
81.90	12.8	1.1E-03	2.4E-04	2.8E-04	4.5E-05
85.12	12.8	1.1E-03	2.4E-04	2.8E-04	4.5E-05
89.97	12.8	1.1E-03	2.4E-04	2.8E-04	4.5E-05
96.23	12.8	1.1E-03	2.4E-04	2.8E-04	4.5E-05
0.00	12.8	2.8E-03	5.9E-04	2.2E-04	3.5E-05
0.86	12.8	2.8E-03	5.9E-04	2.2E-04	3.5E-05
3.90	12.8	2.8E-03	5.9E-04	2.2E-04	3.5E-05
7.12	12.8	2.8E-03	5.9E-04	2.2E-04	3.5E-05
11.97	12.8	2.8E-03	5.9E-04	2.2E-04	3.5E-05
18.23	12.8	2.8E-03	5.9E-04	2.2E-04	3.5E-05
102.41	28.3	2.5E-03	5.3E-04	9.9E-04	1.6E-04
105.24	29.4	2.5E-03	5.3E-04	9.9E-04	1.6E-04
107.22	25.6	2.5E-03	5.3E-04	9.9E-04	1.6E-04
112.05				9.9E-04	1.6E-04
24.41	28.3	8.2E-03	1.7E-03	1.7E-03	2.7E-04
27.24	29.4	4.5E-03	9.3E-04	1.5E-03	2.4E-04
29.22	25.6	3.4E-03	7.1E-04	1.4E-03	2.3E-04
34.05				1.2E-03	2.0E-04
300.00	12.8	1.1E-05	2.4E-06	2.8E-06	4.5E-07
300.00	27.6	2.5E-05	5.3E-06	9.9E-06	1.6E-06

are included in the table of rate constants (Table 3).

MATLAB was used to perform the multivariate linear regression. The MATLAB script file is provided in the Appendix. For both years (2012 and 2013) equations were produced for NO_3-N and PO_4-P release rate constants as a function of temperature and deployment time (Table 4). Figure 17 the shows the results from the multivariate regression for the range of temperatures observed in the field and the regressed data.

Figure 18 shows release rate constants predicted for field conditions based on the multivariate regression equations above coupled to amendment plot deployment times and Willard Spur daily temperatures recorded in the field by the Utah DWQ. For combined extreme long deployment times (e.g., >180 days) and low temperatures (e.g., 5-7 °C), the regressions led to negative $k_{release}$ values, and in these instances the release rate constant was set to zero.

Coupling the release rate constants to the known mass of nutrients deployed in the amended plots (Tables 1 and 2) allows estimating the daily release rate (g/day) for each plot for both 2012 and 2013 (Figure 19). These daily nutrient release rates from the Willard Spur amendments can be compared to other loads into Willard Spur. For the remainder of the discussion of release rate constants, it was assumed that all forms of phosphorus other than PO_4-P are negligible in the water column, and the change in PO_4-P represents the change in total phosphorus (TP).

The cumulative release from the fertilizer amendments to the water column were determined by integrating (summing) over time the mass of nutrients released each day given in Figure 19. The low fraction of the total nutrients released in 2013 shown in Figure 20 is in part due to the variation between the differences in the change in

Table 4. Equations describing nutrient release rates ($k_{release}$) for the 2012 and 2013 fertilizer mixtures.

2012 NO_3-N	$-0.0000147(\textit{deployment time}) + 0.000138(\textit{temperature}) + 0.000101$
2012 PO_4-P	$-0.000000626(\textit{deployment time}) + 0.0000570(\textit{temperature}) + -0.000335$
2013 NO_3-N	$-0.00000308(\textit{deployment time}) + 0.0000291(\textit{temperature}) + 0.000212$
2013 PO_4-P	$-0.000000411(\textit{deployment time}) + 0.0000106(\textit{temperature}) + -0.0000708$

a.

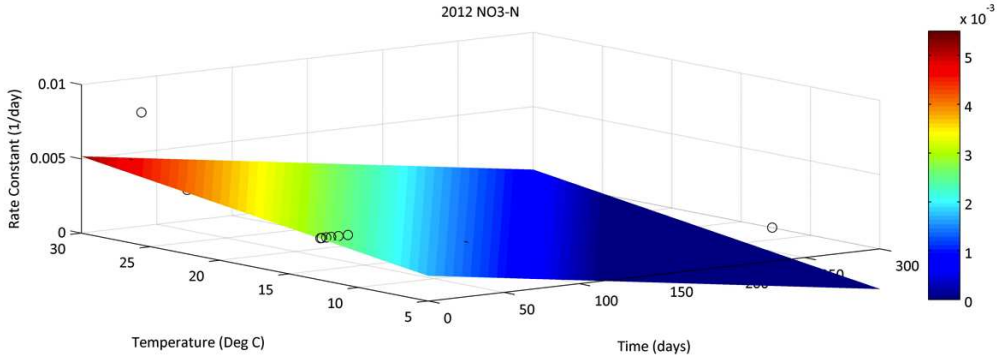

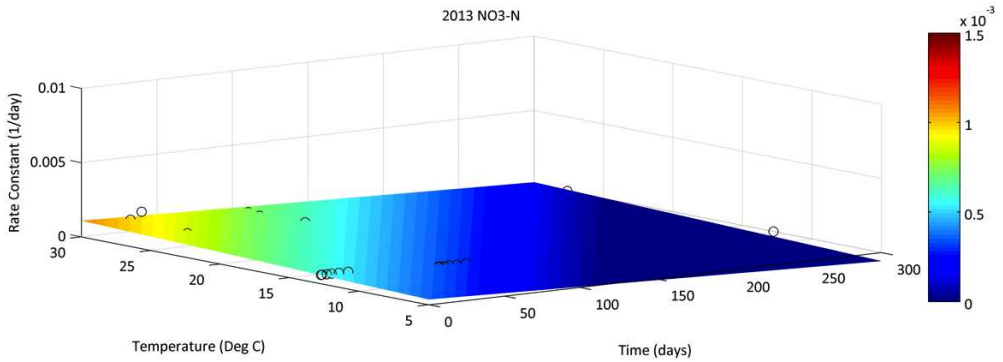

b.

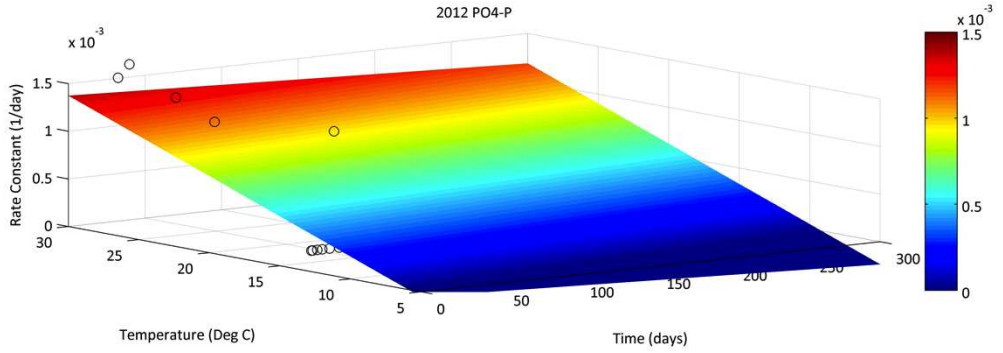

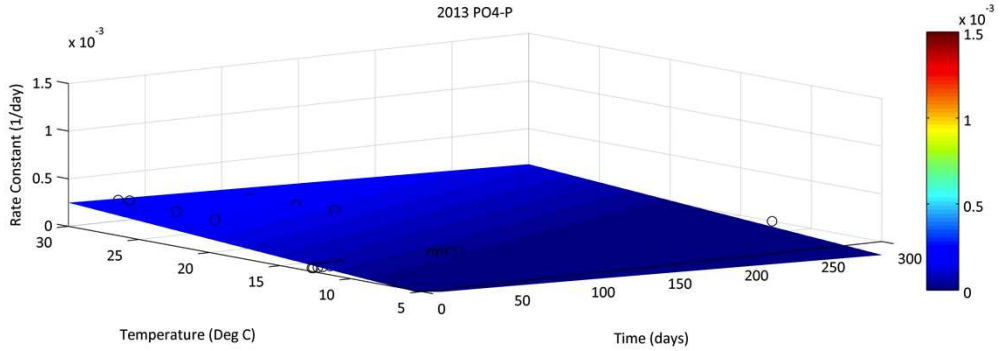

Figure 17. Release rate constants for a) NO_3-N and b) PO_4-P for the range of times fertilizer is submerged and water temperatures. Open circles represent discrete rate constants from the bucket and mesocosm tests. Note the different scale on the 2012 NO_3-N rate constant color bar.

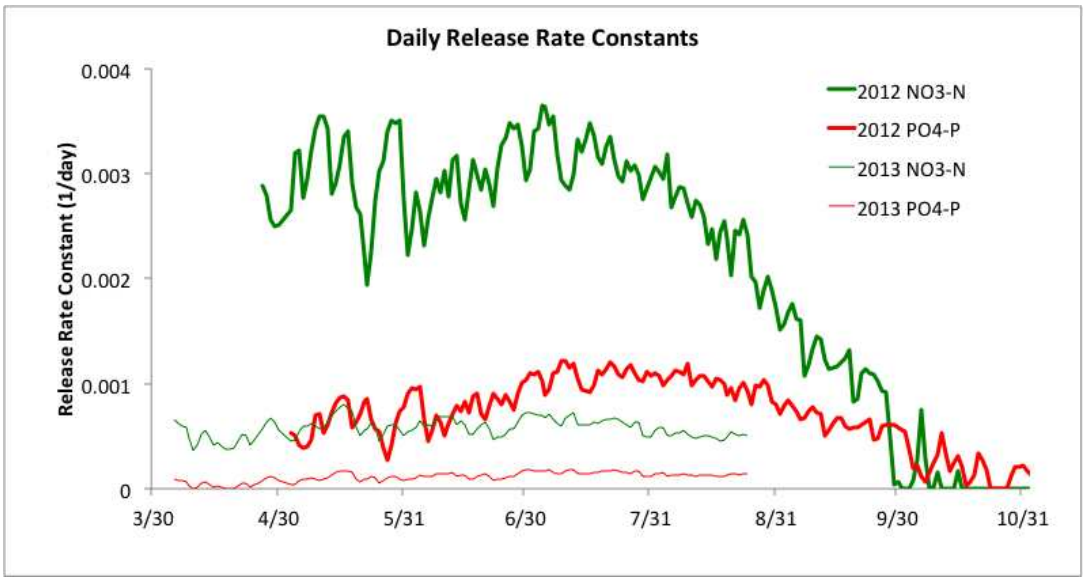

Figure 18. Release rate constants for NO_3-N and PO_4-P for each day during the 2012 and 2013 sampling periods.

a.

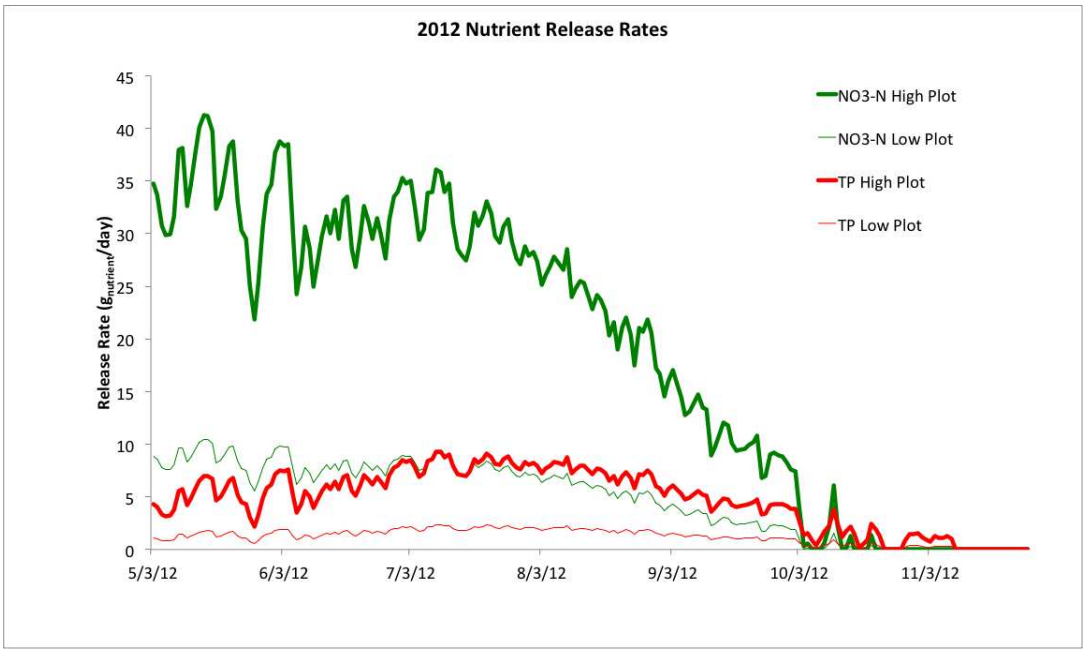

b.

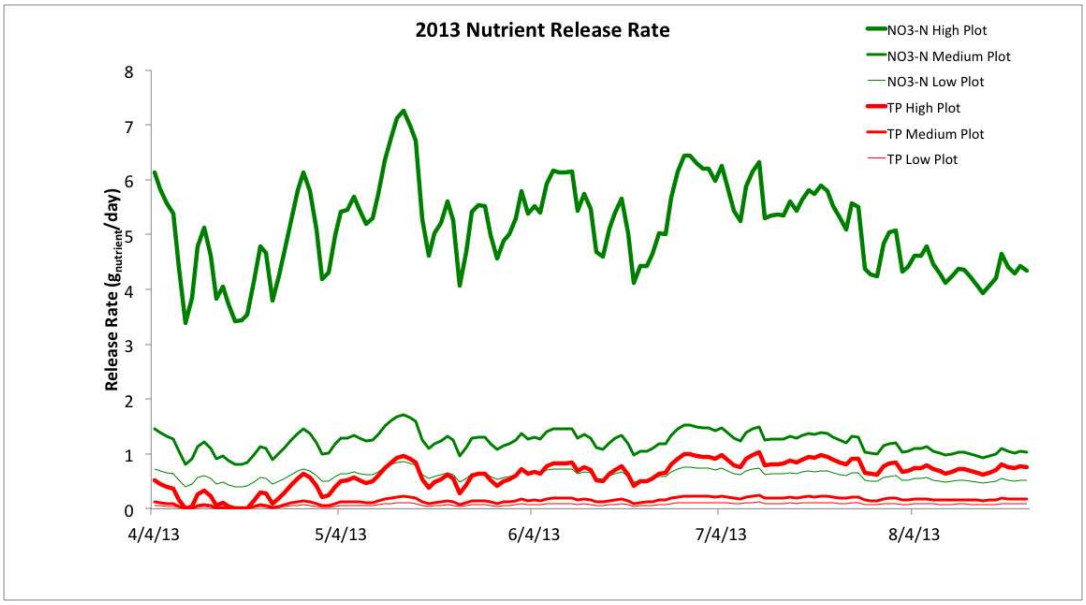

Figure 19. Daily release rates for a) NO_3-N and b) PO_4-P into the water column from the nutrient amendments during the 2012 and 2013 sampling periods.

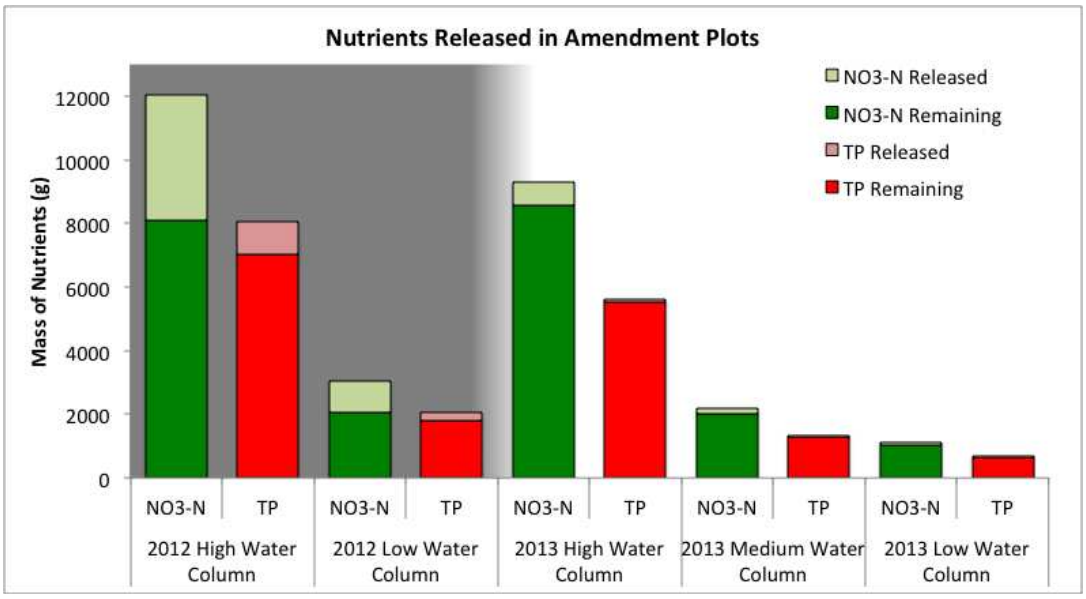

Figure 20. Summary of delivery of NO_3-N and TP to the water column from fertilizer amendments estimated using release rates ($k_{release}$). Shaded area indicates 2012 plots.

concentration in the mesocosms for the 2012 and 2013 fertilizers. In addition, the 2013 amendments were submerged in the field fewer days than the 2012 amendments, 200 days and 140 days for 2012 and 2013, respectively.

2.3.3.4 Mesocosm Nutrient Removal Rates

In this study, the term "nutrient removal" is used to describe a wide variety of processes that remove NO_3-N and TP from the water column. These processes include assimilation by SAV and algae, assimilation by microorganisms in the sediment and water column, and precipitation of nutrients onto the sediment. It does not include loss from dilution or advection because mesocosm experiments were conducted in essentially closed conditions. This term is intentionally broad because the scope of this study did not include quantifying individual physical processes related to the removal of nutrients from the water column.

The change in mass of a given nutrient in the water column, can be described using Equation 2:

$$\frac{\partial M_{water}^{nutr}}{\partial t} = k_{release}\left(f_{fert}^{nutr}\left(M_{fert}\right)\right) - k_{removal}\left(C_{water}^{nutr}\right)\left(V_{water}\right) \qquad (2)$$

where $k_{removal}$ represents the rate at which nutrients leave the water column, $C^{nutr}{}_{water}$ is the steady state concentration of the nutrient in the water, and V_{water} is the volume of water influenced by the fertilizer.

When the system reaches steady state where nutrient release is equal to uptake and the nutrient concentration in the water column reaches a steady value, the following

equation applies:

$$k_{removal} = \frac{k_{release}\left(f_{fert}^{nutr}\left(M_{fert}\right)\right)}{C_{water}^{nut} V_{water}} \quad (3)$$

Mesocosm nutrient concentrations approached steady state during the last 4 days of the experiment (Figure 16), approaching values of 3.65 mg/L and 1.13 mg/L for NO_3-N and PO_4-P, respectively, for the 2012 mixture, and values of 0.906 mg/L and 0.633 mg/L for NO_3-N and PO_4-P, respectively, for the 2013 mixture. Table 5 shows the mesocosm nutrient release and nutrient uptake rate constants calculated using Equation 3 and the steady state nutrient concentrations.

2.3.3.5 Willard Spur Nutrient Removal Rates

Measured nutrient concentrations in the water column amended plots were predominantly equivalent to those in the ambient and control plots for both NO_3-N and PO_4-P in 2012 and 2013 (Figures 6 and 11). The exceptions to this generalization are the months of June, July, and August in 2012 for the high water column amendment. Inserting the corresponding release rate constants and measured nutrient concentrations into Equation 3 for this plot during these months yields a consistent set of removal rate constants ranging from 6.5 to 11.5 day^{-1} for NO_3-N, and from 1.5 to 2.75 day^{-1} for PO_4-P.

2.4 Discussion

Water column NO_2-N+NO_3-N and dissolved P concentrations were significantly greater in the high and low water column amendment relative to the water column control

Table 5. Comparison of nutrient release and removal rate constants in mesocosms.

	Mesocosm Rate Constants (d^{-1})		
	Nutrient	**$k_{release}$**	**$k_{removal}$**
Osmocote™	NO_3-N	0.0743	2.02
	TP	0.0178	1.04
2013 Mix	NO_3-N	0.0260	1.71
	TP	0.00486	0.305

in 2012 (Figure 7). However, significant differences between water column amendments and controls were not observed in 2013 (Figure 12). This reflects the difference in the amendment mixtures between 2012 and 2013. Specifically, the 2013 mixture contained approximately half of the nitrate and phosphorus content relative to the 2012 mixture.

Estimated nutrient release rates into the plots can be compared to the NO_2-N + NO_3-N and TP loads from the PWRWTP (Figure 2.21) as measured throughout 2012 (Denbleyker, 2013b). Loads per volume from the PWRWTP were calculated in kg-day^{-1}-m^{-3} for a relatively dry year similar to water levels in 2012 (elevation of Willard Spur water is approximately 4200.5 ft), a relatively wet year (elevation of approximately 4201.5 ft), the 2012 water column amendment plots, and hypothetical scenarios based on maximum and minimum flows and concentrations anticipated from the plant (Denbleyker, 2013a). Nutrient loads from the 2012 low water column amendments during the spring and early summer were greater than PWRWTP loads in dry conditions (4200.5 ft) by factors of 5 to 40 from April through August, with the exception of the significant decrease in NO_2-N + NO_3-N observed in July. Beginning in September, estimated nutrient loads per volume from the PWRWTP in fall months approach and exceed loads per volume from the 2012 low water column amendment.

Uptake rates in the Willard Spur amended plots and the Farmington Bay mesocosms were similar (in the same order of magnitude). However, Willard Spur uptake rates were approximately a factor of 3-6 and 2-6 times higher than those from the Farmington Bay mesocosms for NO_3-N and PO_4-P, respectively. These differences can be attributed to the location, i.e., the mesocosm experiments were performed at a Farmington Bay impounded wetland (elevated nutrient and legacy contaminant

a.

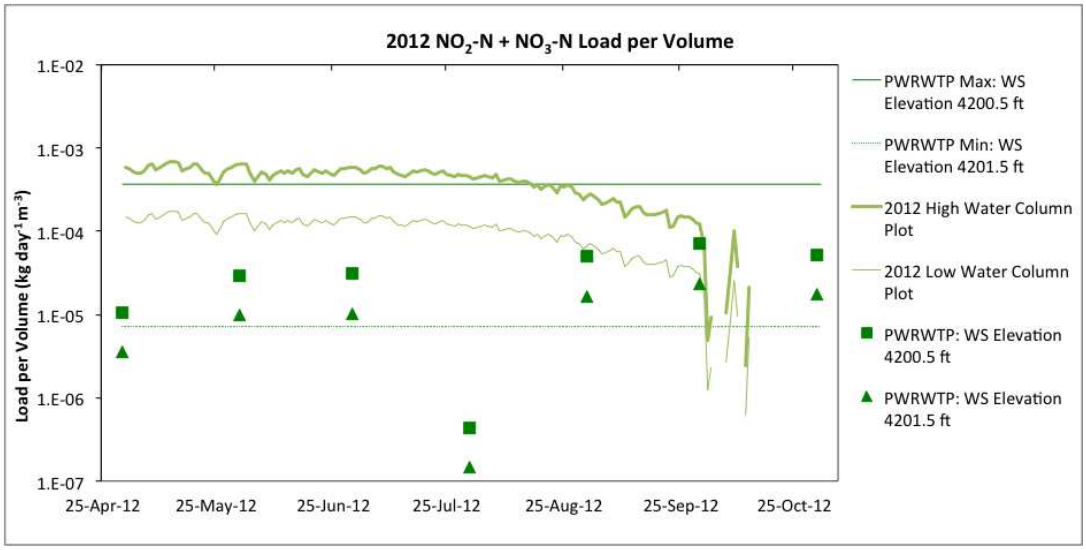

b.

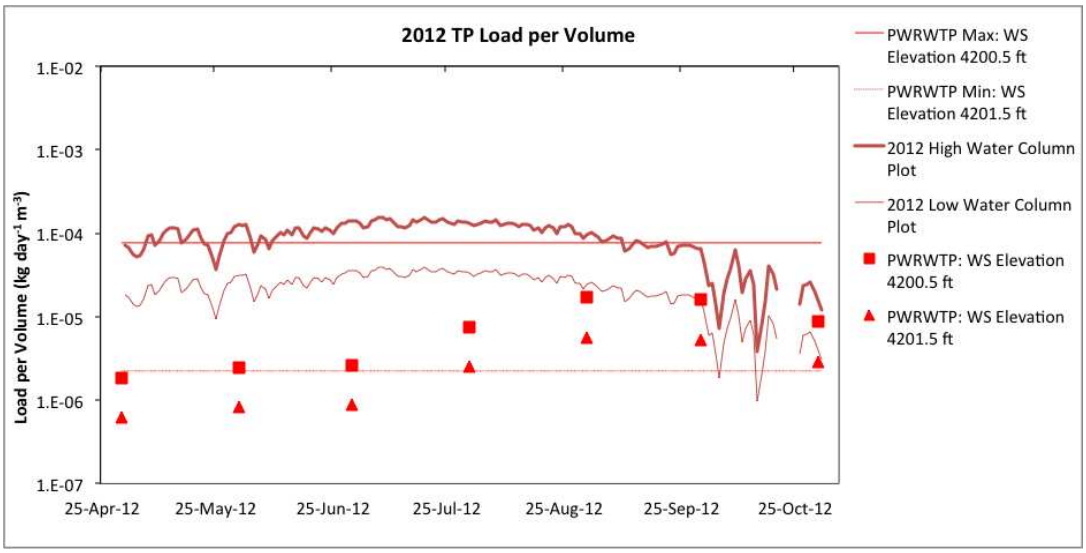

Figure 21. Comparison of estimated NO_3-N and TP loads per volume from 2012 nutrient amendments and the 2012 PWRWTP effluent. Volume of water column plots (60 m^3) assume a water depth of 0.5 m. Estimated storage of Willard Spur elevations of 4200.5 and 4201.5 are 1,480,200 m^3 and 493,400 m^3, respectively.

concentrations) (Carling et al., 2013), and to the season, i.e., the Willard Spur uptake rates correspond to the active growing season (June-August), whereas the mesocosm uptake rates correspond to early fall (September).

Sediment amendments in 2012 yielded measurable increases in nutrient concentrations in sediment (Figures 8). Additionally, nitrogen isotope effects were also observed in the sediment-amended plots. The fertilizer $\delta^{15}N$ was approximately 0‰, whereas the ambient sediment $\delta^{15}N$ was approximately 7.25‰. A simple mixing of these two sources would suggest a negative $\Delta^{15}N_{amendment\text{-}control}$, implying that fertilizer addition to sediment would yield $\delta^{15}N$ values ranging from 0 to 7.25‰. Instead, amended sediment showed enriched $\delta^{15}N$ values (e.g., 8 to 10.5‰), yielding a positive $\Delta^{15}N_{amendment\text{-}control}$ of 1.5‰ in the high sediment amendment (Figure 9). Notably, the corresponding plant leaves were depleted relative to control leaves, with a negative $\Delta^{15}N_{amendment\text{-}control}$ of -1.5‰ in the high sediment amendment (Hoven et al., 2013). In fact, this isotope effect is expected in soils where excess ammonia is available (Heaton, 1986). This occurs when either labile organic nitrogen is rapidly converted into ammonium during the early stages of mineralization or when ammonium is added from an artificial source. Usually the formation of ammonia from organic nitrogen in the soil (Step 1 in Equation 4) is the rate-limiting step in the formation of nitrate.

$$organic - N \xrightarrow{1} NH_4^+ \xrightarrow{2} NO_2^- \xrightarrow{3} NO_3^- \qquad (4)$$

Very little fractionation is observed in this reaction ($\varepsilon_{NH4^+\text{-org. N}}$ approximately 0‰). However, large kinetic fractionation ($\varepsilon_{NO3^-\text{-}NH4^+}$ of up to -35‰) is observed in the

transformation of ammonia to nitrate (steps 2 and 3 in Equation 4). Consequently, nitrogen isotopes of the most available form of nitrogen to plants, nitrate, are significantly depleted. Therefore when the transformation of ammonia to nitrate is the rate-limiting step, plant tissue is depleted in ^{15}N and sediment is subsequently enriched in ^{15}N.

For the most part, the amendments to the water column did not yield dramatic accumulation of nutrients in the water column, presumably due to dilution and losses via plant and sediment uptake, settling of particle associated forms, and other potential factors in the Willard Spur system. The measured concentration depends on both the rate of release of the nutrients from Osmocote™ and the residence time of the nutrients within the plot, both of which are unknown. Factors such as wind, surface water flow, and plant and sediment uptake influence residence time of nutrients in the water column within the plots. The rate of nutrient release from Osmocote™ decreases below 60 °F and after 2-3 weeks of deployment (Heck et al., 2000).

Despite an apparent lack of nutrient accumulation in the water column, the amendments appeared to influence plant health as indicated by plant metrics in 2012 and 2013 (Hoven et al., in preparation). In May and June of 2012 significant treatment effects were observed on percent cover of algae on SAV (attached or loosely associated macroalgal epiphytes) and branch densities (Hoven et al., 2013). There were stronger and more lasting effects from the sediment amendments relative to the water column amendments in 2012. In 2013 gross observations include plot scale visual observations. For example, in 2013 areal coverage by plants was distinctly different within versus outside the amended area. In late July the high water column amendment showed no

SAV on the surface, decreased areal coverage of SAV, and increased bleached appearance relative to the low water column amendment (Figure 22). Furthermore, SAV were prevalent on the surface in the low water column amended area (Figure 22b) but not outside the amended area. Areal coverage and the bleached appearance decreased from the high to low amendments.

Plant responses measured in the Willard Spur test plots demonstrate that the fertilizer amendments succeeded in bracketing the range of nutrient loads below which no impacts to plant health are expected, and above which plant health is known to decline. Sensitive indicators of detrimental impacts to plant health are now being developed from this range of nutrient loads (Hoven et al., in preparation).

a. b.

c. d.

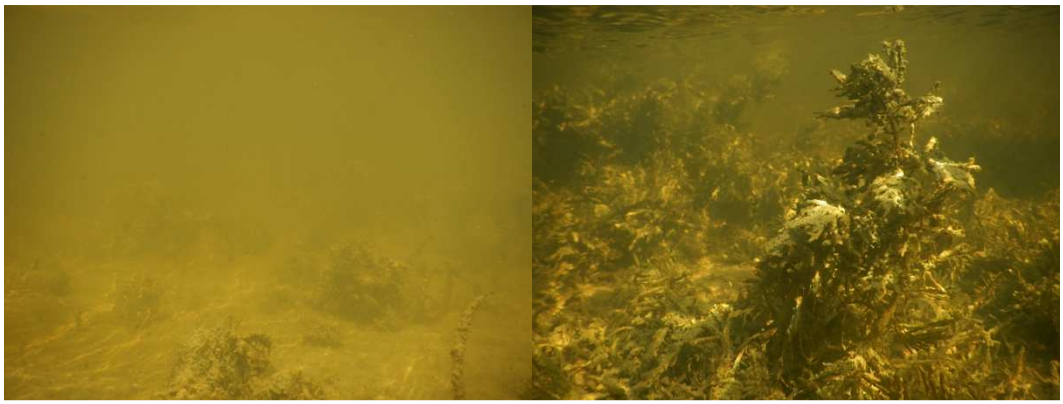

Figure 22. Surface SAV branch coverage in a) high water column plot and b) low water column plot. Areal SAV coverage and color of SAV varied significantly between c) the high water column plot and d) the low water column plot.

3. EFFECTS OF DRYING ON SEDIMENT NUTRIENTS

3.1 Background

Impounded wetlands surrounding the Great Salt Lake are heavily relied upon for removal of anthropogenic nutrients from two main inflows, the Bear River from the north and Jordan River from the south. Plants in constructed wetlands consume high nutrient loads from agricultural and urban runoff. However, macrophytes are sensitive to changes in sediment, pore water, and surface water (Carling et al., 2013). The health of Great Salt Lake wetlands has been threatened by anthropogenic influences that include trace element contamination and eutrophication (Carling et al., 2011; Dicataldo et al., 2011; Hoven and Miller, 2009; Vest and Conover, 2011; Waddell et al., 2009). Food sources for migratory birds in the Great Salt Lake have been negatively effected by this contamination (Johnson, 2008; Vest and Conover, 2011), including early senescence of SAV (Hoven and Miller, 2009).

Internal loading of phosphorus from the sediment to the water column is related to biological activity influenced by seasons, redox-sensitive sorption to iron compounds, macrophyte density, dissolved oxygen, and pH (Sondergaard et al., 2003). One method for reducing deleterious internal nutrient loading (i.e., mobilization of nutrients from the sediment that produces algae blooms and are possibly related to SAV senescence) is mineralization of nutrients by oxidation through drying and rewetting. When sediment is

dried, nutrients, particularly phosphorus, mineralize into soluble forms such as PO_4-P. When the sediment is rewetted, the soluble phosphorus is mobilized into the water column and removed from the system by flow (Gilbert et al., 2014; Olila et al., 1997). Impounded wetlands surrounding the Great Salt Lake are particularly well suited for this type of remediation due to their relatively small size and the flexibility managers have to adjust water levels of the entire body of the wetland.

The wetland chosen for this study, FB1, is located in Farmington Bay and has an area of approximately 1,100 acres. FB1 varies in depth between 0 and 2 m. Managers from the Utah Department of Wildlife Resources (DWR) and local runoff control the wetland's area and depth. Working with the Utah DWR allowed for scheduling sample collection before draining, after FB1 was drained and the upper 8-10 cm of sediment had dried, and after re-flooding.

This experiment also assessed the capacity of QEMSCAN electron microscopy to quantify changes in sediment elemental content. QEMSCAN can conduct a raster scans of a mineral grain at resolutions as low as 1 μm. From the raster scans it is possible to quantify mineral content and the prevalence of elements on extremely small scales. A high-energy accelerated electron beam produces energy dispersive x-ray spectra to identify elemental content. Elemental composition is used along with back-scattered electron brightness and x-ray count rate to assign a mineral to each pixel in the raster scan.

3.2 Methods

Sediment squeezer cores were collected using the same method as described in section 2.2.2. Samples were processed and analyzed at multiple laboratories, as described below.

3.2.1 Field Methods

In the summer of 2013 the Utah Division of Wildlife Resources intentionally drained a Farmington Bay impounded wetland, FB1. Samples were collected on June 20 when water levels at the sample site were approximately 0.4 m (Figure 23a) and again in August when the June sample site had been dry for approximately one month (Figure 23b). A small channel developed in the dried sediment between the remaining water in the center of the wetland and its outlet. A third core was collected October 31, after the wetland had been re-flooded and water levels were approximately 0.8 m.

Surface water samples and sediment squeezer cores were collected in June, August, and October of 2013. Surface water was collected near an outlet of FB1 where water was assumed to represent the chemistry of the pond. Pore water samples were collected for dissolved anion analysis by forcing water through syringe filters (Whatman 0.45 μm PES). Pore water was collected from ports in the core between 0 and 35 cm. Following extraction of pore water from the cores, the sediment was extruded from the core in 3 cm sections for depths up to 12 cm.

In June pore water samples were collected from depths 3 to 30 cm. In August no pore water was extracted between 0 and 8 cm. A dried block of sediment approximately 10 cm thick was removed from the surface and cut into 3 cm horizons. The squeezer core

a. b.

Figure 23. Sample location a) before FB1 was drained (June 20, 2013) and b) after one month of dry conditions (August 14, 2013).

was inserted into the saturated sediment exposed when the dry block of sediment was removed. Pore water samples were collected for depths between 10 and 35 cm. In October pore water was collected at depths between 0 and 18 cm. The sediment core sample sites were within 5 m of each other. In October the increased water depth did not allow for collecting a core as far from the shore as the June and August cores.

3.2.2 Laboratory Methods

Phosphorus in FB1 was characterized in three ways. Dissolved phosphorus from surface water and pore water extracted from sediment was analyzed using ion chromatography. Available phosphorus, calcium phosphates and adsorbed phosphorus on calcite and iron oxide surfaces, was measured for each horizon using the Olsen $NaHCO_3$ method (Olsen et al., 1954).

QEMSCAN was used to characterize elemental content of sediment grains. Sediment from each horizon between 0 and 12 cm were dried overnight at 100°C. To prepare sediment grains for QEMSCAN analysis, dried sediment samples were impregnated in 25 mm epoxy plugs and polished in kerosene to avoid allowing clays to absorb water and swell. Three random locations on each sample were selected for the raster scan. The area of each scan was 4E6 μm^2 with each pixel representing 25 μm^2. This resolution was intended to match estimated grain size of the sediment, which was mostly silty clay.

3.3 Results

Sediment profiles of available phosphorus showed decreasing phosphorus with depth (Figure 24). August sediment samples that had been dried showed increased available phosphorus for horizons 6-9 cm and 9-12 cm. A 10-50% increase in available phosphorus was observed in dried and rewetted sediment, except for the 3-6 cm horizon. However, only one sample was collected and analyzed for sediment horizon

Significant increases in pore water dissolved phosphorus were observed between samples collected before drying (21-Jun) and after re-flooding (31-Oct). Dissolved phosphorus increased by 50-200% at sample depths between 4 and 18 cm (Figure 25). Surface water dissolved phosphorus increased by approximately 35%, from 0.246 mg/L in June to 0.331 mg/L in August, despite a 0.5 m increase in water depth at the sample site. Again, only one sample was collected and analyzed for each depth.

Carbon and nitrogen was also analyzed at the SIRFER lab for 3 cm intervals (Figure 26). Following drying, more than 0.5-2.5‰ increase in $\delta^{15}N$ was observed in all horizons except organic nitrogen between 6 and 9 cm. The enrichment is especially pronounced in total nitrogen. A corresponding decrease in total % nitrogen was observed in the upper two horizons but not between 6 and 12 cm (Figure 26).

QEMSCAN analysis was only performed on samples collected before the wetland was drained (June 21) and after the sediment had dried (August 14). Figure 27 shows results from raster scans for apatite and total phosphorus. Before the wetland was drained the greatest % area measured for both apatite and total phosphorus was found at depths of 3-6 cm and 9-12 cm. Following drying, the total phosphorus increased on the upper layer (0-3 cm) and similar or decreasing values were observed between 3 and 12 cm. More

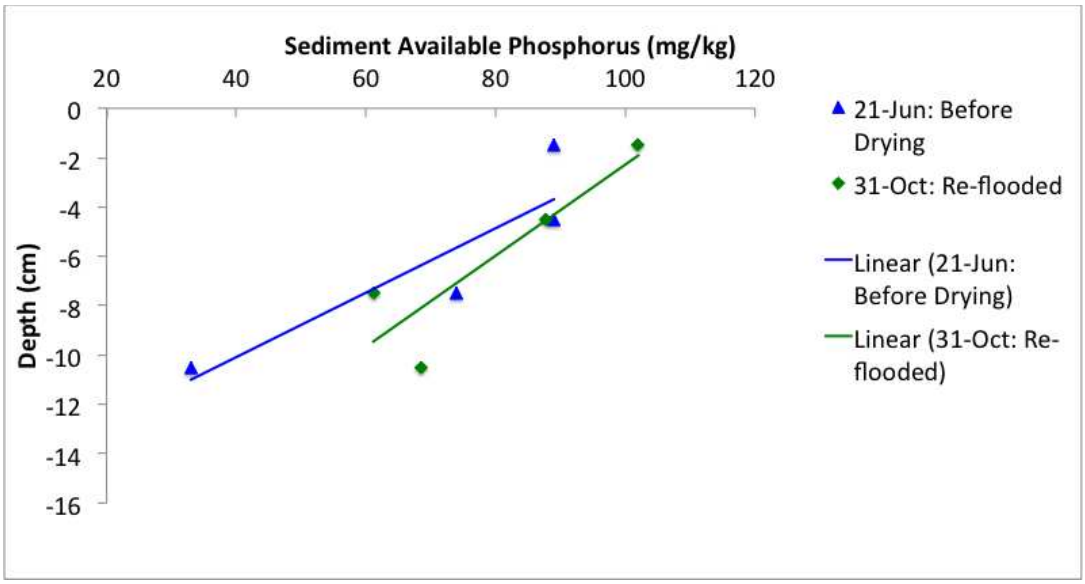

Figure 24. Concentration of available phosphorus in FB1 sediment relative to depth of sample before drying (21-Jun) and re-flooded (31-Oct).

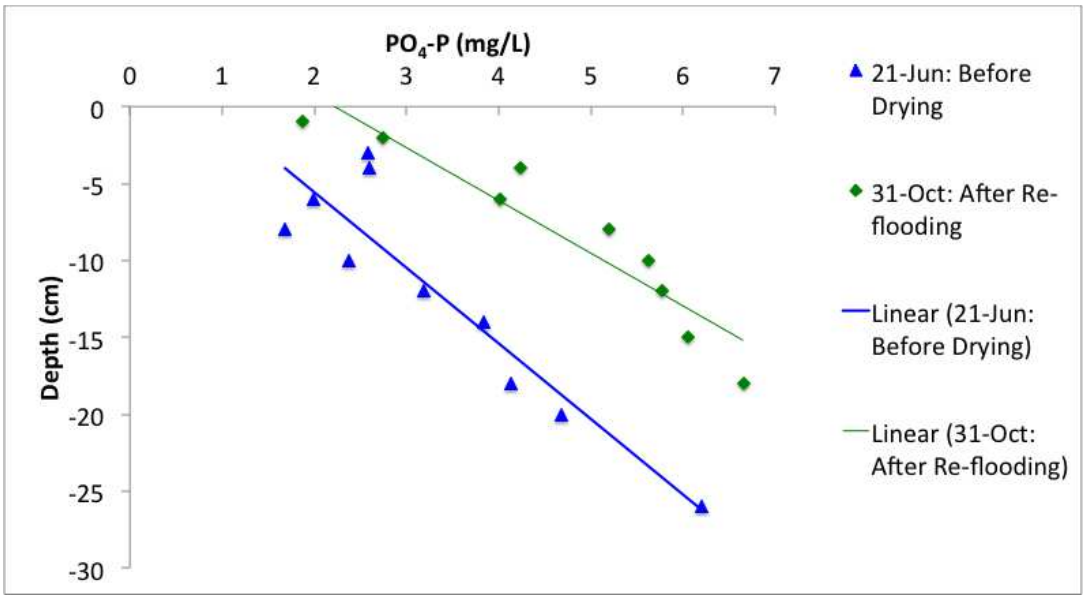

Figure 25. Concentration of dissolved phosphorus in FB1 sediment pore water relative to the depth of sample before drying (21-Jun) and re-flooded (31-Oct).

a.

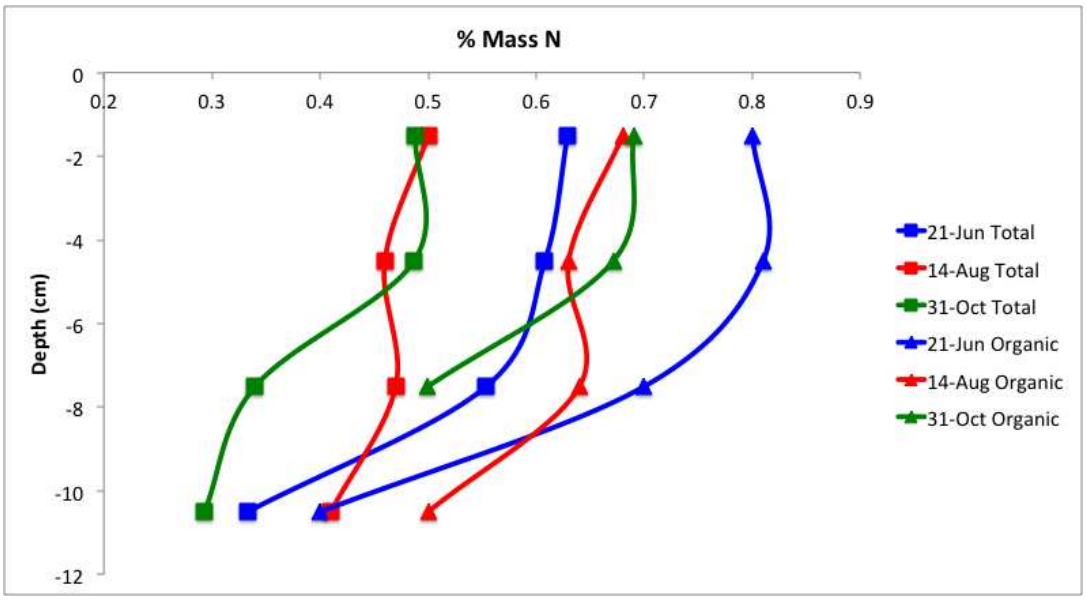

b.

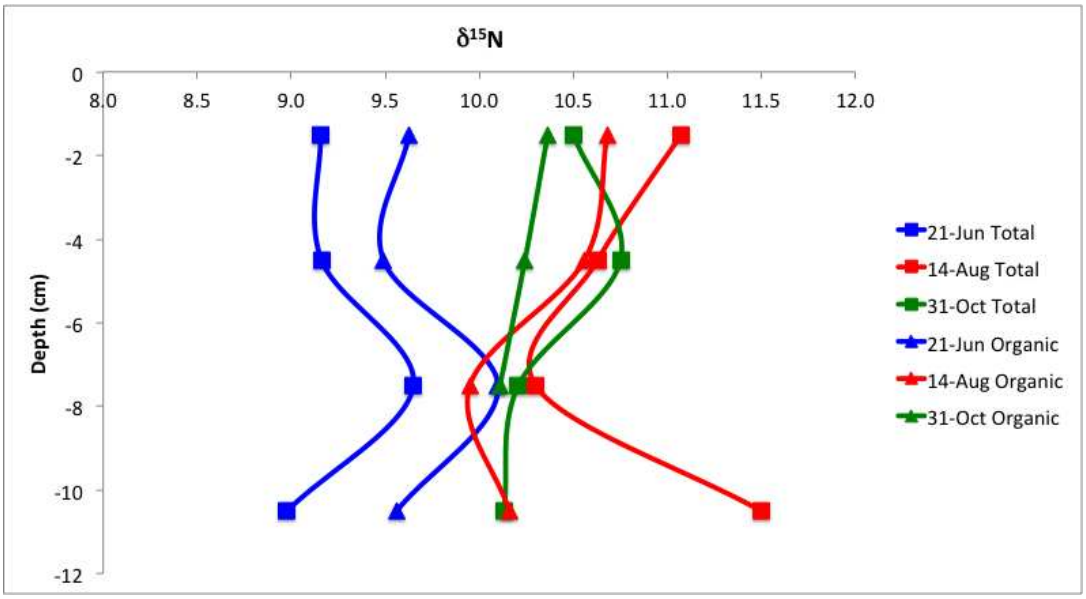

Figure 26. Depth profiles of total and organic a) nitrogen isotope values and b) % nitrogen for FB1 sediment before drying (21-Jun), dried (14-Aug), and re-flooded (31-Oct).

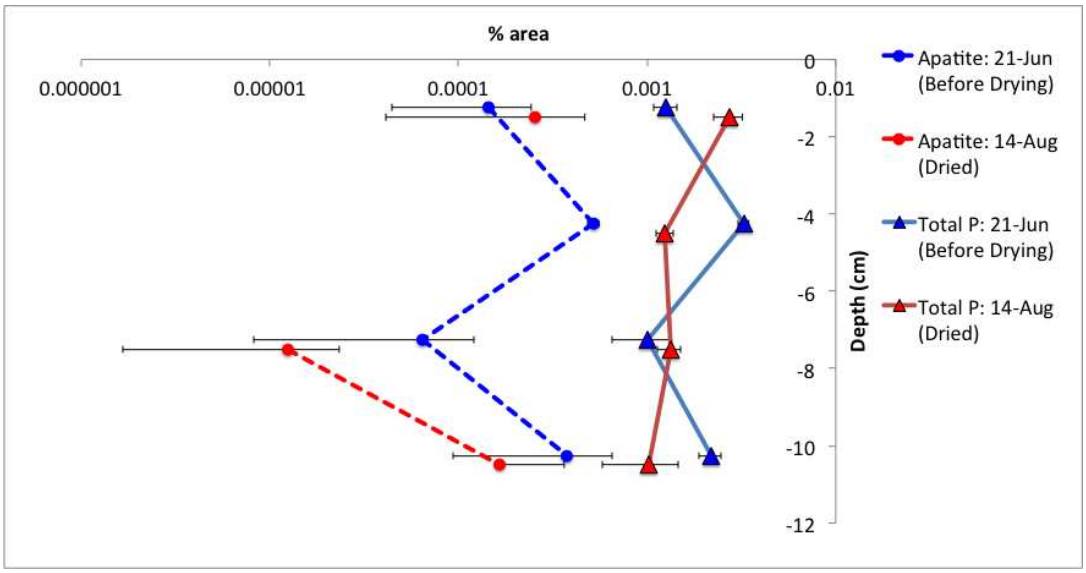

Figure 27. Depth profiles of total P and apatite in sediment before drying (21-Jun) and dried (14-Aug).

QEMSCAN results showing mineral content are included in the Appendix.

Figure 28 shows QEMSCAN results for one sample (before drying, 0-3 cm). This image shows all of the minerals identified in the three scans. Values represent the sum of the pixels from all three scans for each mineral characterized by the QEMSCAN software.

Changes in the mineralogy were observed when comparing mineral composition of sediment horizons before drying and after drying (Figure 29). Here a series of four mineral categories (series 1: iron and other sulphides, sulphates, Fe-Cu-Ti-Oxides and carbonates, and apatite) are shown in dark colors. A second series of mineral categories (series 2: silicates, carbonates, and the background) are shown in white. Figure 29 indicates an increase in series 1 minerals in the upper horizon (0-3 cm), a decrease in horizons 3-6 and 9-12 cm, and minimal change for horizon 6-9 cm.

Iron and other sulphides decrease by 50-100% in all horizons except for the top horizon, which shows a 200% increase. All horizons show up to a 100% decrease in sulphates and Fe-Cu-Ti-Ox/CO_3 minerals. The sum of the area of coverage of the six mineral categories, excluding background, determines the total area used to calculate percent areal coverage for the six categories. Background percent areal coverage is determined using the total area of the scan (4E6 μm^2). Iron and other sulphides drive the increase of series 1 minerals seen in Figure 29 in the horizon from 0-3 cm (>200% increase), specifically, the unknown pixels containing sulphur and silicon atoms.

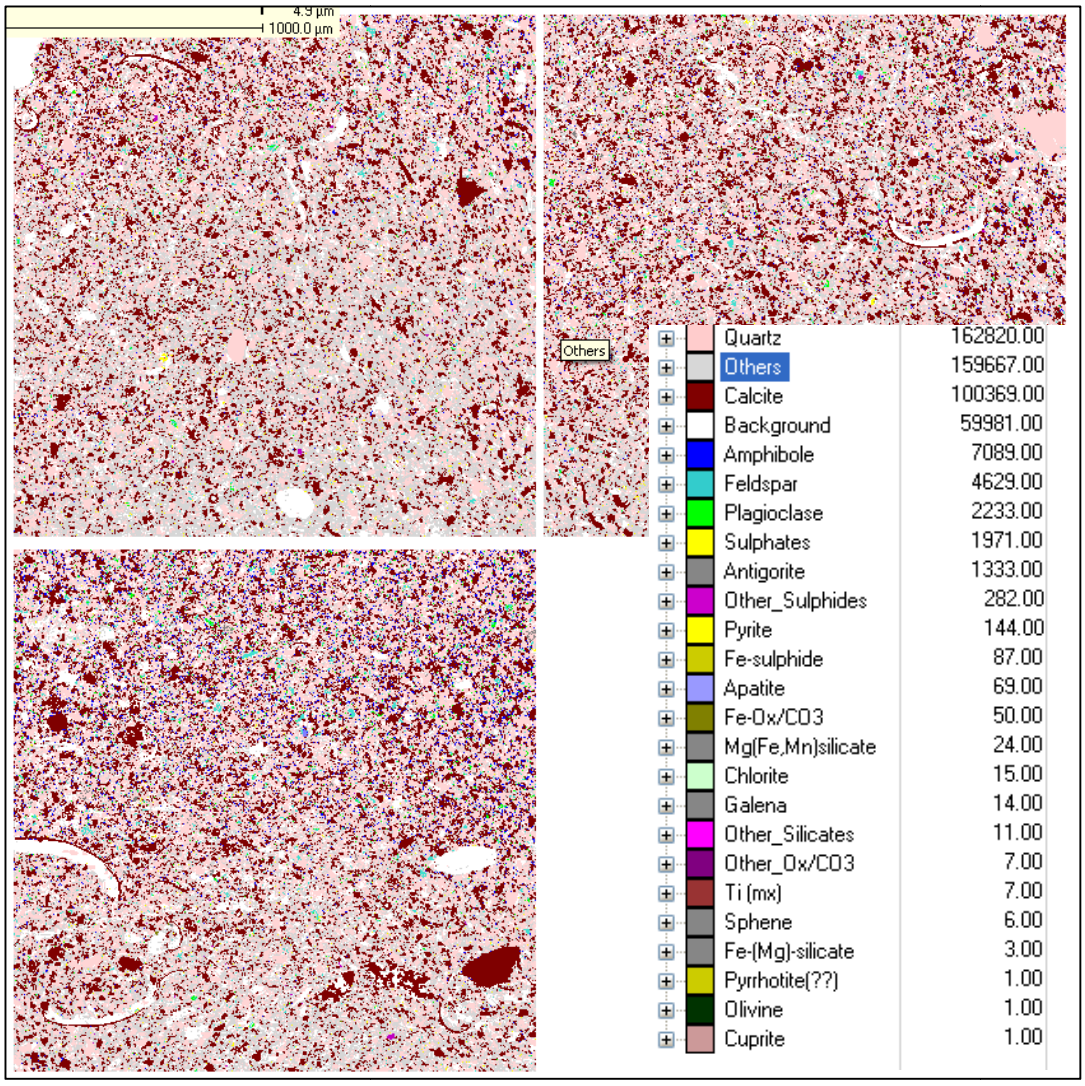

Figure 28. Results from three raster scans of sediment from horizon 0-3 cm before drying (21-Jun).

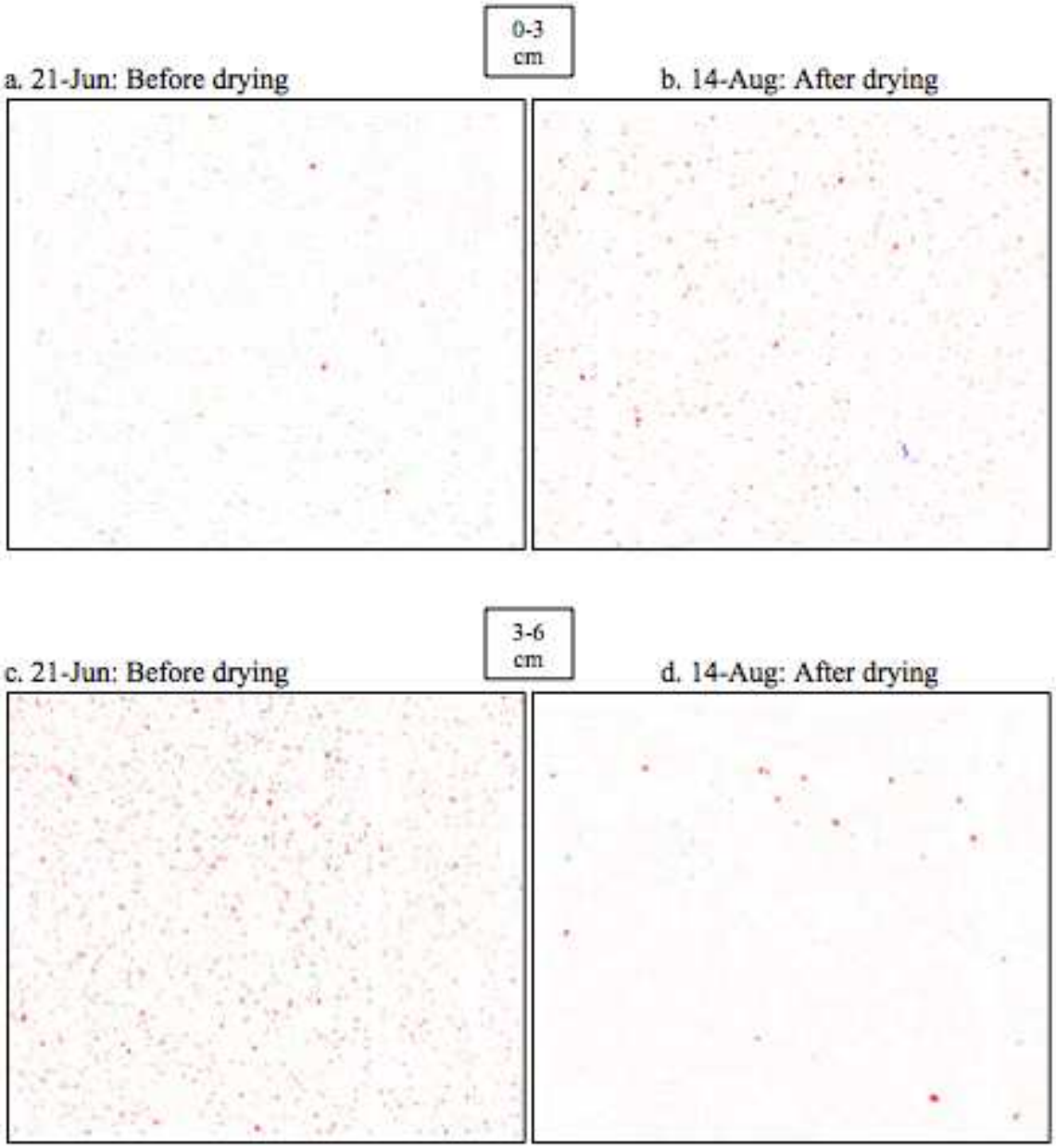

Figure 29. Representative images of each sample from QEMSCAN results before drying (left) and after drying (right) for horizons between 0-3 cm (a and b), 3-6 cm (c and d), 6-9 cm (e and f), and 9-12 cm (g and h). Dark colors, red, orange, green, and blue, indicate iron and other sulfides, sulphates, Fe-Cu-Ti-Ox/CO_3, and apatite, respectively. White represents silicates, carbonates, and background.

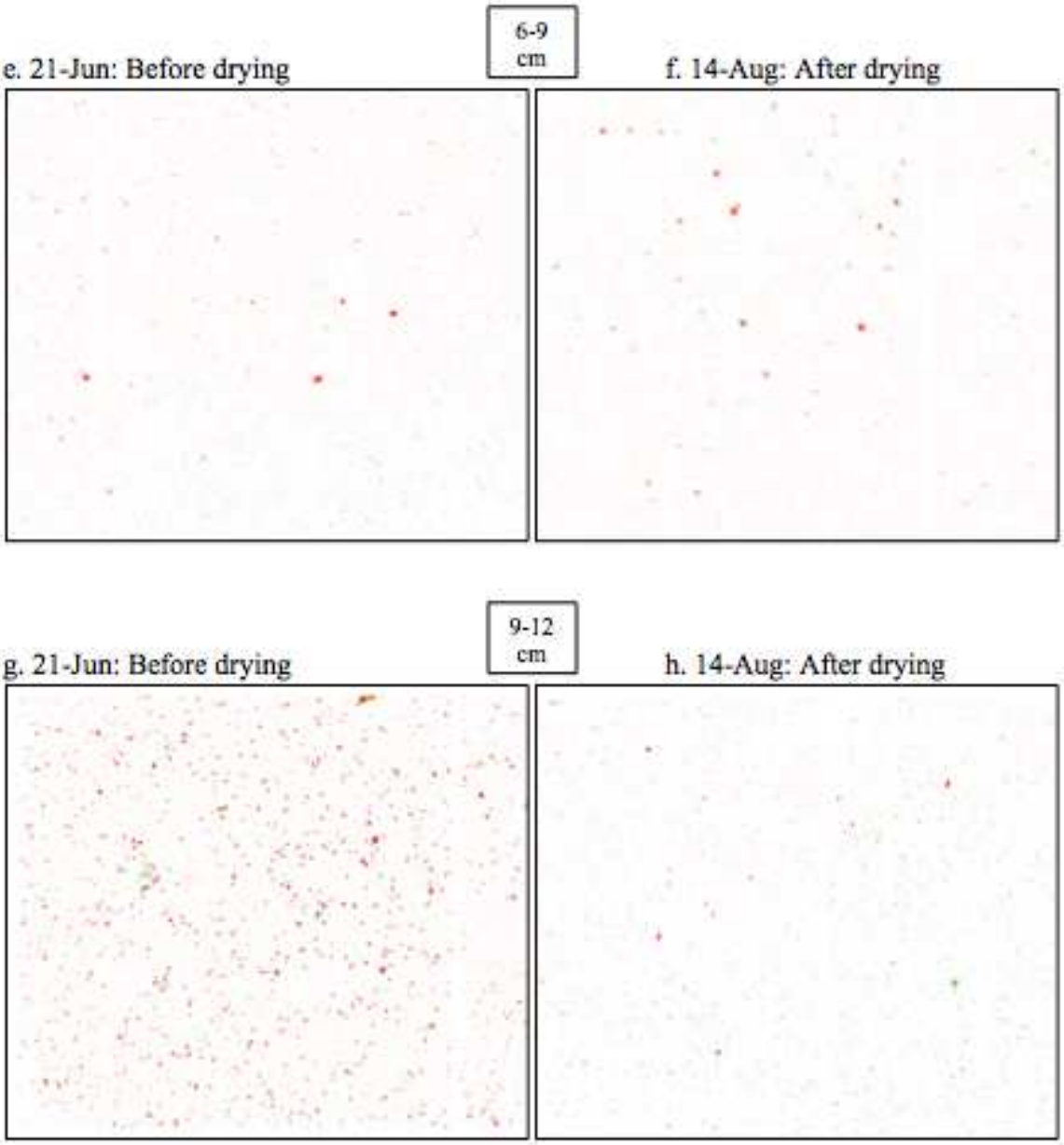

Figure 29. Continued.

3.4 Discussion

Changes in both sediment available phosphorus (Figure 24) and pore water dissolved phosphorus (Figure 25) indicate possible changes in the mobility of sediment phosphorus following the drying and re-flooding process. Pore water dissolved phosphorus increased 50 to 200% following oxidation and re-flooding. This could reflect oxidation of the upper 10 cm of sediment that oxidized during the months of July, August, and September. Enrichment of nitrogen isotopes following drying may indicate kinetic fractionation caused by the loss of nitrogen through volatilization (Figure 26).

Though it may not represent all labile phosphorus, the Olsen method is also used to approximate bioavailable phosphorus that can be taken up by algae or macrophytes in carbonate rich soils (Pierzynski, 2000). The Olsen method does not provide total phosphorus and is not suitable for determining net loss of phosphorus from the sediment. Available phosphorus data (Figure 24) indicates transformations of phosphorus that is more available for use by biological organisms. The 10% increase in available phosphorus at the top horizon of the sediment (0-3 cm) indicates oxidation of organic phosphorus, increasing its mobility to the water column.

QEMSCAN was relied upon to characterize total phosphorus on the sediment. This method was able to quantify changes in the sediment, such as the % area decrease in phosphorus at depths between 3-6 cm and 9-12 cm following drying (Figure 27). While apatite measurements are highly variable and undetectable in some samples, individual scans for total phosphorus of samples showed statistically significant changes following drying and oxidation.

Percent areal coverage (Figure 30) of iron and other sulphides, sulphates, and Fe-

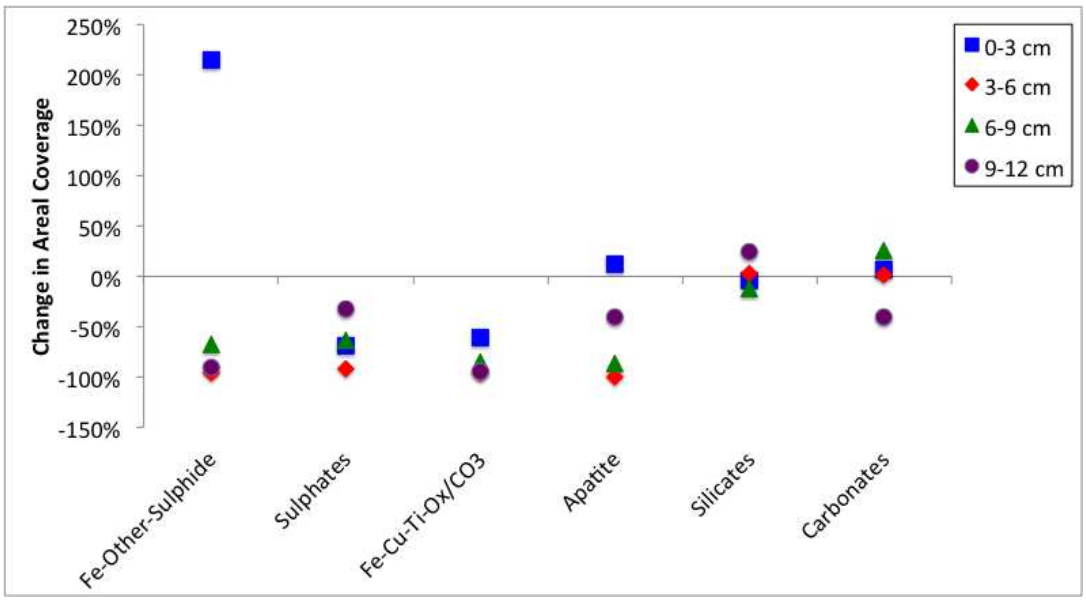

Figure 30. Change in percent areal coverage of each mineral category defined by QEMSCAN software for sediment horizons before and after drying.

Cu-Ti-Ox/CO_3 all decreased except for iron and other sulphides in the top horizon of the sediment (0-3 cm). This indicates a decrease in sulphur in the sediment following drying. A general decrease in iron and other sulphides was observed in all samples following drying and oxidation except for the 0-3 cm horizon. The small grain size led to edge effects, causing some uncertainty in the software when identifying sulphur and silicon minerals. The software creates an identity for the pixel that falls under the Fe-sulphide category and indicates that sulphur and silicon atoms are present in that pixel. This unknown mineral, labeled "S/Si Other ??," described 50-90% of the "Fe-Other-Sulphide" category and was the primary driver of differences between sediment before and after drying. This made it difficult to describe changes in sulphur species more quantitatively.

Elements of interest may have been washed into horizons below 12 cm due to rain events during the summer months when the sediment was dry. In order to determine if these minerals are removed from the sediment, analysis of samples collected after FB1 was re-flooded is necessary. The possibility of washing minerals lower into the sediment also requires analysis of sediment horizons below 12 cm. Dry FB1 sediment in 2013 was cracked down to approximately 10 cm, forming the blocks described above. Near 10 cm the consistency and appearance of the sediment changed and was similar to before the wetland was drained. To test the hypothesis of series 1 minerals washing into lower horizons, it is necessary to analyze sediment horizons well below the cracked and dried layer that develops after the wetland has been drained.

While QEMSCAN measurements provide extensive information at very high resolutions, that information may not be representative of the wetland or even the individual layer. Embedding sediment samples in epoxy and polishing the surface to

prepare for QEMSCAN analysis was problematic and often only 10-20% of the polished surface of the sediment was ideal for QEMSCAN analysis. It is unknown whether or not analyzing multiple locations on only one sample from each layer is representative of the entire sample, much less the horizon throughout the entire wetland. Analyzing multiple points on multiple samples from each layer and including multiple squeezer cores from the water body is required to more completely assess QEMSCAN's efficacy for characterizing changes in the sediment due to drying and oxidation.

4. SUMMARY

During 2012 and 2013 the Willard Spur nutrient cycling plots were exposed to a broad range of nutrient loads through the nutrient amendments. A significant difference in nutrient concentrations between plots was not measureable in the water column but plant responses varied significantly. Easy to measure parameters such as nutrient concentrations in the water column did not reflect the stress experienced by the plants demonstrated in sensitive SAV plant metrics.

Beginning around July 2012 and throughout 2013 the Willard Spur water levels decreased to where it was no longer flowing into the Great Salt Lake. This impoundment could possibly have a profoundly negative effect on the Willard Spur. The storage of the Willard Spur ranged between close zero when it dried in August 2013 and over 1,400 acre-feet in 2011 when it was flowing into the Great Salt Lake.

Impounded wetlands and sheet flow wetlands have distinct differences. The hydrologic and biologic conditions are far more varied in sheet flow wetlands relative to impounded wetlands (Carling et al., 2013). During high water years when the Willard Spur is connected to the Great Salt Lake soluble and suspended constituents are transported out of the wetland. Figure 21 shows the effect of the PWRWTP effluent would have on dissolved nutrient concentrations for 2012 water levels. However, these estimates do not include estimates for the uptake capacity of the Willard Spur and the

channel that connects the effluent outfall and the main body of the Willard Spur. Impounded conditions in the Willard Spur are vastly different than wet years where the area and volume of water is much greater. The increase in the area of the Willard Spur likely corresponds with an increase in its total uptake capacity as more sediment is submerged and SAV habitat expands.

Parameters indicating sheet flow wetland health are extraordinarily difficult to define and constrain. It is challenging to identify indicators of wetland health in systems with multiple "functional states" (Ostermiller, 2013). These results indicate that sediment and surface water chemistry both influence plant health in the various functional states of the Willard Spur. This is especially true in sheet flow wetlands with wide ranges of hydrologic conditions that support SAV growth. Plant health metrics such as those developed by Hoven et al. (2013) coupled with a variety of sediment and surface water parameters, possibly specific to individual water bodies, provide the most complete picture of wetland health.

APPENDIX

SUPPLEMENTAL INFORMATION

A.1 Details of Experimental Design

Figures 31 and 32 show the experimental design for 2012 and 2013, respectively. Only Osmocote™ was used in the 2012 amendments (Table 6). Osmocote™ has mass ratio of 19-6-12 NPK (nitrogen-phosphorus-potassium) ratio with 9% of the nitrogen in the form of nitrate and 10% in the form of ammonia. Dissolved phosphorus target concentrations in the 2012 high and low water column plots of 0.4 and 0.1 mg/L, respectively, became the 2013 high and medium water column plots (Table 7). The 2013 low water column plot dissolved phosphorus target concentration was set at 0.05 mg/L.

In 2013 about 4% (by mass) of the fertilizer mixture was uncoated urea (46-0-0 NPK ratio). Urea is soluble and this fertilizer dissolved within two days during dissolution tests. This fraction of the mixture was intended to be a short-term source of nutrients early in the growing season. About 36% of the fertilizer mixture was polymer-coated urea fertilizer (39-0-0 NPK ratio) designed to release nitrogen for about 45 days. Release of the coated urea was dependent on the breakdown of the polymer coating over time.

The remaining 60% of the mixture was coated Osmocote Smart Release™

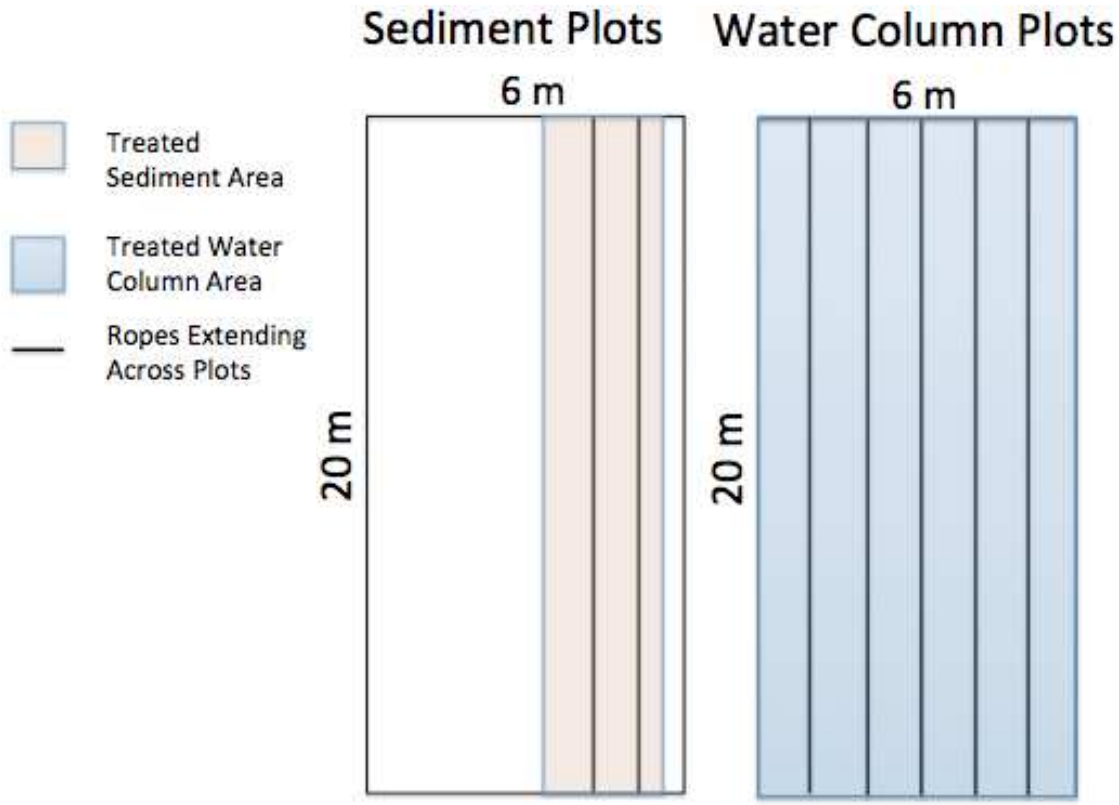

Figure 31. The area of plots where sediment and water column was amended with Osmocote Smart Release ™ fertilizer.

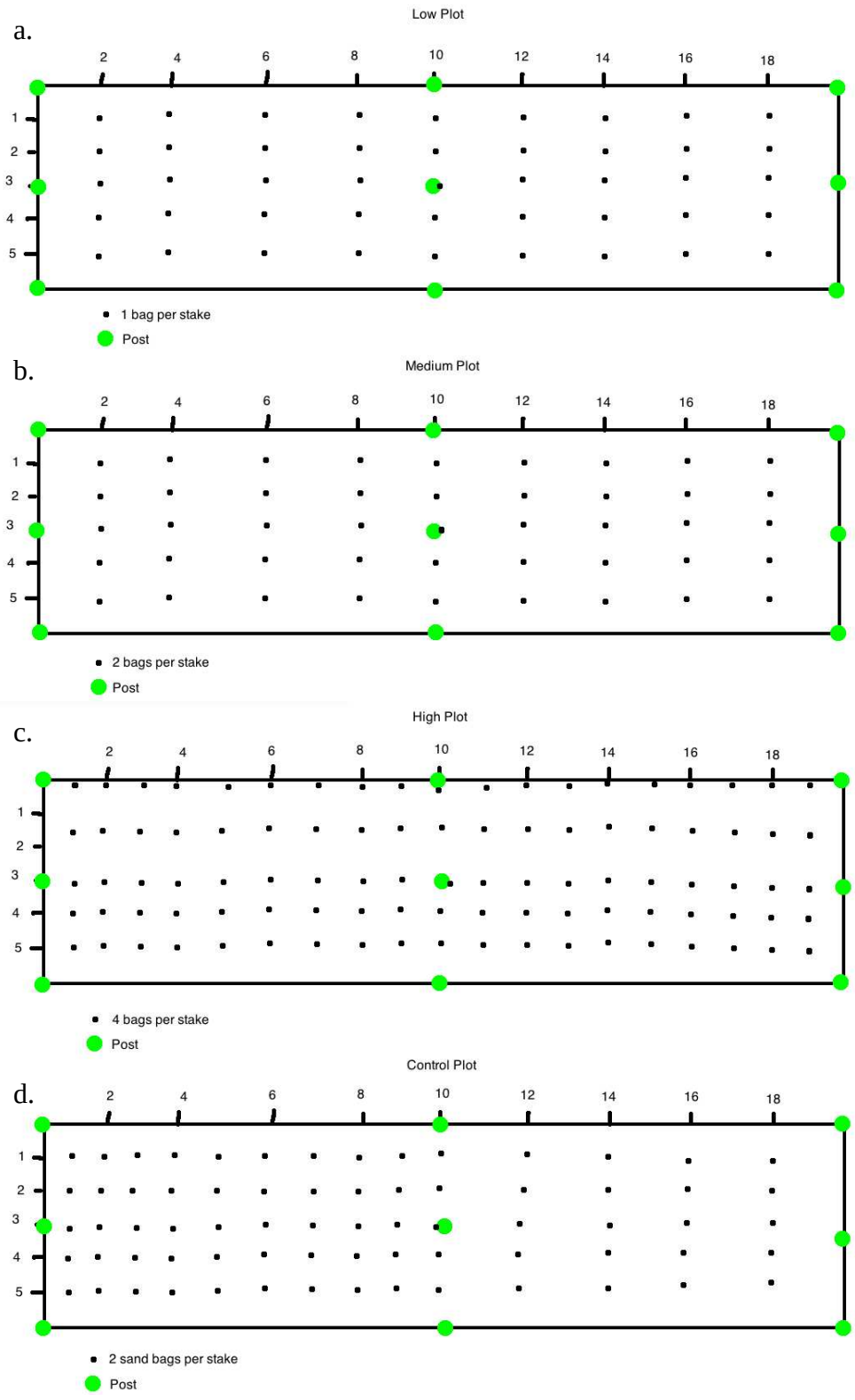

Figure 32: Distribution of stakes and fertilizer in a) low, b) medium, c) high, and d) control 2013 water column plots.

Table 6. Mass of fertilizer in 2012 sediment and water column plots.

Mass of Fertilizer Added		
	Osmocote Smart Release™ per plot (kg)	Total Mass of Fertilizer per plot (kg)
High Sediment	160	160
Low Sediment	80	80
High Water Column	134	134
Low Water Column	34	34

Table 7. Mass of fertilizer in 2013 water column amendment plots.

Mass of Fertilizer Added			
	Osmocote Smart Release™ (kg)	Urea (coated and uncoated) (kg)	Total Mass of Fertilizer (kg)
High Water Column	91.2	60.8	152
Medium Water Column	21.6	14.4	36
Low Water Column	10.8	7.2	18

fertilizer (19-6-12 NPK ratio), the same fertilizer that was used in 2012. As mentioned previously, Osmocote ™ is designed to release nutrients for 3-4 months, depending on the temperature. This fraction was intended to release nutrients throughout the warmer months. Temperatures during sample events did not begin to consistently reach above 60 °F until early to mid June 2013.

A.2 2012 and 2013 Sample Analysis Plans

Tables 8 and 9 describe the sample analysis plans for 2012 and 2013, respectively. Analysis was conducted at three laboratories at the University of Utah; SIRFER in the Department of Biology and the ICP MS Metals Lab and Johnson Lab, both in the Department of Geology and Geophysics. Sediment samples were also sent to the USUAL lab at Utah State. Surface water samples were analyzed at the Utah State Health Laboratory in Taylorsville, UT.

A.3 2012 and 2013 Supplementary Data

Figures 33 through 46 show supplementary sediment and surface water data collected and analyzed in 2012. Figures 47 through 55 show supplementary sediment and surface water data collected and analyzed in 2013. Figures 56 and 57 show supplementary data from FB1 collected in 2013. These results do not show significant differences between plots. This data indicates seasonal changes observed over the sampling season and was analyzed to look for possible influences on SAV. Details are provided in a collaborative report that summarizes results from the entire project (Hoven et al., in preparation).

Table 8. 2012 water and sediment chemistry and number of samples per metric, per treatment plot by month and total sample number for all six plots. The number of samples collected each month per plot is provided for each metric. ‡ = up to six plots.

Surface Water	Method	June	July	Aug	Sept	Oct	2012 Total
U of U: Johnson Lab							
Field Parameters		3-4	1	1	1	1	47
Filtered Trace Elements[1]	EPA 200.8-Metals	3-4					23
Total and Methyl Mercury	EPA 1631E-THg; EPA 1630-MeHg	1	1	1		1	24
Dissolved NO_3-N and PO_4-P	EPA 300.0-DISS	3-4	4	3	3	3	101
Utah State Health Lab							
Filtered Trace Metals[2]	EPA 200.8-DISS	3-4					23
Carbonaceous BOD	EPA 405.1	3-4	1	1	1	1	47
Unfiltered Nutrients							
Ammonia, NO_3-N+NO_2-N, TP, TKN	EPA 350.3, 353.2, 365.1, 351.4	3-4	3	3	3	3	95
Filtered Nutrients							
NO_3-N+NO_2-N, TP, TN	EPA 353.2-DISS, 365.1-DISS, 4500N-DISS	3-4	3	3	3	3	95
General Chemistry							
TSS, TVS, Turbidity, Alkalinity, TDS, Sulfate	EPA 160.2, 160.4, 180.1, 2320B, 2540C, 375.2	3-4	3	3	3	3	95
Sediment	**Method**	**June**	**July**	**Aug**	**Sept**	**Oct**	**2012 Total**
U of U: SIRFER Lab							
N, C Content: Total/organic, isotopes		3	1	1	1	1	42
U of U: Johnson Lab							
Trace elements	EPA 200.8-Metals	3					18
Total and methyl mercury	EPA 1631E-THg; EPA 1630-MeHg	3	1	1	1	1	42
Utah State University Analytical Laboratories							
Nutrients (NO_3-N, P, K)		3	1	1	1	1	42
pH/Salinity		3	1	1	1	1	42
Metals (Zn, Fe, Cu, Mn, S)		3	1	1	1	1	42
Organic Matter		3	1	1	1	1	42
Nutrient Flux		Up to 3			Up to 3		Up to 36 ‡

1. Li, Be, Na, Mg, Al, P, K, Ca, Sc, Ti, V, Cr, Mn, Fe, Co, Ni, Cu, Zn, As, Se, Rb, Sr, Y, Mo, Ag, Cd, Sb, Cs, Ba, La, Ce, Nd, Sm, Gd, Tb, Dy, Ho, Lu, Tl, Pb, U.
2. B, Ca, Fe, Mg, K, As, Ba, Cd, Cr, Cu, Pb, Mn, Ni, Al.

Table 9. 2013 water and sediment chemistry and number of samples per metric, per treatment plot and total sample number for the four plots. The number of samples collected each month is provided for each metric. Three samples were collected per plot and one sample was collected at the ambient site.

Surface Water	**Method**	**Samples Per Event**	**Sample Events Collected**	**2013 Total**
U of U: Johnson Lab				
Field Parameters		5	8	40
Total and Methyl Mercury	EPA 1631E-THg; EPA 1630-MeHg	5	3	15
Dissolved NO_3-N and PO_4-P	EPA 300.0-DISS	13	8	104
Utah State Health Lab				
Carbonaceous BOD	EPA 405.1	5	8	40
Ammonia, NO_3-N+NO_2-N, TP, TKN	EPA 350.3, 353.2, 365.1, 351.4	13	8	104
NO_3-N+NO_2-N, TP, TN	EPA 353.2-DISS, 365.1-DISS, 4500N-DISS	13	8	104
TSS, TVS, Turbidity, Alkalinity, TDS, Sulfate	EPA 160.2, 160.4, 180.1, 2320B, 2540C, 375.2	13	8	104
Sediment	**Method**	**Samples Per Event**	**Sample Events Collected**	**2013 Total**
U of U: SIRFER Lab				
Total/organic: N/C Content, isotopes		12	4	48
Utah State University Analytical Laboratories				
Nutrients (NO_3-N, ammonia, available P)		12	4	48
Organic Matter		12	4	48

a.

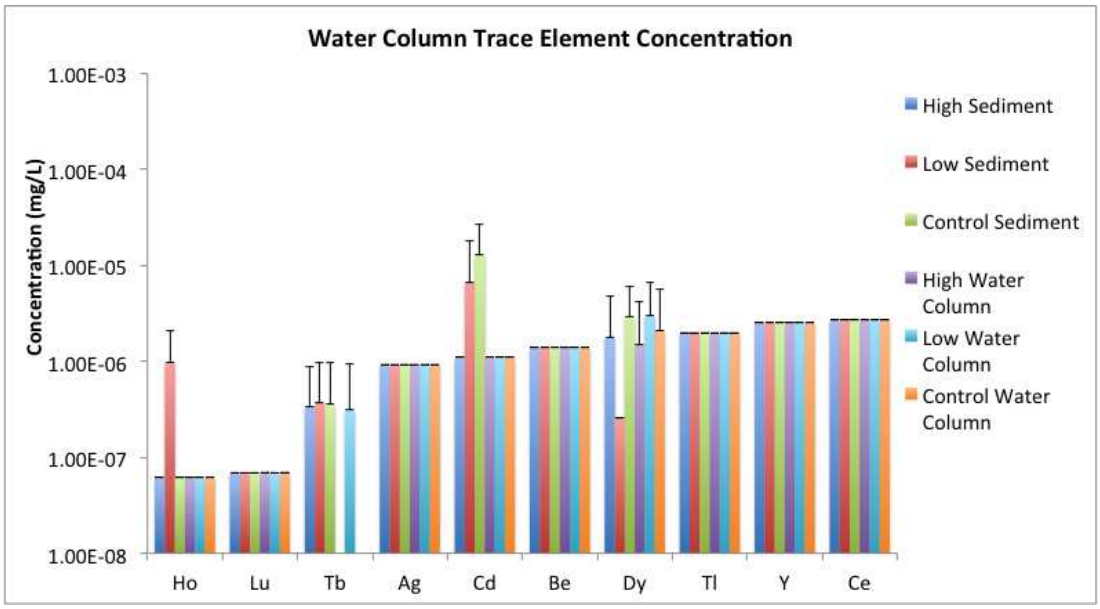

b.

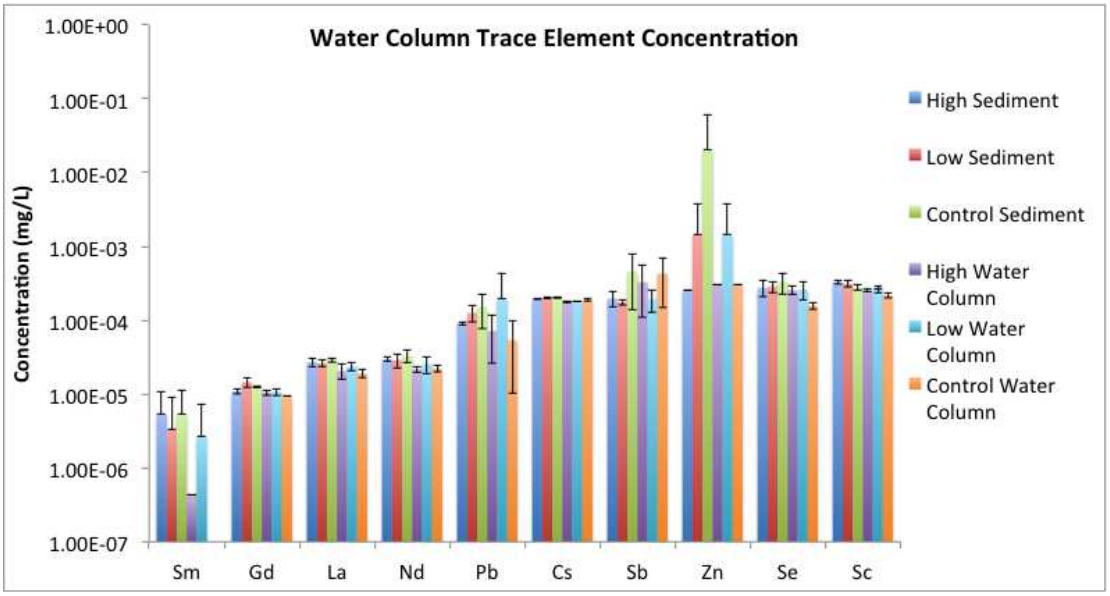

Figure 33. Dissolved trace element concentrations for all elements measured with concentrations primarily less than a) 1E-5 mg/L, b) 1E-3 mg/L, c) 1E-2 mg/L, and d) all concentrations remaining. Error bars represent one standard deviation (n=4 excluding Control Water Column where n=3).

c.

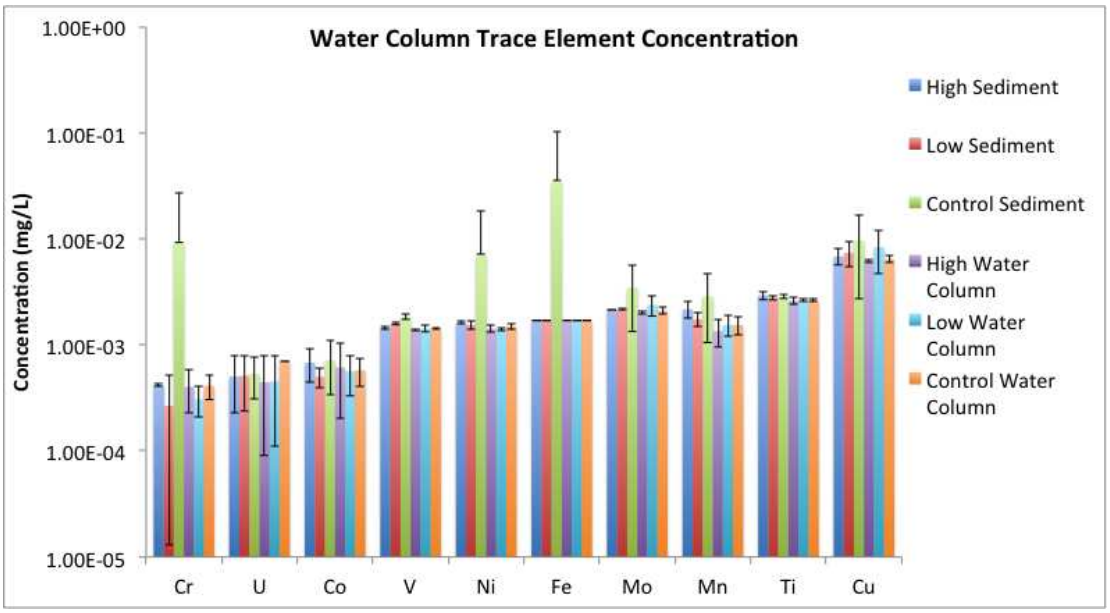

d.

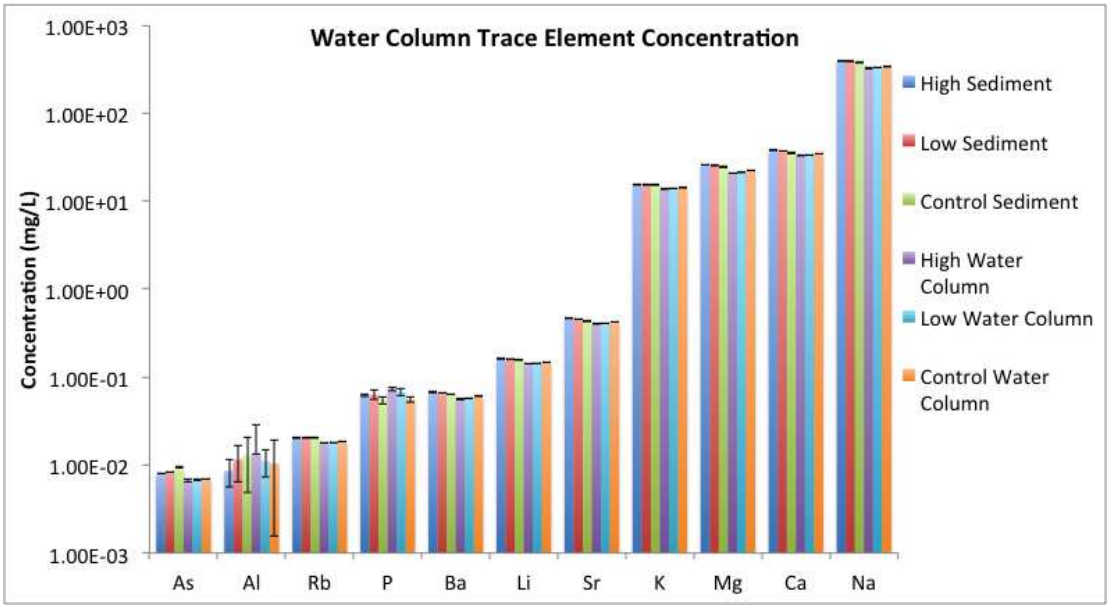

Figure 33. Continued.

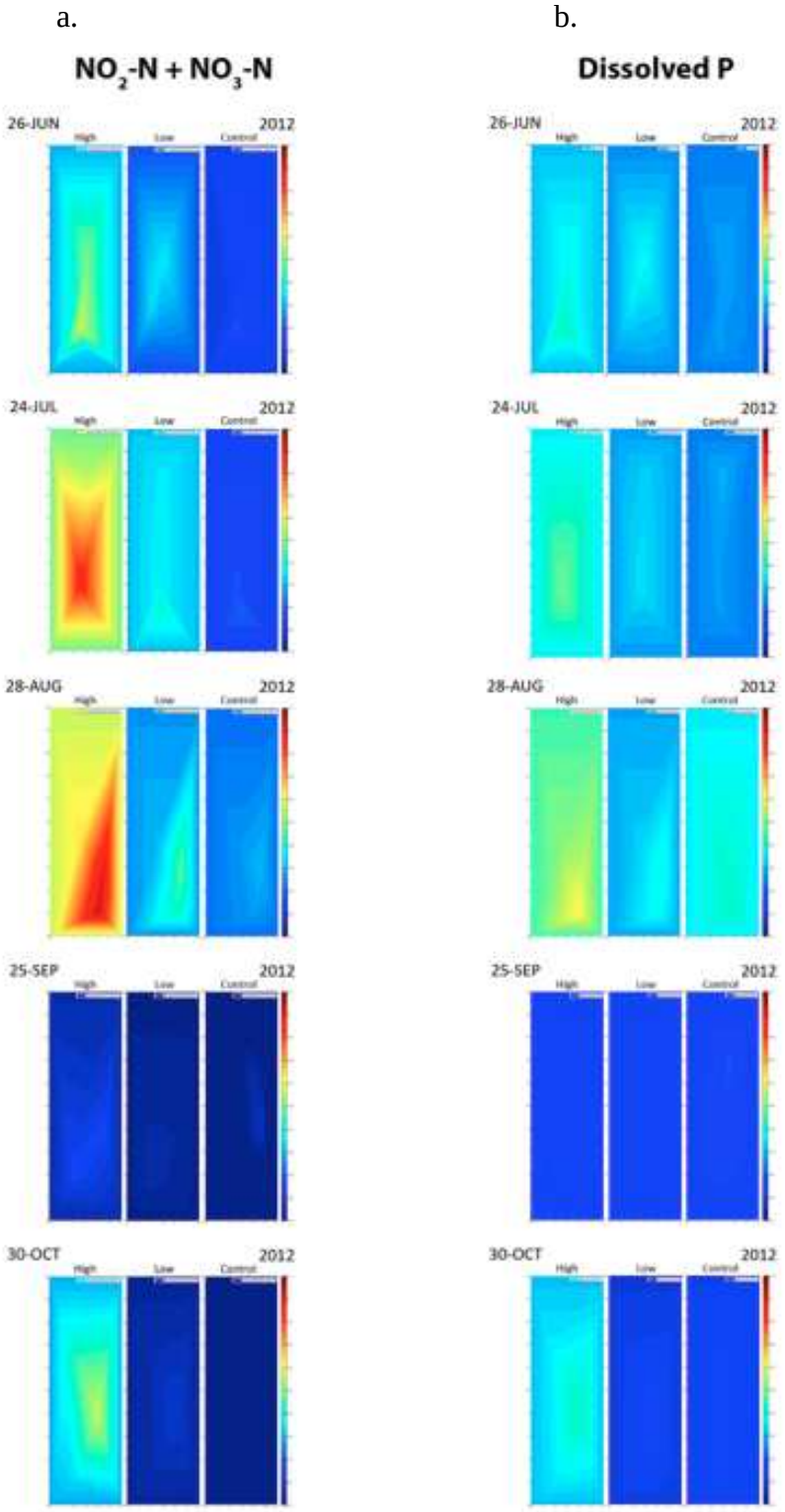

Figure 34. 2D plots of a) dissolved nitrite + nitrate and b) dissolved P concentrations for filtered surface water samples. Boundary values were set at 90% of lowest value measured in the plot (n=3 except for June samples where n=4, excluding June Control Water Column where n=3).

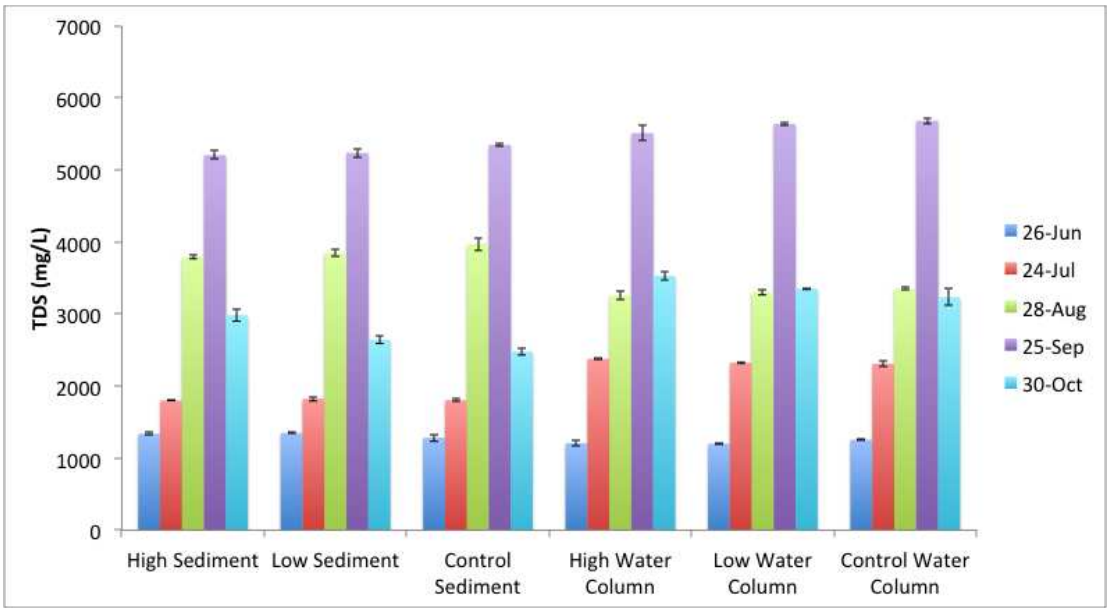

Figure 35. Total dissolved solids for unfiltered surface water samples. Error bars represent one standard deviation (n=3 except for June samples where n=4, excluding June Control Water Column where n=3).

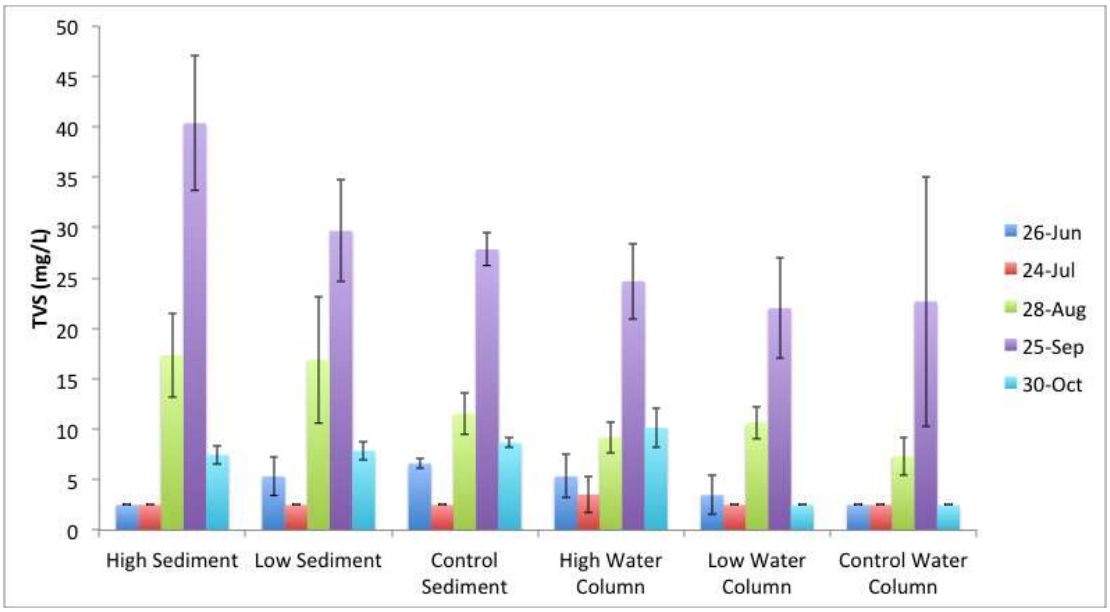

Figure 36. Total volatile solids for unfiltered surface water samples. Error bars represent one standard deviation (n=3 except for June samples where n=4, excluding June Control Water Column where n=3).

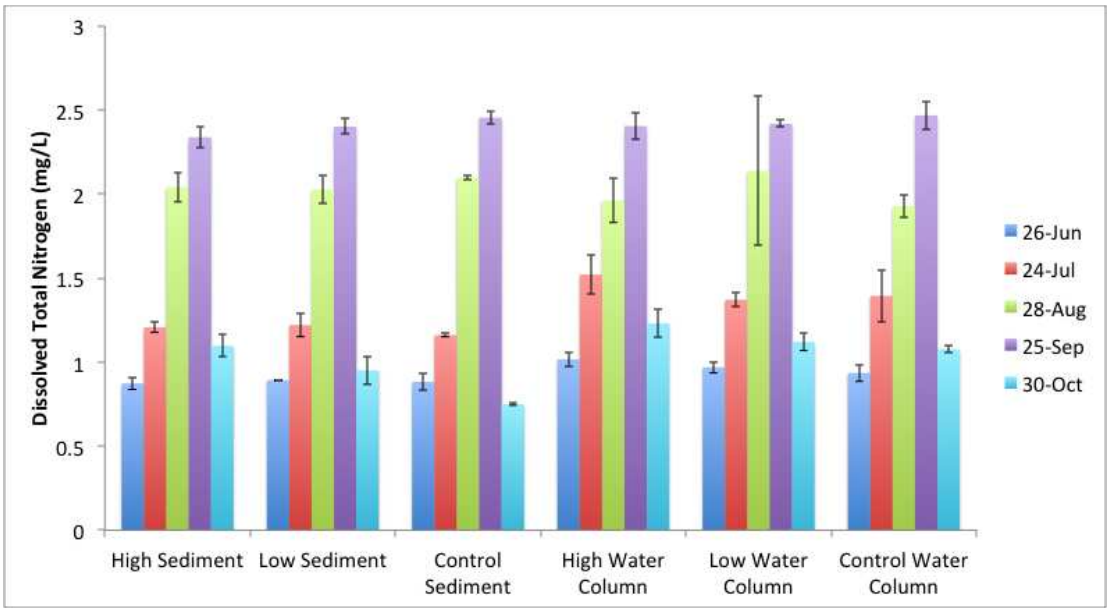

Figure 37. Dissolved total nitrogen for filtered surface water samples. Error bars represent one standard deviation (n=3 except for June samples where n=4, excluding June Control Water Column where n=3).

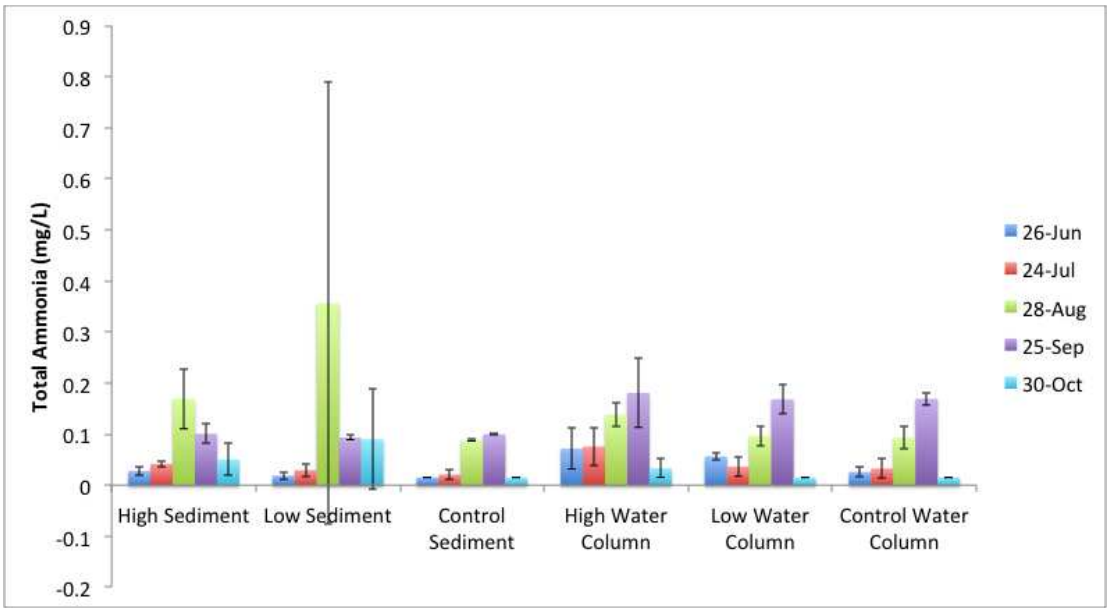

Figure 38. Total ammonia for unfiltered surface water samples. Error bars represent one standard deviation (n=3 except for June samples where n=4, excluding June Control Water Column where n=3).

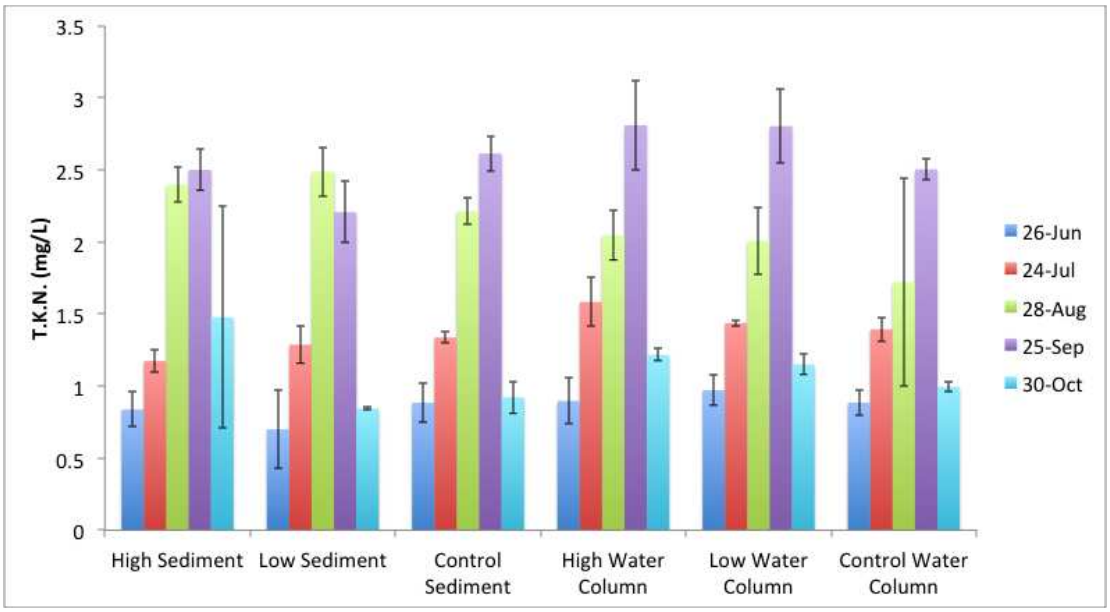

Figure 39. TKN for unfiltered surface water samples. Error bars represent one standard deviation (n=3 except for June samples where n=4, excluding June Control Water Column where n=3).

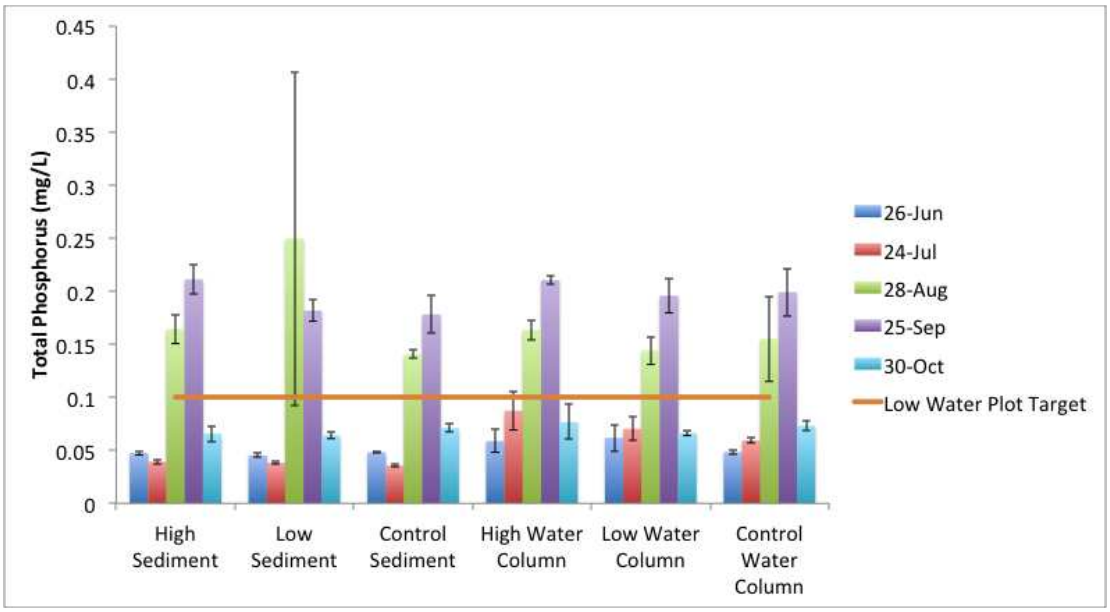

Figure 40. Unfiltered total phosphate (n=3 except for June samples where n=4, excluding June Control Water Column where n=3).

a.

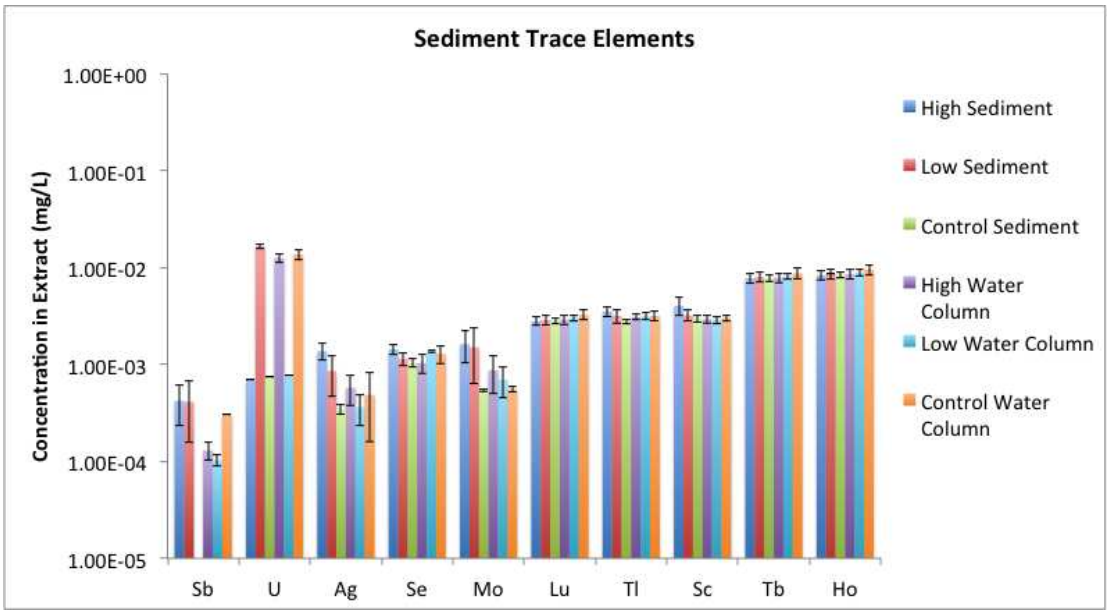

b.

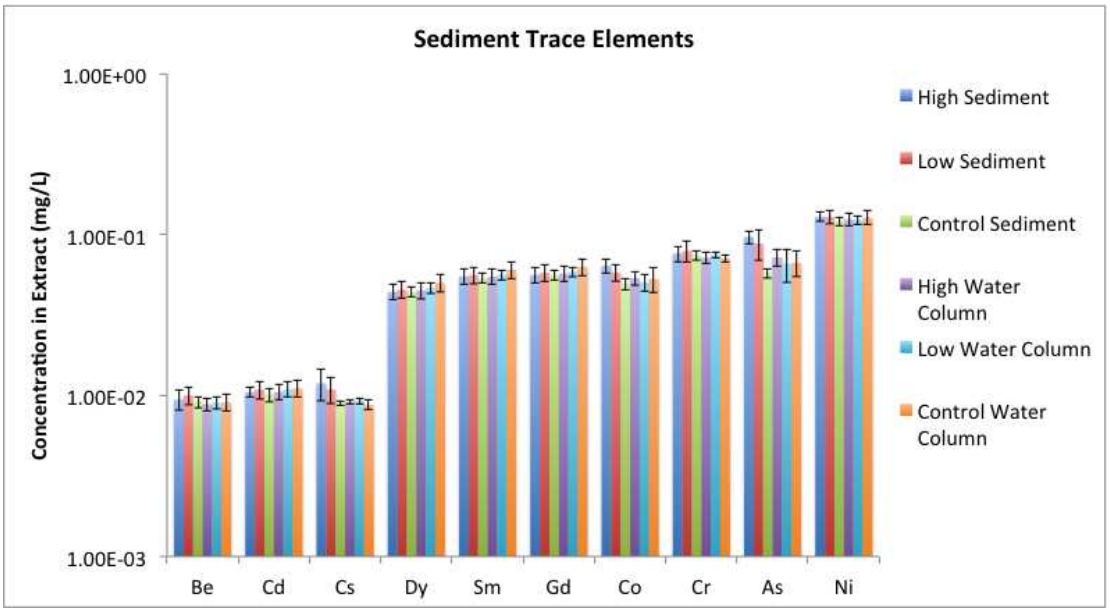

Figure 41. Sediment trace metals represented by the concentration of trace elements in the extract for concentrations primarily less than a) 1E-2 mg/L, b) 1E-1 mg/L, c) 1 mg/L, and d) all concentrations remaining.. Error bars represent one standard deviation (n=3).

c.

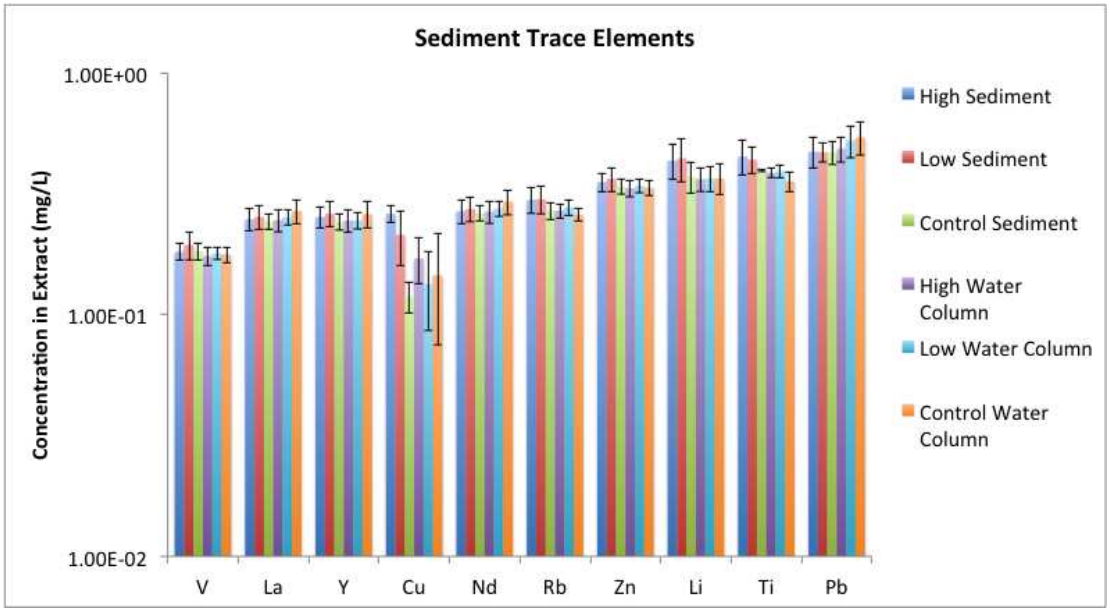

d.

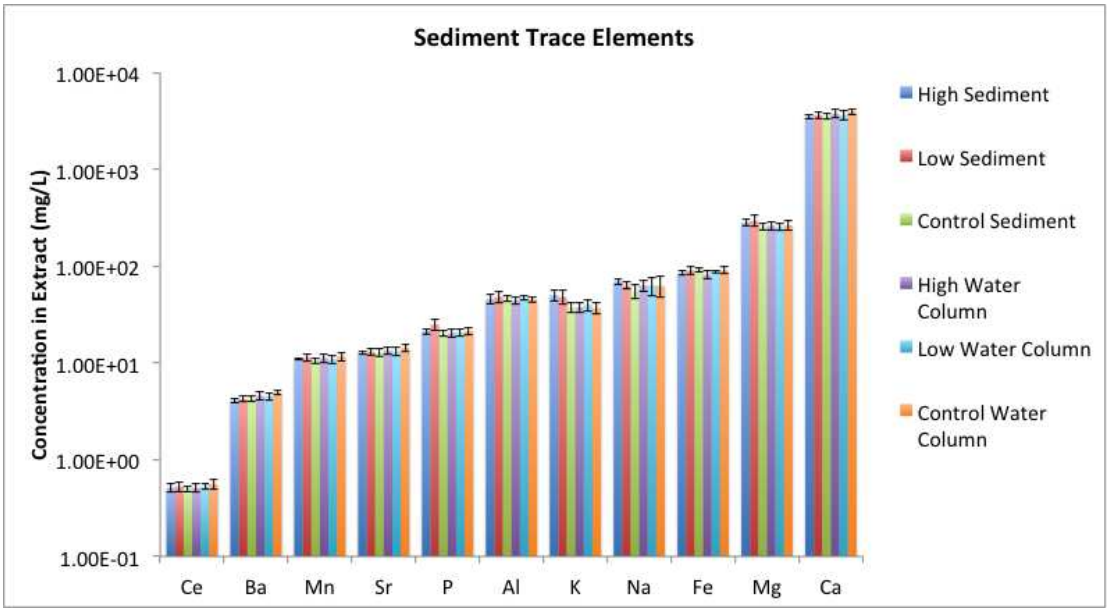

Figure 41. Continued.

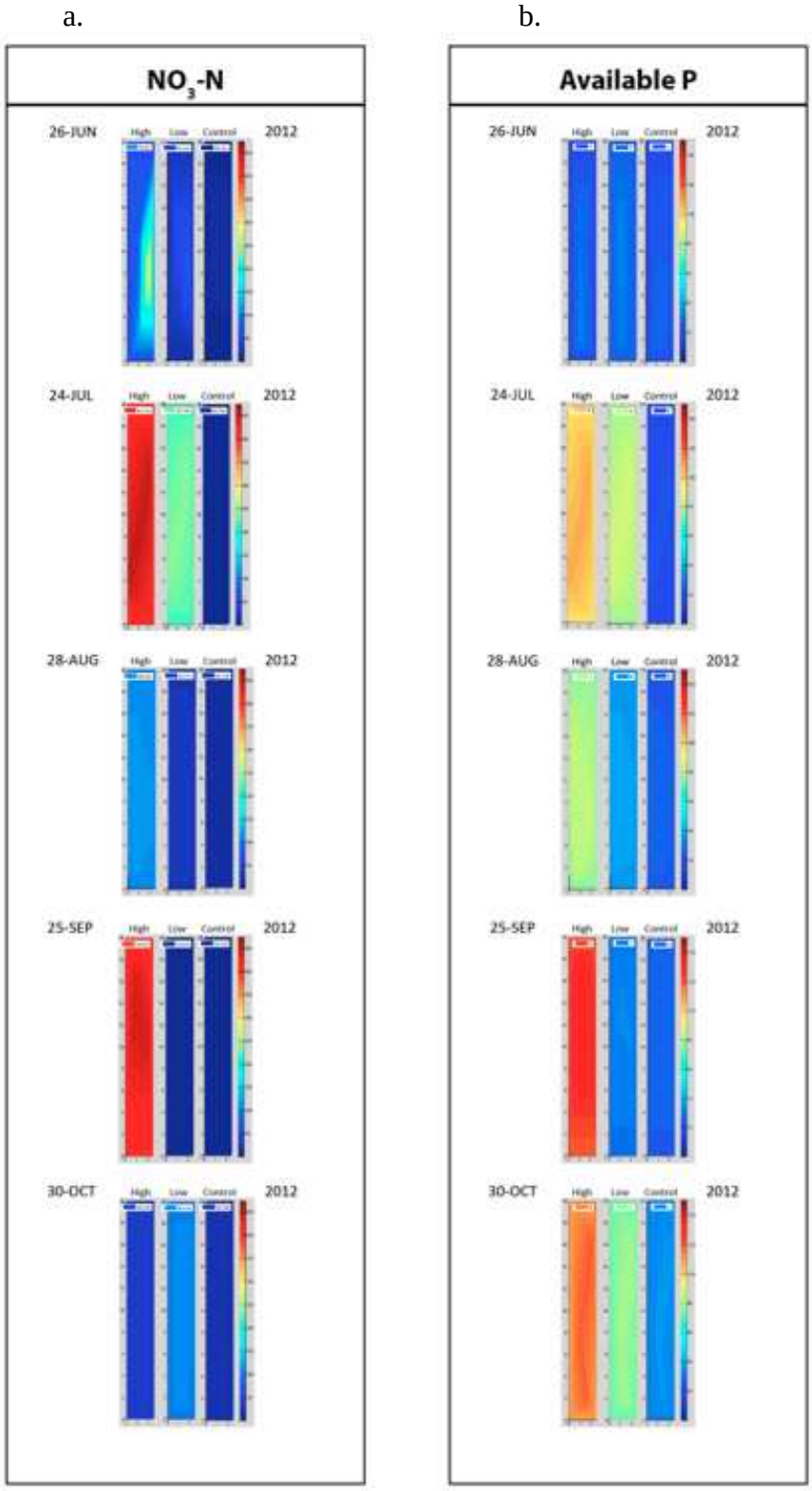

Figure 42. Sediment concentrations for a) nitrate and b) available phosphorus in amended sediment plots. Three samples were collected in random locations. Boundary values were set at 90% of lowest value measured in the plot (n=3 except for June samples where n=4, excluding June Control Water Column where n=3).

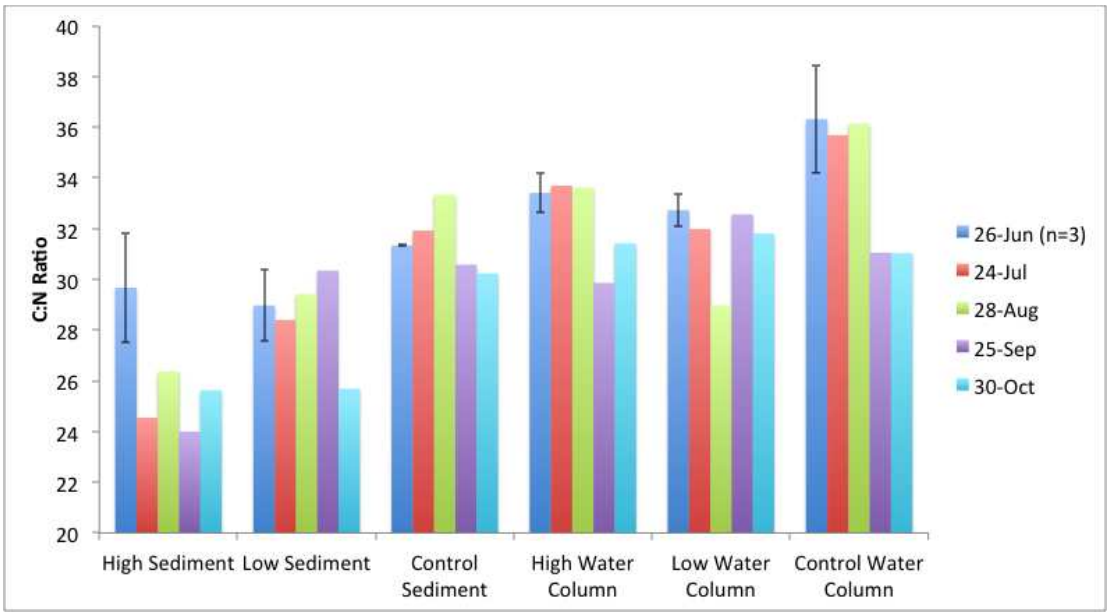

Figure 43. Sediment C:N ratio. Error bars represent one standard deviation (n=3).

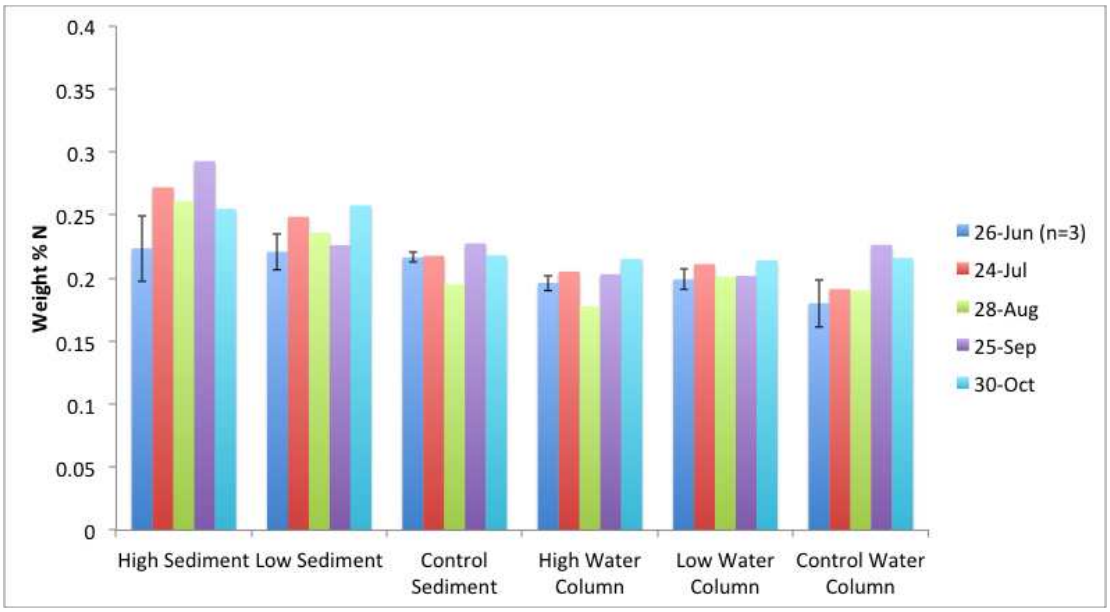

Figure 44. Total weight percent nitrogen. Error bars represent one standard deviation (n=3).

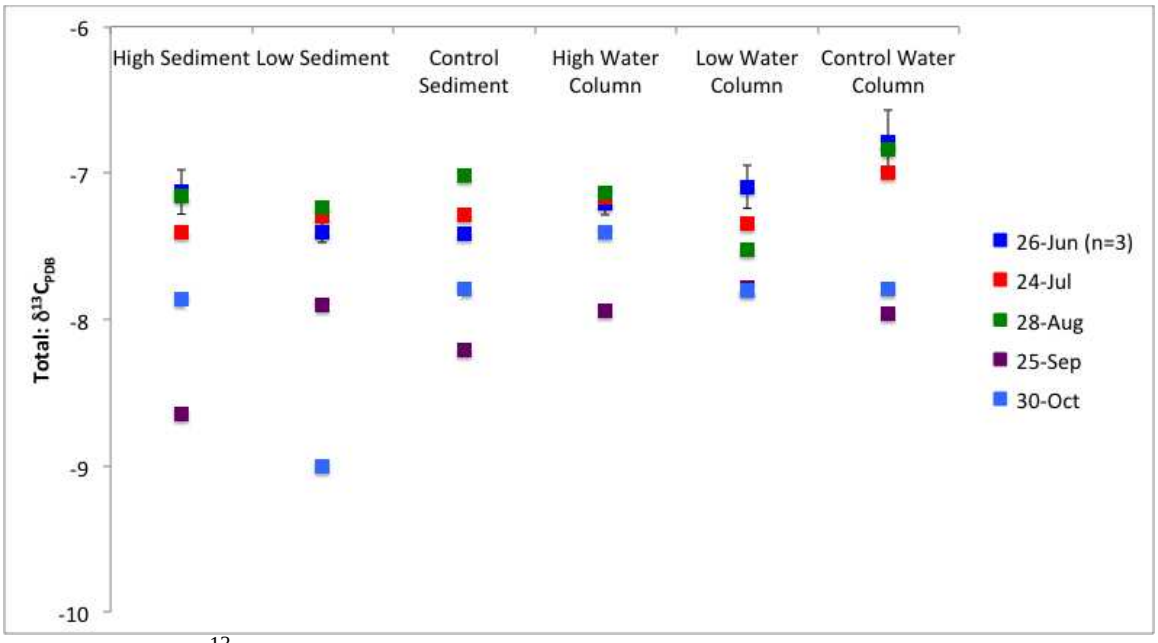

Figure 45. Total $\delta^{13}C_{PDB}$. Error bars represent one standard deviation (n=3).

a. b.

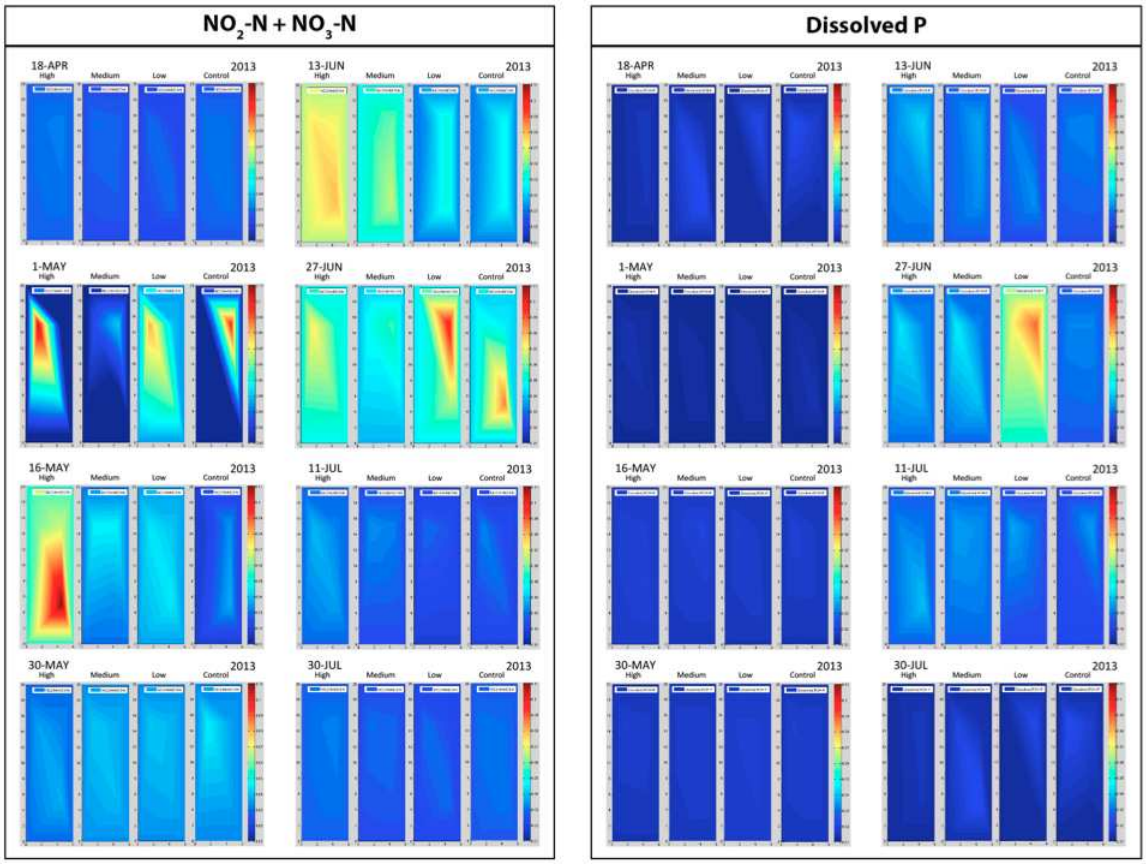

Figure 46. Surface water concentrations for a) dissolved nitrite + nitrate and b) dissolved P 2D plots for filtered surface water samples. Error bars represent one standard deviation (n=3 except for June samples where n=4, excluding June Control Water Column where n=3).

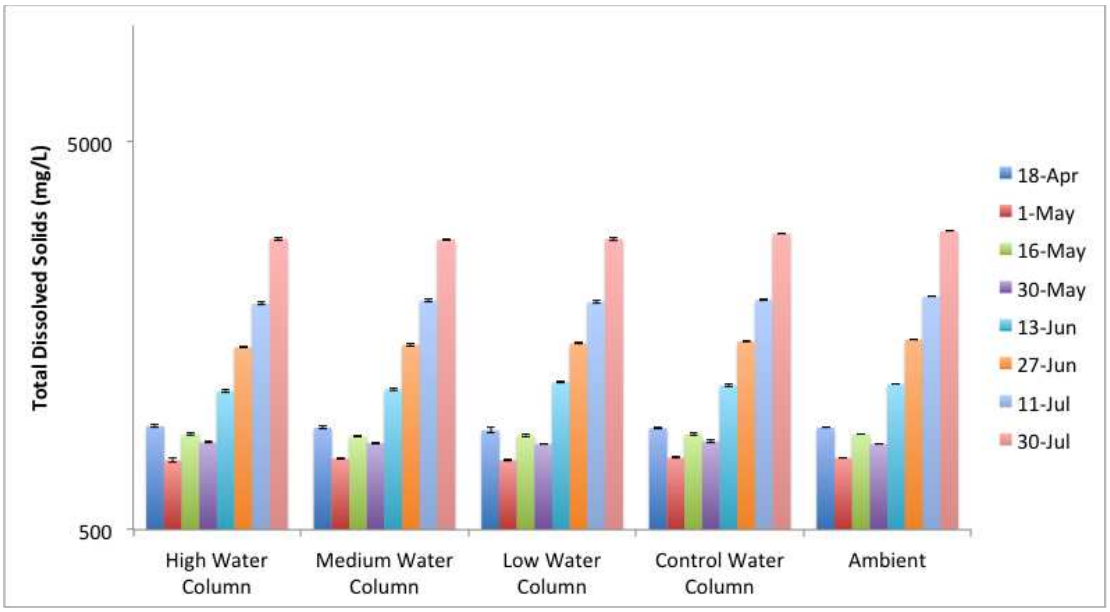

Figure 47. Total dissolved solids for unfiltered surface water samples. Error bars represent one standard deviation (n=3 except for June samples where n=4, excluding June Control Water Column where n=3).

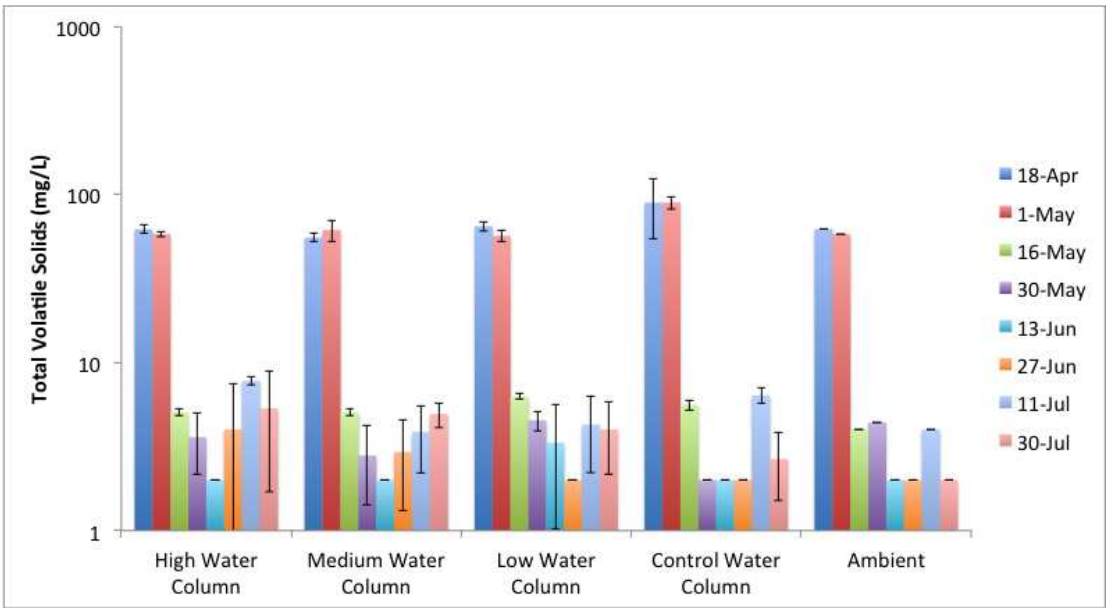

Figure 48. Total volatile solids for unfiltered surface water samples. Error bars represent one standard deviation (n=3 except for June samples where n=4, excluding June Control Water Column where n=3).

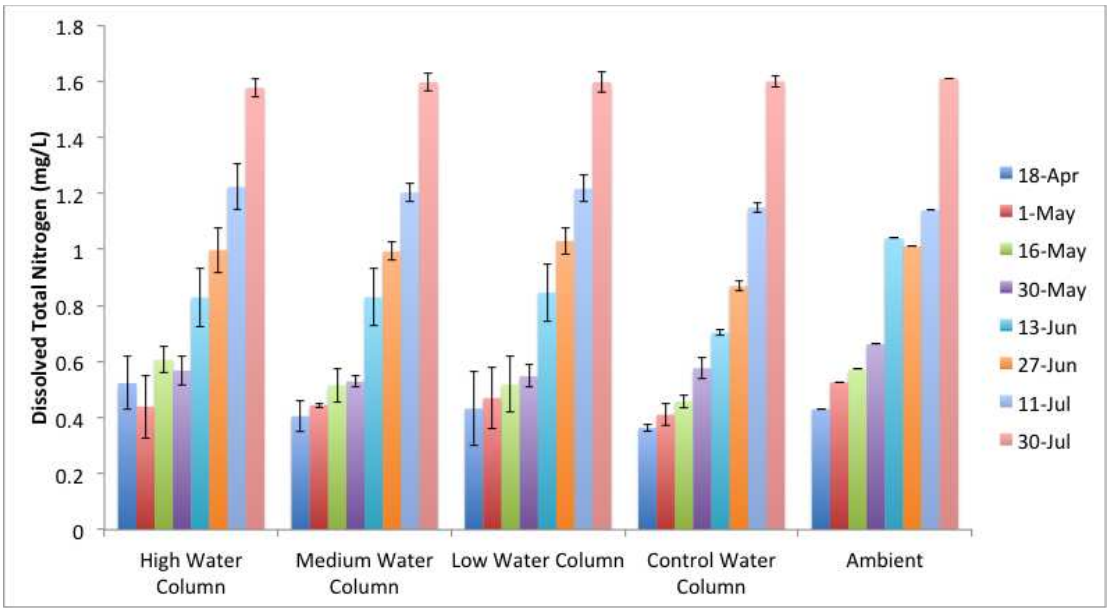

Figure 49. Dissolved total nitrogen for filtered surface water samples. Error bars represent one standard deviation (n=3 except for June samples where n=4, excluding June Control Water Column where n=3).

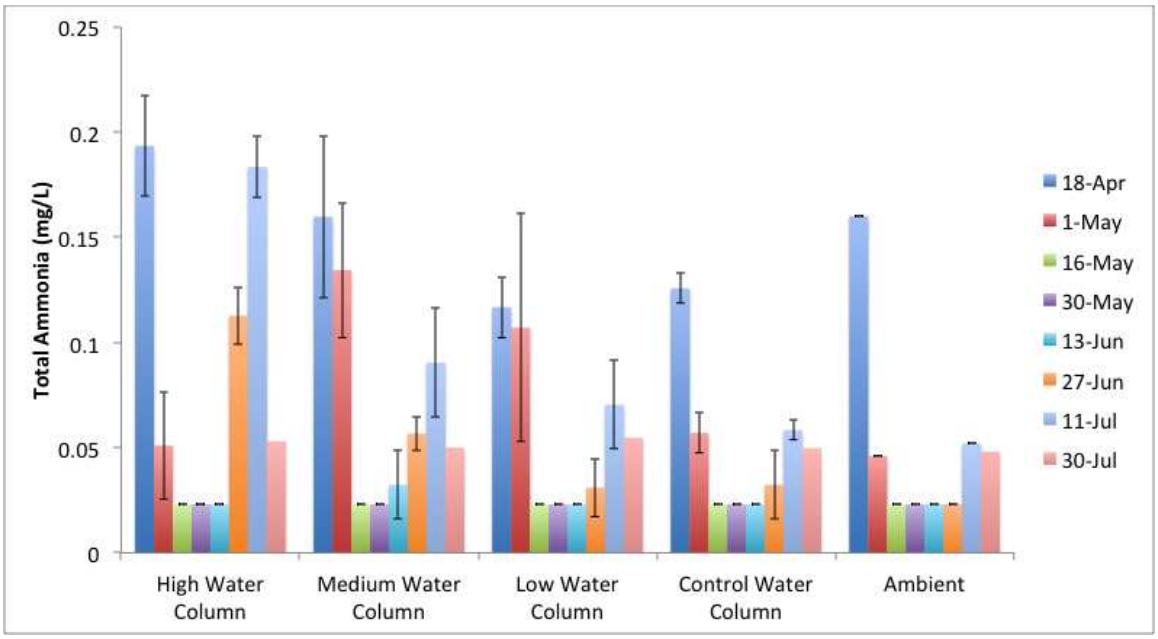

Figure 50. Total ammonia for unfiltered surface water samples. Error bars represent one standard deviation (n=3 except for June samples where n=4, excluding June Control Water Column where n=3).

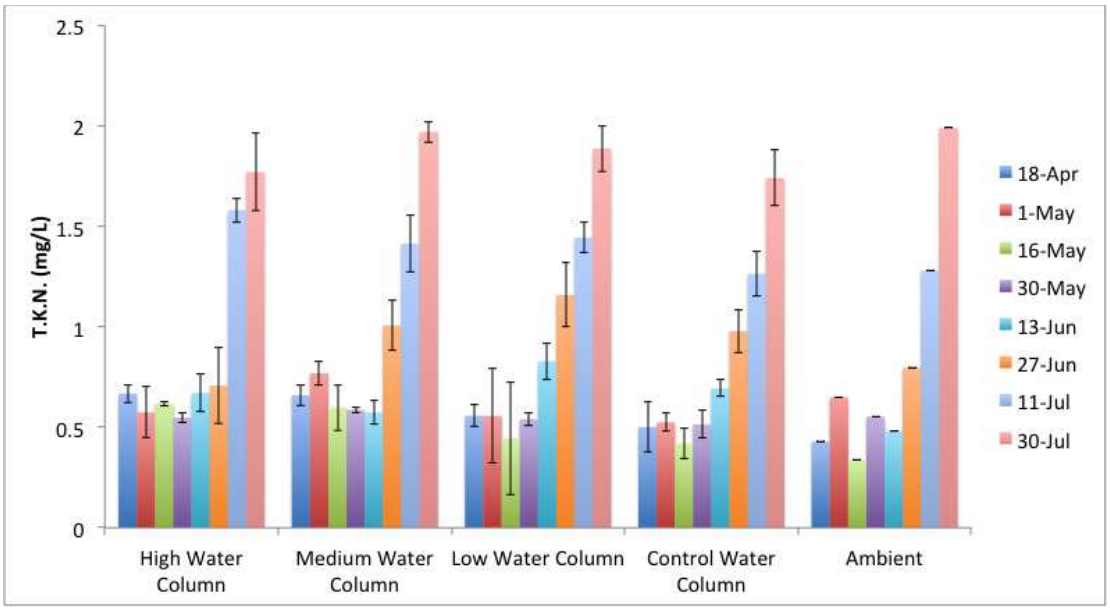

Figure 51. TKN for unfiltered surface water samples. Error bars represent one standard deviation (n=3 except for June samples where n=4, excluding June Control Water Column where n=3).

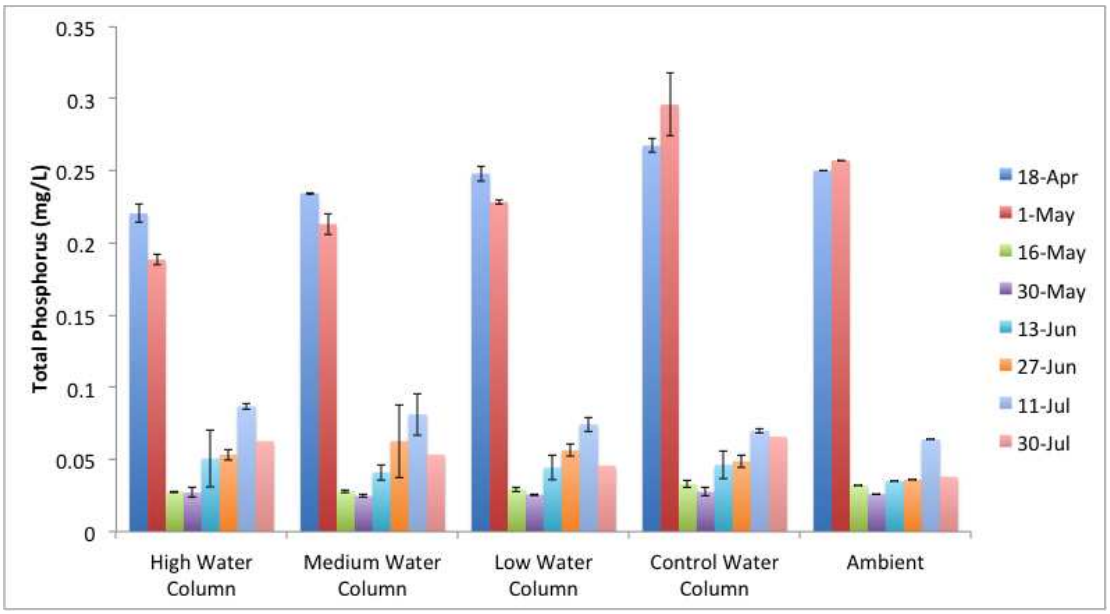

Figure 52. Unfiltered total phosphate (n=3 except for June samples where n=4, excluding June Control Water Column where n=3).

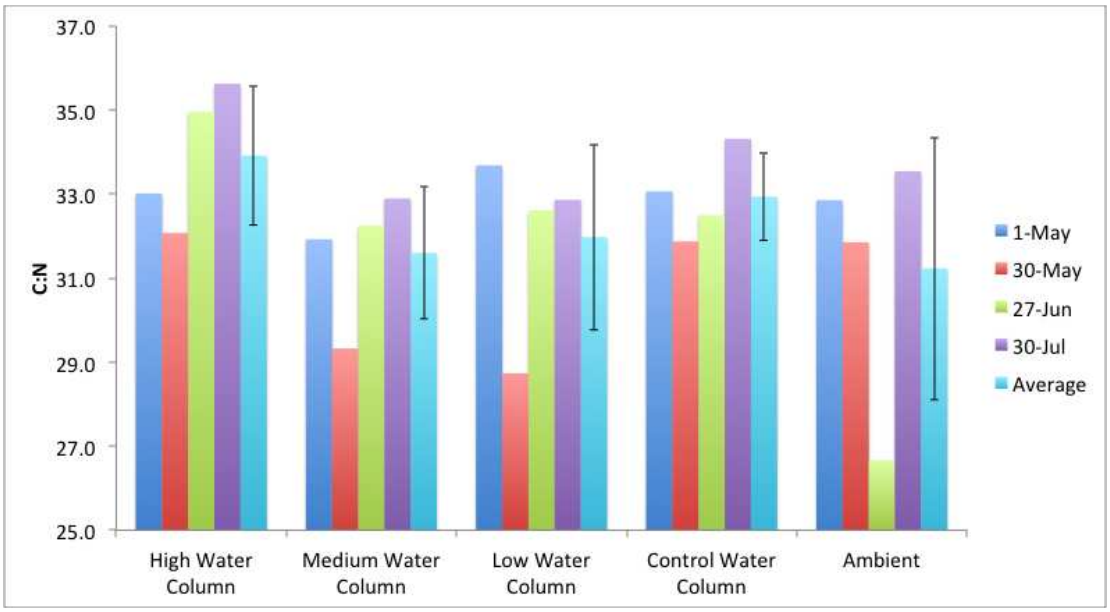

Figure 53. Sediment C:N ratio. Error bars represent one standard deviation (n=3).

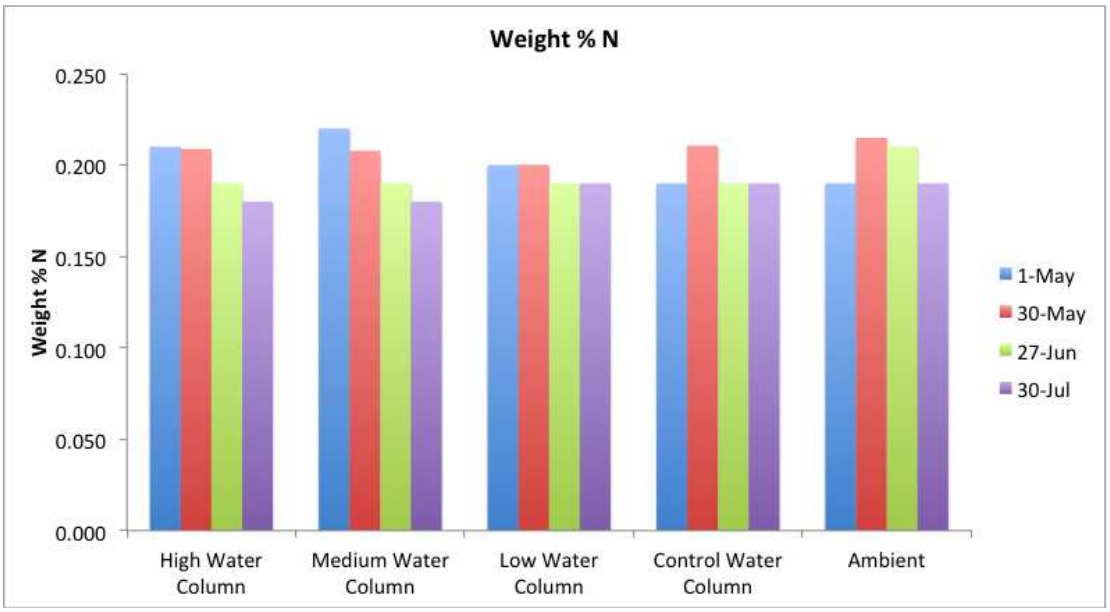

Figure 54. Total weight percent nitrogen. Error bars represent one standard deviation (n=3).

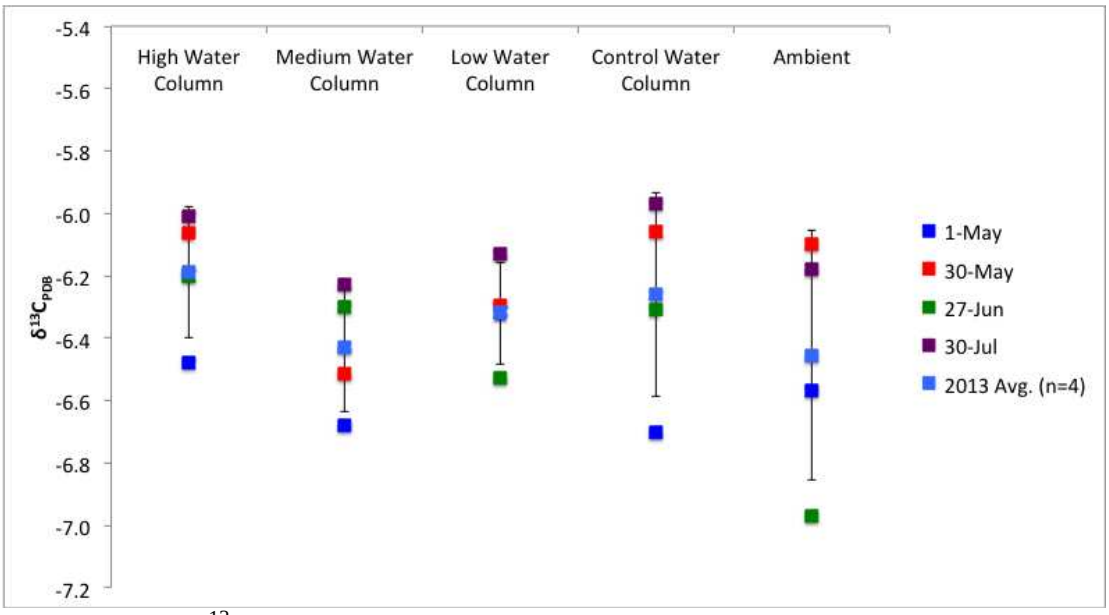

Figure 55. Total $\delta^{13}C_{PDB}$. Error bars represent one standard deviation (n=3).

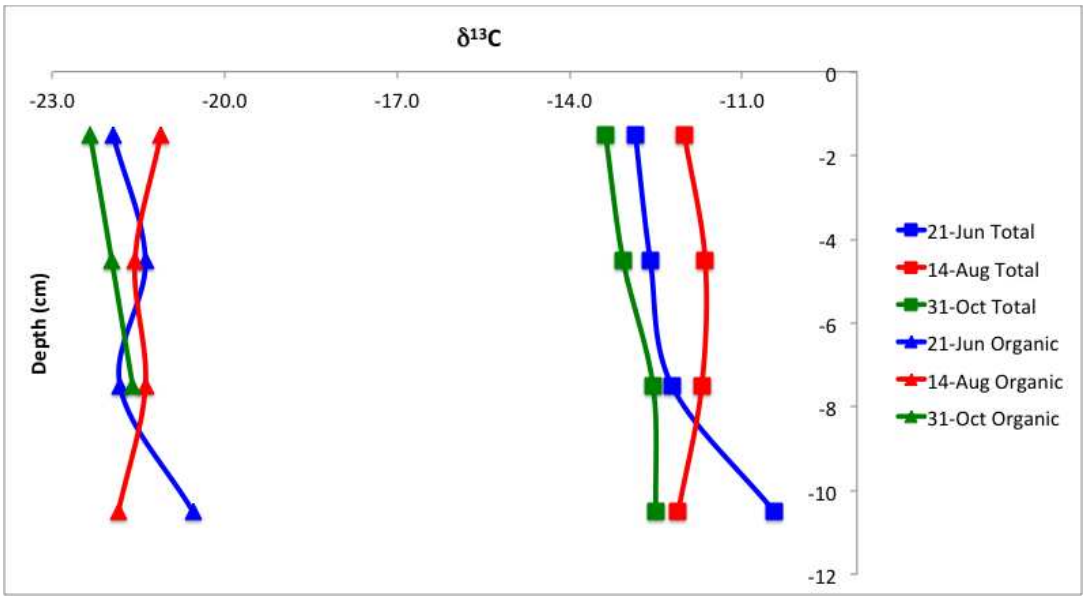

Figure 56. Depth profiles of total and organic carbon isotope values for FB1 sediment before drying (21-Jun) and dried (14-Aug).

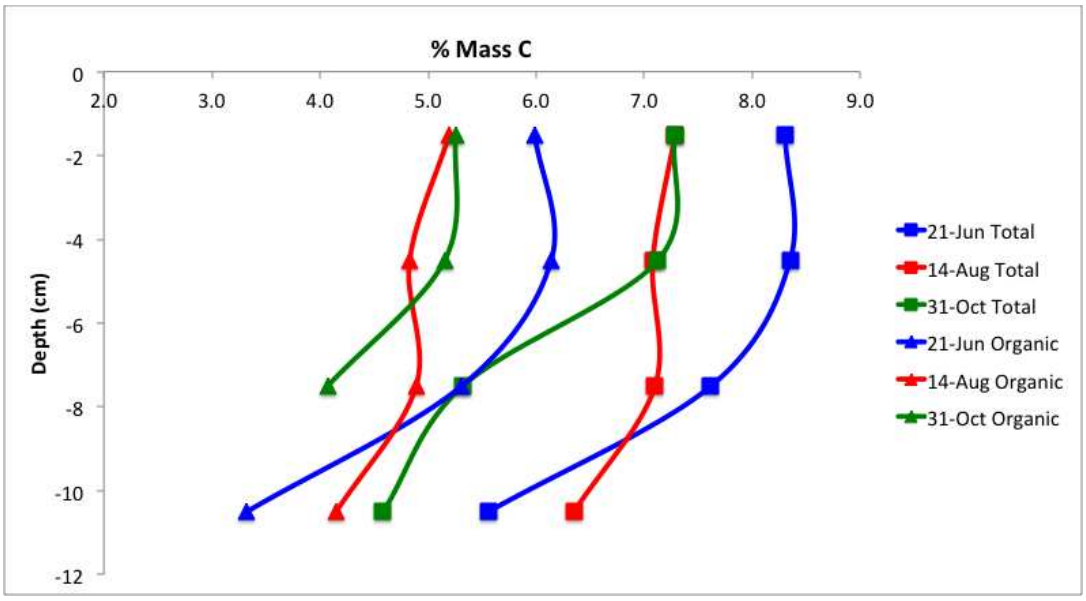

Figure 57. Depth profiles of total and organic % carbon for FB1 sediment before drying (21-Jun) and dried (14-Aug).

5.4 Rate Constant Regression

Contents of text files for the MATLAB script below include data from bucket tests.

- Column 1 – number of days fertilizer has been submerged
- Column 2 – temperature of water when sample was collected
- Column 3 – rate constant according to derivative of the line of best fit
- Column 4 – rate constant calculated by resulting equation from regressed data (not used in MATLAB script)

N2012.txt

```
78.00416667 12.77777778 0.001138889 0.001631569
78.86180556 12.77777778 0.001138889 0.001618974
81.90138889 12.77777778 0.001138889 0.001574335
85.11875    12.77777778 0.001138889 0.001527086
89.96597222 12.77777778 0.001138889 0.001455901
96.23333333 12.77777778 0.001138889 0.00136386
0.004166667 12.77777778 0.002813889 0.002777058
0.861805556 12.77777778 0.002813889 0.002764463
3.901388889 12.77777778 0.002813889 0.002719824
7.11875 12.77777778 0.002813889 0.002672575
11.96597222 12.77777778 0.002813889 0.00260139
18.23333333 12.77777778 0.002813889 0.002509349
102.4069444 28.33333333 0.002530556 0.003427409
105.2402778 29.44444444 0.002530556 0.003539672
107.2194444 25.55555556 0.002530556 0.002972053
24.40694444 28.33333333 0.008153282 0.004572898
27.24027778 29.44444444 0.004451369 0.004685161
29.21944444 25.55555556 0.00337952  0.004117542
300 12.77777778 1.13889E-05 -0.001628608
300 27.61904762 2.53056E-05 0.000426688
```

N2013.txt

```
78.00416667 12.77777778 0.000239167 0.000342629
78.86180556 12.77777778 0.000239167 0.000339985
81.90138889 12.77777778 0.000239167 0.00033061
85.11875    12.77777778 0.000239167 0.000320688
89.96597222 12.77777778 0.000239167 0.000305739
96.23333333 12.77777778 0.000239167 0.000286411
0.004166667 12.77777778 0.000590917 0.000583182
0.861805556 12.77777778 0.000590917 0.000580537
3.901388889 12.77777778 0.000590917 0.000571163
7.11875 12.77777778 0.000590917 0.000561241
11.96597222 12.77777778 0.000590917 0.000546292
18.23333333 12.77777778 0.000590917 0.000526963
102.4069444 28.33333333 0.000531417 0.000719756
105.2402778 29.44444444 0.000531417 0.000743331
107.2194444 25.55555556 0.000531417 0.000624131
24.40694444 28.33333333 0.001712189 0.000960309
```

```
27.24027778 29.44444444 0.000934787 0.000983884
29.21944444 25.55555556 0.000709699 0.000864684
300 12.77777778 2.39167E-06 -0.000342008
300 27.61904762 5.31417E-06 8.96044E-05
```

P2012.txt

```
78.00416667 12.77777778 0.000279167 0.00034422
78.86180556 12.77777778 0.000279167 0.000343683
81.90138889 12.77777778 0.000279167 0.000341781
85.11875    12.77777778 0.000279167 0.000339768
89.96597222 12.77777778 0.000279167 0.000336735
96.23333333 12.77777778 0.000279167 0.000332814
0.004166667 12.77777778 0.000220833 0.000393025
0.861805556 12.77777778 0.000220833 0.000392489
3.901388889 12.77777778 0.000220833 0.000390587
7.11875 12.77777778 0.000220833 0.000388574
11.96597222 12.77777778 0.000220833 0.000385541
18.23333333 12.77777778 0.000220833 0.000381619
102.4069444 28.33333333 0.0009875   0.001215224
105.2402778 29.44444444 0.0009875   0.001276756
107.2194444 25.55555556 0.0009875   0.00105395
112.0458333 23.33333333 0.0009875   0.000924319
24.40694444 28.33333333 0.001707164 0.00126403
27.24027778 29.44444444 0.001529598 0.001325562
29.21944444 25.55555556 0.001425991 0.001102755
34.04583333 23.33333333 0.00122384  0.000973125
300 12.77777778 2.79167E-06 0.000205314
300 25.81196581 0.000009875 0.000947933
```

P2013.txt

```
78.00416667 12.77777778 4.46667E-05 3.3025E-05
78.86180556 12.77777778 4.46667E-05 3.26726E-05
81.90138889 12.77777778 4.46667E-05 3.14236E-05
85.11875    12.77777778 4.46667E-05 3.01015E-05
89.96597222 12.77777778 4.46667E-05 2.81097E-05
96.23333333 12.77777778 4.46667E-05 2.55343E-05
0.004166667 12.77777778 3.53333E-05 6.5077E-05
0.861805556 12.77777778 3.53333E-05 6.47246E-05
3.901388889 12.77777778 3.53333E-05 6.34756E-05
7.11875 12.77777778 3.53333E-05 6.21535E-05
11.96597222 12.77777778 3.53333E-05 6.01616E-05
18.23333333 12.77777778 3.53333E-05 5.75862E-05
102.4069444 28.33333333 0.000158    0.000188426
105.2402778 29.44444444 0.000158    0.000199079
107.2194444 25.55555556 0.000158    0.000156908
112.0458333 23.33333333 0.000158    0.000131292
24.40694444 28.33333333 0.000273146 0.000220478
27.24027778 29.44444444 0.000244736 0.000231131
29.21944444 25.55555556 0.000228159 0.00018896
34.04583333 23.33333333 0.000195814 0.000163344
300 12.77777778 4.46667E-07 -5.81981E-05
300 25.81196581 0.00000158  8.04169E-0
```

MATLAB function file: “importdmap”

```
function importdmap(fileToRead1)
%IMPORTFILE(FILETOREAD1)
%  Imports data from the specified file
%  FILETOREAD1:  file to read

%  Auto-generated by MATLAB on 15-Sep-2012 02:50:12
```

```
% Import the file
rawData1 = importdata(fileToRead1);

% For some simple files (such as a CSV or JPEG files), IMPORTDATA might
% return a simple array.  If so, generate a structure so that the output
% matches that from the Import Wizard.
[~,name] = fileparts(fileToRead1);
newData1.(genvarname(name)) = rawData1;

% Create new variables in the base workspace from those fields.
vars = fieldnames(newData1);
for i = 1:length(vars)
    assignin('base', vars{i}, newData1.(vars{i}));
end
```

MATLAB script file: “Regress_Plots201213_3DSurface_NoPoints”

```
%Multiple Linear Regression
%Example 15.2
%Use matrices from "2012 Bucket and 2013 Mesocoms Test" spreadsheet

%1. Adjust "Bucket Test Data" as desired
%2. Copy paste columns AU-AW into "Regress_Plots201213_3DSurface" script
%3. Run "Regress_Plots201213_3DSurface" script
%4. Use output C array to populate green cells below regression data
%5. Use "Flux Results" and update txt files used by
"Regress_Plots201213_3DSurface" script
%6. Run  "Regress_Plots201213_3DSurface" script twice to get plot scales
to be the same.

%2012 matrices
ANO3N2012 = [
20.0000000  1547.9041667    360.3968254
1547.9041667    259404.0984057  30155.2119709
360.3968254 30155.2119709   7531.0216679
];

bNO3N2012 = [
0.047329198378
1.926151141626
0.963213609099
];

APO4P2012 = [
22.0000000  1093.9958333    366.6666667
1093.9958333    183117.4859404  21444.9699074
366.6666667 21444.9699074   7693.8271605
];

bPO4P2012 = [
0.012836593591
0.740772968750
0.302108421040
];

CNO3N2012 = ANO3N2012\bNO3N2012
CPO4P2012 = APO4P2012\bPO4P2012
AINO3N = inv(ANO3N2012);
AIPO4P = inv(APO4P2012);
```

```
%2013 matrices
ANO3N2013 = [
20.0000000  1547.9041667    360.3968254
1547.9041667    259404.0984057  30155.2119709
360.3968254 30155.2119709   7531.0216679
];

bNO3N2013 = [
0.009939131659
0.404491739742
0.202274857911
];

APO4P2013 = [
22.0000000  1693.9958333    405.2564103
1693.9958333    273117.4859404  33021.8929843
405.2564103 33021.8929843   8523.3563445
];

bPO4P2013 = [
0.002055881641
0.118997675000
0.048378130272
];

CNO3N2013 = ANO3N2013\bNO3N2013
CPO4P2013 = APO4P2013\bPO4P2013
AINO3N2013 = inv(ANO3N2013);
AIPO4P2013 = inv(APO4P2013);

%plot 2012 NO3-N and PO4-P flux

tempa = 5;
tempb = 30;
timea = 0;
timeb = 300;
coloraxisa = 0;
coloraxisb1 = 0.0015;
coloraxisb2 = 0.01;
coloraxisb3 = 0.0055;
res = .1;

time = linspace(timea,timeb);
temp1 = linspace(tempa,tempb);

NO3Nflux2012=CNO3N2012(1)+CNO3N2012(2).*time+CNO3N2012(3).*temp1;% NO3-N
2012 5-30 deg C
PO4Pflux2012=CPO4P2012(1)+CPO4P2012(2).*time+CPO4P2012(3).*temp1;% PO4-P
2012 5-30 deg C

%Plot 2013 NO3-N and PO4-P flux

%Using 2013 time/temp coefficients
NO3Nflux2013=CNO3N2013(1)+CNO3N2013(2).*time+CNO3N2013(3).*temp1;% NO3-N
2013 5-30 deg C
PO4Pflux2013=CPO4P2013(1)+CPO4P2013(2).*time+CPO4P2013(3).*temp1;% PO4-P
2013 5-30 deg C


%Creating meshgrids and grid data for surf command.

[XI,YI] = meshgrid (timea:res:timeb, tempa:res:tempb);
```

```
%2012
%N

Nflux2012 = CNO3N2012(1)+CNO3N2012(2).*XI+CNO3N2012(3).*YI;% Equation
for 2012 NO3-N rate constant
importdmap('N2012.txt')
for n =1:20
    X2012N(n,1)=N2012(n,1);
    Y2012N(n,1)=N2012(n,2);
    Z2012BucketkN(n,1)=N2012(n,3);
    Z2012EquationkN(n,1)=N2012(n,4);

end

figure(1)
subplot(2,1,1)
hold on
ZIN2012 = griddata(XI, XI, Nflux2012,XI,YI);
surf(XI,YI,Nflux2012,'EdgeColor','none');
colorbar
shading interp
colormap jet
axis([timea timeb tempa tempb coloraxisa coloraxisb2])
caxis([coloraxisa coloraxisb3]) %Set range of colorbar. Use % to use
auto range for full spectrum.
%scatter3 (X2012N, Y2012N, Z2012EquationkN,
'o','MarkerEdgeColor','r',...
%    X2012N, Y2012N, Z2012BucketkN,'x','MarkerEdgeColor','k');
scatter3 (X2012N, Y2012N, Z2012BucketkN,'o','MarkerEdgeColor','k');

xlabel 'Time (days)'
ylabel 'Temperature (Deg C)'
zlabel 'Rate Constant (1/day)'
title ('2012 NO3-N')

V=axis;
view(3)
grid on

%2013
%N
Nflux2013=CNO3N2013(1)+CNO3N2013(2).*XI+CNO3N2013(3).*YI;% Equation for
2013 NO3-N rate constant
importdmap('N2013.txt')
for n =1:20
    X2013N(n,1)=N2013(n,1);
    Y2013N(n,1)=N2013(n,2);
    Z2013BucketkN(n,1)=N2013(n,3);
    Z2013EquationkN(n,1)=N2013(n,4);
end

subplot(2,1,2)
hold on
ZIN2013 = griddata(XI, XI, Nflux2013,XI,YI);
surf(XI,YI,Nflux2013,'EdgeColor','none');
colorbar EastOutside
shading interp
colormap jet
axis([timea timeb tempa tempb coloraxisa coloraxisb1])
caxis([coloraxisa coloraxisb1]) %Set range of colorbar. Use % to use
auto range for full spectrum.
%scatter3 (X2013N, Y2013N, Z2013EquationkN,
```

```
'o','MarkerEdgeColor','r',...
%    X2013N, Y2013N, Z2013BucketkN,'x','MarkerEdgeColor','k');
scatter3 (X2013N, Y2013N, Z2013BucketkN,'o','MarkerEdgeColor','k');

xlabel 'Time (days)'
ylabel 'Temperature (Deg C)'
zlabel 'Rate Constant (1/day)'
title ('2013 NO3-N')

axis(V);
view(3)
grid on

%2012
%P
Pflux2012 = CPO4P2012(1)+CPO4P2012(2).*XI+CPO4P2012(3).*YI;% Equation
for 2012 PO4-P rate constant
importdmap('P2012.txt')
for n =1:22 %number of rows in .txt file
    X2012P(n,1)=P2012(n,1);
    Y2012P(n,1)=P2012(n,2);
    Z2012BucketkP(n,1)=P2012(n,3);
    Z2012EquationkP(n,1)=P2012(n,4);

end

figure(2)
subplot(2,1,1)
hold on
ZIP2012 = griddata(XI, XI, Pflux2012,XI,YI);
surf(XI,YI,Pflux2012,'EdgeColor','none');
colorbar EastOutside
axis([timea timeb tempa tempb coloraxisa coloraxisb1])
caxis([coloraxisa coloraxisb1]) %Set range of colorbar. Use % to use
auto range for full spectrum.
shading interp
colormap jet
%scatter3 (X2012P, Y2012P, Z2012EquationkP,
'o','MarkerEdgeColor','r',...
%    X2012P, Y2012P, Z2012BucketkP,'x','MarkerEdgeColor','k');
scatter3 (X2012P, Y2012P, Z2012BucketkP,'o','MarkerEdgeColor','k');

xlabel 'Time (days)'
ylabel 'Temperature (Deg C)'
zlabel 'Rate Constant (1/day)'
title ('2012 PO4-P')

V=axis;
view(3) %default for 3d plots
grid on


%2013
%P
Pflux2013=CPO4P2013(1)+CPO4P2013(2).*XI+CPO4P2013(3).*YI;% Equation for
2013 PO4-P rate constant

importdmap('P2013.txt')
for n =1:22
    X2013P(n,1)=P2013(n,1);
    Y2013P(n,1)=P2013(n,2);
    Z2013BucketkP(n,1)=P2013(n,3);
```

```
    Z2013EquationkP(n,1)=P2013(n,4);
end

subplot(2,1,2)
hold on
ZIP2013 = griddata(XI, XI, Pflux2013,XI,YI);
surf(XI,YI,Pflux2013,'EdgeColor','none');
colorbar EastOutside
axis([timea timeb tempa tempb coloraxisa coloraxisb1])
caxis([coloraxisa coloraxisb1]) %Set range of colorbar. Use % to use
auto range for full spectrum.
shading interp
colormap jet


%scatter3 (X2013P, Y2013P, Z2013EquationkP,
'o','MarkerEdgeColor','r',...
%    X2013P, Y2013P, Z2013BucketkP,'x','MarkerEdgeColor','k');
scatter3 (X2013P, Y2013P, Z2013BucketkP,'o','MarkerEdgeColor','k');

xlabel 'Time (days)'
ylabel 'Temperature (Deg C)'
zlabel 'Rate Constant (1/day)'
title('2013 PO4-P')

axis(V);
view(3) %default for 3d plots
grid on
```

REFERENCES

Aldrich, T.W. and Paul, D.S., 2002. Avian ecology of Great Salt Lake. Great Salt Lake: An Overview of Change. Special publication of the Utah Department of Natural Resources, Salt Lake City, Utah: 343-374.

Baggett, L.P., Heck Jr, K.L., Frankovich, T.A., Armitage, A.R., and Fourqurean, J.W., 2010. Nutrient enrichment, grazer identity, and their effects on epiphytic algal assemblages: Field experiments in subtropical turtlegrass Thalassia testudinum meadows. Marine Ecology Progress Series, 406: 33-45.

Bellrose, F.C. and Low, J.B., 1978. Advances in waterfowl management research. Wildlife Society Bulletin: 63-72.

Carling, G.T., Fernandez, D.P., Rudd, A., Pazmino, E., and Johnson, W.P., 2011. Trace element diel variations and particulate pulses in perimeter freshwater wetlands of Great Salt Lake, Utah. Chemical Geology, 283(1-2): 87-98.

Carling, G.T., Richards, D. C., Hoven, H., Miller, T., Fernandez, D. P., Rudd, A., Pazmino, E., and Johnson, W. P., 2013. Relationships of surface water, pore water, and sediment chemistry in wetlands adjacent to Great Salt Lake, Utah, and potential impacts on plant community health. Science of The Total Environment, 443: 798-811.

Denbleyker, Jeff. "Hydrology and Nutrient Loads." Utah Division of Water Quality: Science Panel Meetings. Utah Division of Water Quality, 29 01 2013. Web. 10 Oct 2013. <http://www.willardspur.utah.gov/panel/meetings.htm>.

Denbleyker, Jeff. "Plant effluent." Message to Joel Pierson. 28 10 2013. E-mail.

Dicataldo, G., Johnson, W. P., Naftz, D. L., Hayes, D. F., Moellmer, W. O., and Miller, T., 2011. Diel variation of selenium and arsenic in a wetland of the Great Salt Lake, Utah. Applied Geochemistry, 26(1): 28-36.

Downing, J.A., 2010. Emerging global role of small lakes and ponds: little things mean a lot. Limnetica, 1(29): 9-24.

Furman, B.T. and Heck, K., 2008. Effects of nutrient enrichment and grazers on coral reefs: an experimental assessment. Mar Ecol Prog Ser, 363: 89-101.

Gilbert, J.D., Guerrero, F., and de Vicente, I., 2014. Sediment desiccation as a driver of phosphate availability in the water column of Mediterranean wetlands. Science of The Total Environment, 466-467(0): 965-975.

Gorrell, J.V., Andersen, M. E., Bunnell, K. D., Canning, M. F., Clark, A. G., Dolsen D. E., and Howe F. P., 2005. Utah comprehensive wildlife conservation strategy (CWCS). Utah Division of Wildlife Resources Salt Lake City, UT.

Heaton, T., 1986. Isotopic studies of nitrogen pollution in the hydrosphere and atmosphere: a review. Chemical Geology, 59(1): 87-102.

Heck, K.L., Jr., Pennock, J.R., Valentine, J.F., Coen, L.D., and Sklenar, S.A., 2000. Effects of nutrient enrichment and small predator density on seagrass ecosystems: An experimental assessment. Limnology and Oceanography, 45(5): 1041-1057.

Hoven, H.M. and Miller, T.G., 2009. Developing vegetation metrics for the assessment of beneficial uses of impounded wetlands surrounding Great Salt Lake, Utah, USA. Natural Resources and Environmental Issues, 15(1): 11.

Hoven, H.M. , Johnson, W.P., Goel, R.K., Richards, D.C., and Rushforth S. "Nutrient Cycling." Utah Division of Water Quality: Science Panel Meetings. Utah Division of Water Quality, 29 01 2013. Web. 10 Oct 2013. <http://www.willardspur.utah.gov/panel/meetings.htm>.

Hoven, H.M. , Johnson, W.P., Goel, R.K., Richards, D.C., and Rushforth S. In preparation.

Johnson, A.M., 2008. Food abundance and energetic carrying capacity for wintering waterfowl in the Great Salt Lake wetlands. Thesis, Oregon State University, Corvallis, Oregon, USA.

Kadlec, J.A., 2002. Avian botulism in Great Salt Lake marshes: perspectives and possible mechanisms. Wildlife Society Bulletin, 30(3): 983-989.

McCormick, P.V. and Laing, J.A., 2003. Effects of increased phosphorus loading on dissolved oxygen in a subtropical wetland, the Florida Everglades. Wetlands Ecology and Management, 11(3): 199-216.

Naftz, D., Angeroth, C., Kenney, T., Waddell, B., Darnall, N., Silva, S., Perschon C., and Whitehead, J., 2008. Anthropogenic influences on the input and biogeochemical cycling of nutrients and mercury in Great Salt Lake, Utah, USA. Applied Geochemistry, 23(6): 1731-1744.

Olila, O.G., Reddy, K.R., and Stites, D.L., 1997. Influence of draining on soil phosphorus forms and distribution in a constructed wetland. Ecological Engineering, 9(3): 157-169.

Olsen, S.R., Cole, C., Watanabe, F.S., and Dean, L., 1954. Estimation of available phosphorus in soils by extraction with sodium bicarbonate, 939. US Department of Agriculture Washington, DC.

Ostermiller, Jeff. "Hydrology & Nutrient Loads." Utah Division of Water Quality: Science Panel Meetings. Utah Division of Water Quality, 05 04 2012. Web. 15 Sep 2013. <http://www.willardspur.utah.gov/panel/meetings.htm>.

Ostermiller, Jeff. "Water Chemistry." Utah Division of Water Quality: Science Panel Meetings. Utah Division of Water Quality, 29 01 2013. Web. 15 Sep 2013. <http://www.willardspur.utah.gov/panel/meetings.htm>.

Pierzynski, G.M., 2000. Methods of phosphorus analysis for soils, sediments, residuals, and waters. North Carolina State University, Raleigh.

Poulton, P., Johnston, A., and White, R., 2012. Plant-available soil phosphorus. Part I: the response of winter wheat and spring barley to Olsen P on a silty clay loam. Soil Use and Management. 29 (1): 4–11.

Sondergaard, M., Jensen, J.P., and Jeppesen, E., 2003. Role of sediment and internal loading of phosphorus in shallow lakes. Hydrobiologia, 506(1-3): 135-145.

Utah. Division of Water Quality. Willard Spur: willardspurgenerallocation. 2013. Photograph. willardspur.utah.gov, Salt Lake City. Web. 12 Sep 2013. <http://www.willardspur.utah.gov/images/maps/willardspurgenerallocation.jpg>.

Vahtera, E., Conley, D. J., Gustafsson, B. G., Kuosa, H., Pitkanen, H., Savchuk, O. P., Tamminen, T., Viitasalo, M., Voss, M., and Wasmund N., 2007. Internal ecosystem feedbacks enhance nitrogen-fixing cyanobacteria blooms and complicate management in the Baltic Sea. AMBIO: A journal of the Human Environment, 36(2): 186-194.

Vest, J.L., Conover, and M.R., 2011. Food habits of wintering waterfowl on the Great Salt Lake, Utah. Waterbirds, 34(1): 40-50.

Waddell, B., Cline, C., Darnall, N., Boeke, E., and Sohn, R., 2009. Assessment of Contaminants in the Wetlands and Open Waters of the Great Salt Lake, Utah. 1996-2000 Final Report for U.S. Fish and Wildlife Services.

Waddell, K.M. and Giddings, E.M., 2004. Trace elements and organic compounds in sediment and fish tissue from the Great Salt Lake basins, Utah, Idaho, and Wyoming, 1998-99. Water Resources Investigations Report 03-4283.

Zhu, M., Zhu, G., Li, W., Zhang, Y., Zhao, L., and Gu, Z., 2013. Estimation of the algal-available phosphorus pool in sediments of a large, shallow eutrophic lake (Taihu,

China) using profiled SMT fractional analysis. Environmental Pollution, 173(0): 216-223.